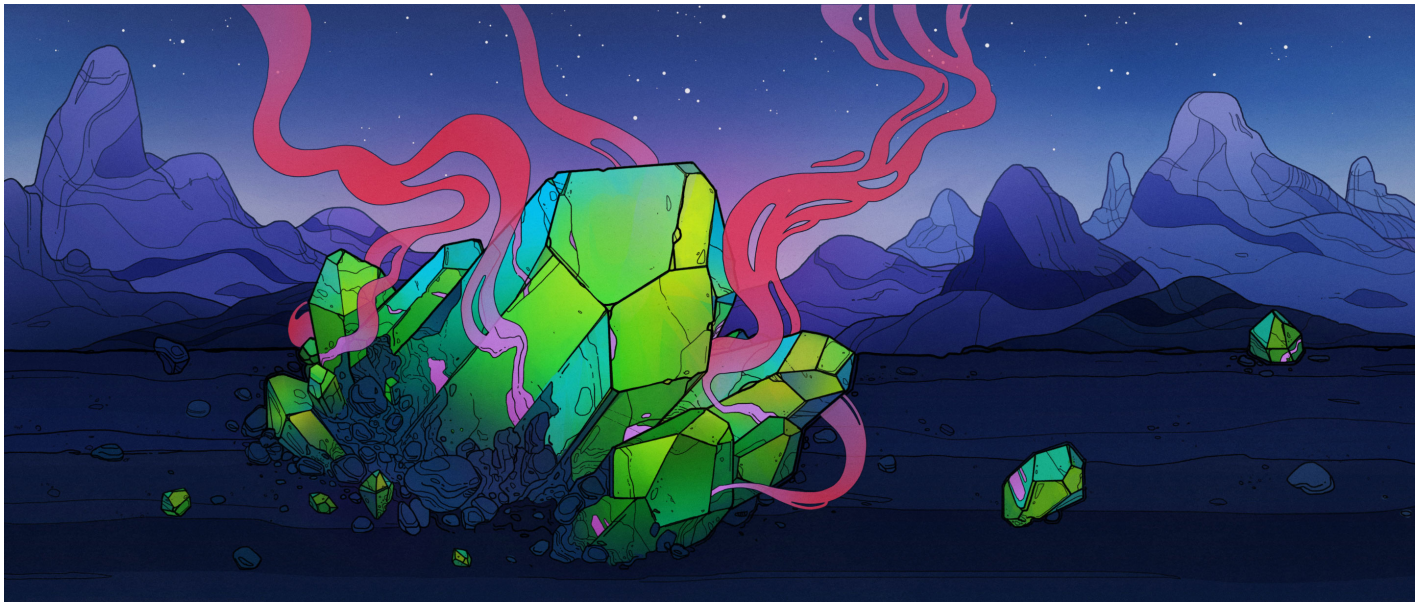
Detectors that rock!



SQUASH
Slovenian Quantum Science Hub

Jožef Stefan Institute
Ljubljana, Slovenia

Co-funded by the European Union

The program is co-funded by the Marie Skłodowska-Curie Actions programme (GA-101177446) and the Slovenian Research and Innovation Agency (ARIS), contract number 5110-18/2025-5.

Figure: Olena Shmahalo/Quanta Magazine

arXiv

Physics > Instrumentation and Detectors

[Submitted on 17 Sep 2026]

Mineral Detection of Neutrinos and Dark Matter 2026 Proceedings

Alexey Elykov, Patrick Stengel, Natsue Abe, Daniel Ang, Lorenzo Apollonio, Levente Balogh, Laura Baudis, Chinmay Bharathulwar, Priyanshu Bhattacharya, Yilda Boukhtouchen, Joseph Bramante, Vincent Breton, Andrew Buchanan, Jens Burkhart, Lorenzo Caccianiga, Andrew Calabrese-Day, Mason Camp, Jordan Chapman, Anson Cook, Reza Ebadi, Denis Erkal, Katherine Freese, Audrey Fung, Shota Futamura, Claudio Galelli, Kevin Gao, Peter W. Graham, Thomas Haddock, Minako Hashiguchi, Alexander Hayes, Adam A. Hecht, Samuel C. Hedges, Shigenobu Hirose, Luisa M. Hötzsch, Patrick Huber, Yohei Igami, Vsevolod Ivanov, Florian Jörg, Ayuki Kamada, Takenori Kato, Yoji Kawamura, Katharina Kehl, Chris Kelso, Holger Kluck, Emilie M. LaVoie-Ingram, Matthew Leybourne, Gavishta H. M. Liyanage, Thalles Lucas, Brenden A. Magill, Paolo Magnani, Jennika McIntosh, Naoki Mizutani, Kohta Murase, Tatsuhiro Naka, Lina Necib, Pranav Parvathaneni, Andre Peterson, Zachary S. C. Picker, Rabeya Rabu, Harikrishnan Ramani, Anupam Ray, Morteza Roostaeinia, Hannah Ross, Issei Saikyo, Lukas Scherne, Maximilian Shen, Aaron Shugar, Joshua Spitz, Kai Sun, Jiashen Tang, Erwin H. Tanin, Dionysios P. Theodosopoulos, Yoichi Usui, Pieter Vermeesch, Aaron Vincent, Ronald Walsworth, Jin-Wei Wang, David Waters, Samuel S. Y. Wong, Audrey Wu, Gregory Wurtz, Wen Yin, Xiuyuan Zhang, Zhexian Zhang

MDνDM community

- Groups across Europe, North America and Asia
- Astroparticle theorists, experimentalists, geologists, and materials scientists

arXiv:2301.07118, 2405.01626, 2508.20482, 2609.20552 series

- Tracks development of crystal detector experiments
- Phenomenological and computational studies

NSF GCR Mineral Detection of Dark Matter Autumn '24



Passive **A**synchronous **L**attice **E**xposure **O**bservatory (**PALEO**)
collaboration formed in Spring '26 **www.paleoscience.org**

UC Berkeley — Igor Jovanovic

Lawrence Livermore National Laboratory — Xianyi Zhang

SLAC NATIONAL ACCELERATOR LABORATORY — Arianna Gleason, Kazu Terao

UNIVERSITY OF MICHIGAN — Thomas Haddock, Josh Spitz, Kai Sun, Emilie LaVoie-Ingram, Audrey Wu, Pranav Parvathaneni, Hannah Ross

IMPERIAL — Christian Wittweg

Jožef Stefan Institute — Patrick Stengel

UNF UNIVERSITY of NORTH FLORIDA — Zane Cable, Chris Kelso, Andre Peterson, Rabeya Rabu, Greg Wurtz

TEXAS The University of Texas at Austin — Katie Freese, Dionysios Theodosopoulos

UNIVERSITY OF MARYLAND — Daniel Ang, Jiashen Tang, Chinmay Bharathulwar, Priyanshu Bhattacharya, Anson Cook, Gavi Liyanage, Maximilian Shen, Mason Camp, Ronald Walsworth

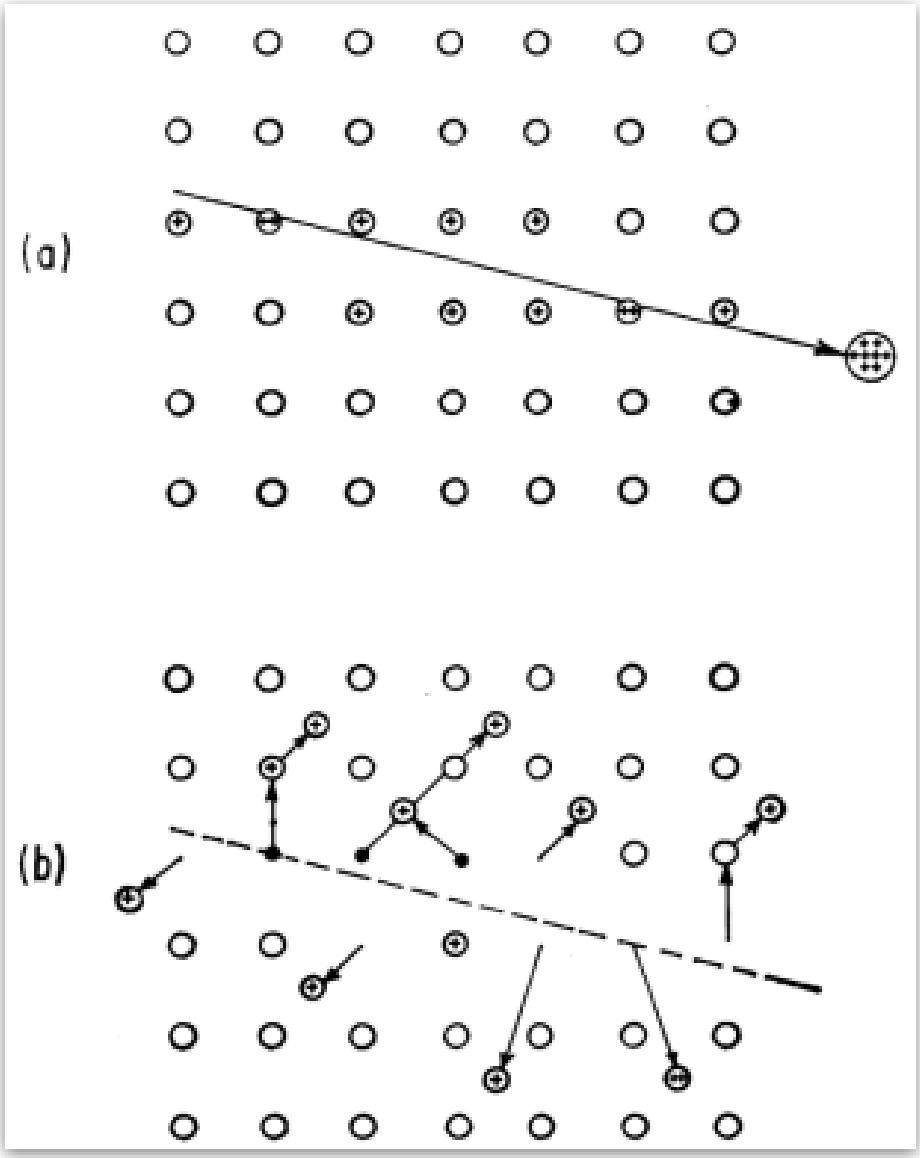
Universität Zürich[UZH] — Laura Baudis, Luisa Hotzsch, Florian Joerg, Nikita Vladimirov

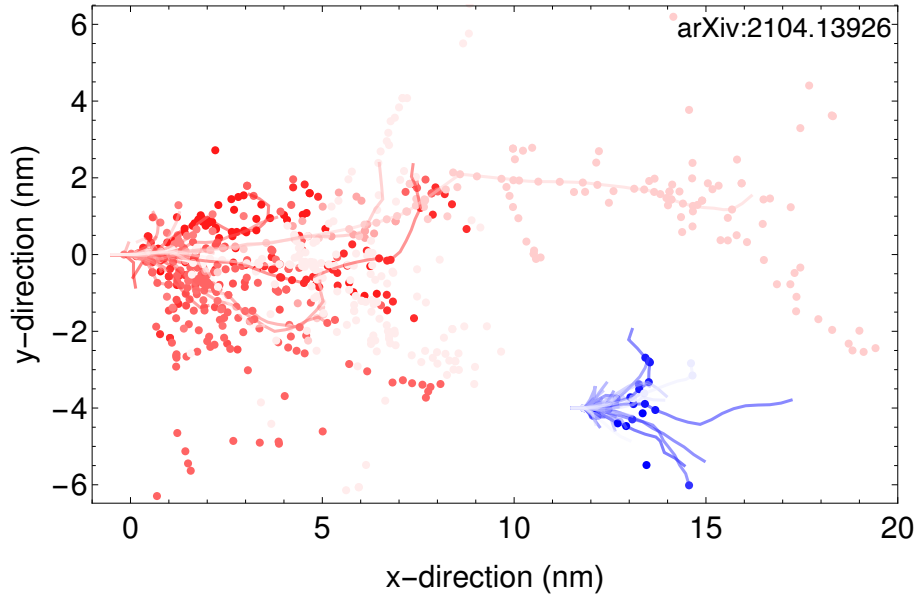
VIRGINIA TECH — Jordan Chapman, Samuel Hedges, Patrick Huber, Giti Khodaparast, Brenden Magill, Tommy O'Donnell, Jackson Skidmore, Vsevolod Ivanov

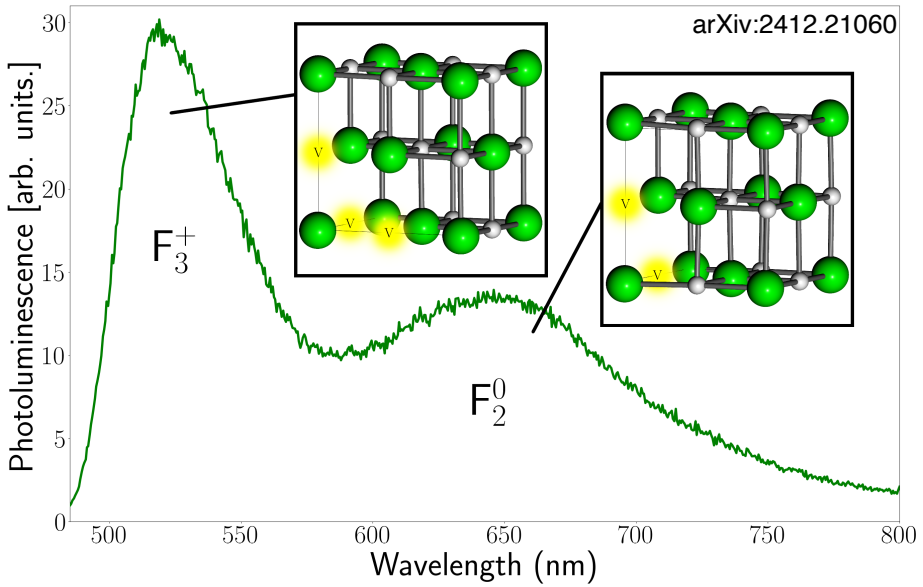
Outline

1. Introduction to paleo-detectors
2. Dark matter direct detection
3. Summary and outlook

Damage induced by nuclear recoils in crystal detectors

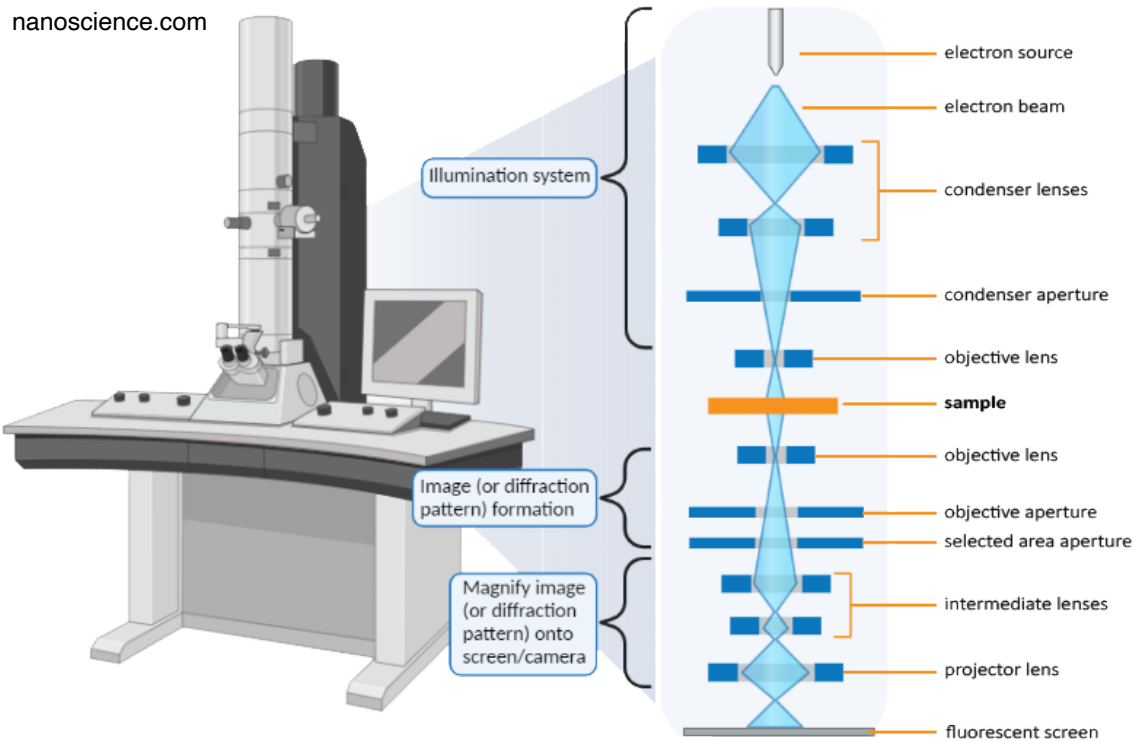




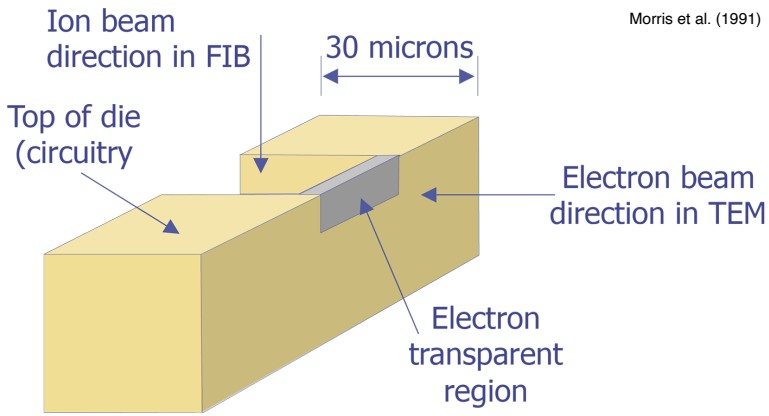


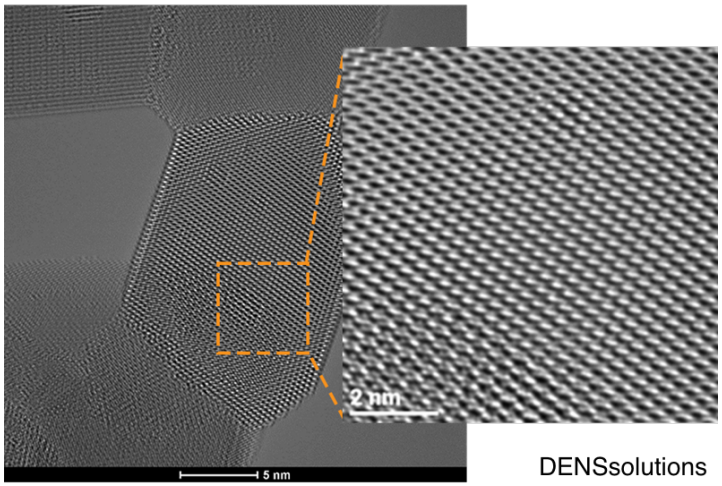
STEM imaging and FIB milling of samples

nanoscience.com



Morris et al. (1991)





DENSsolutions

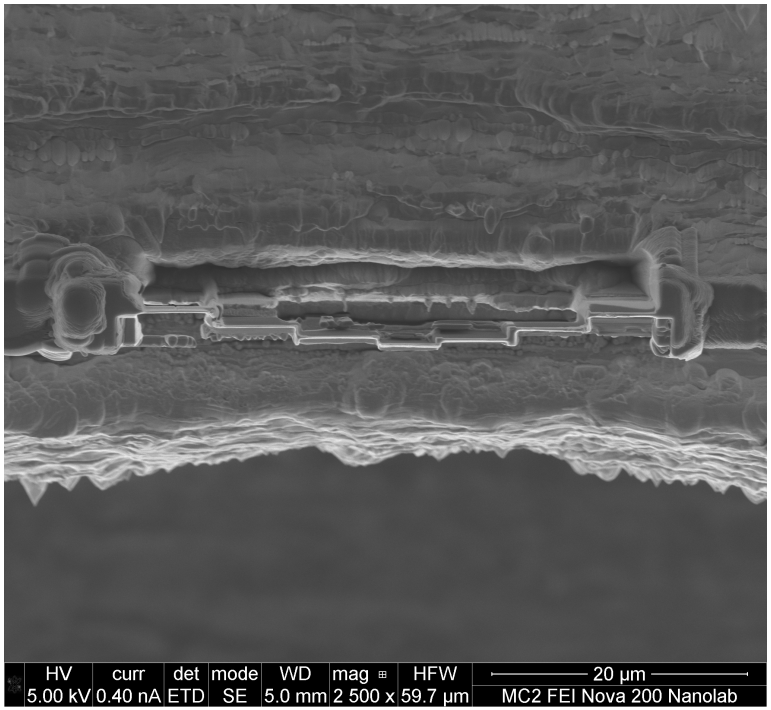
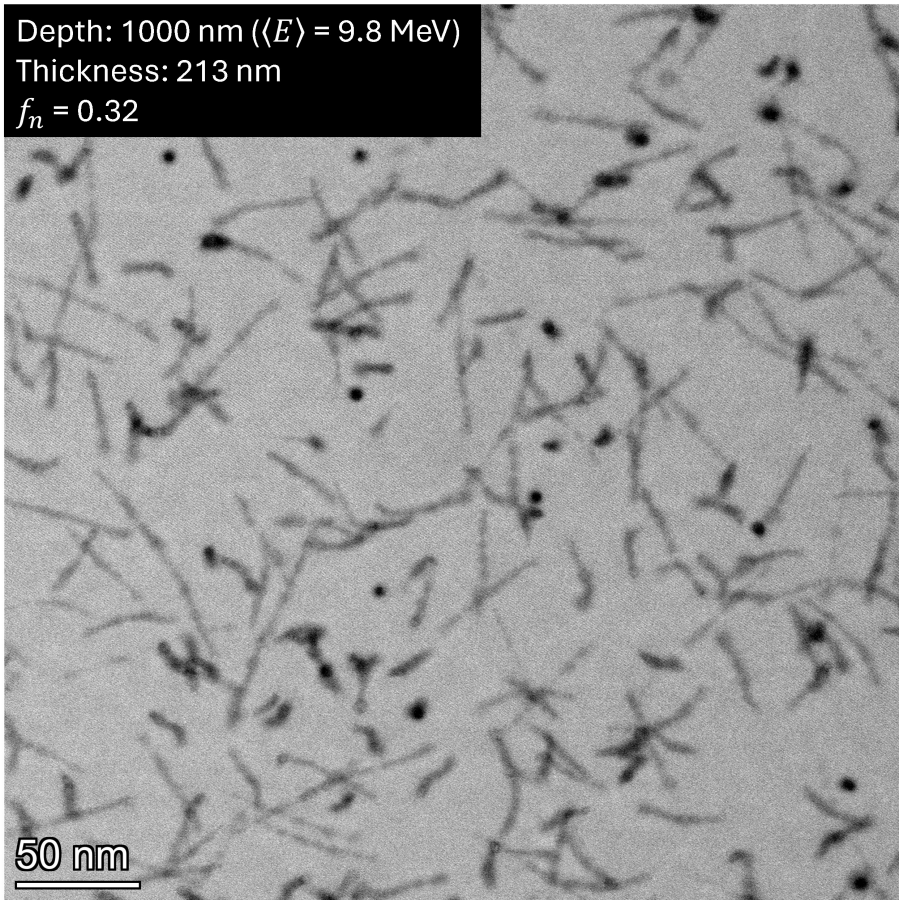
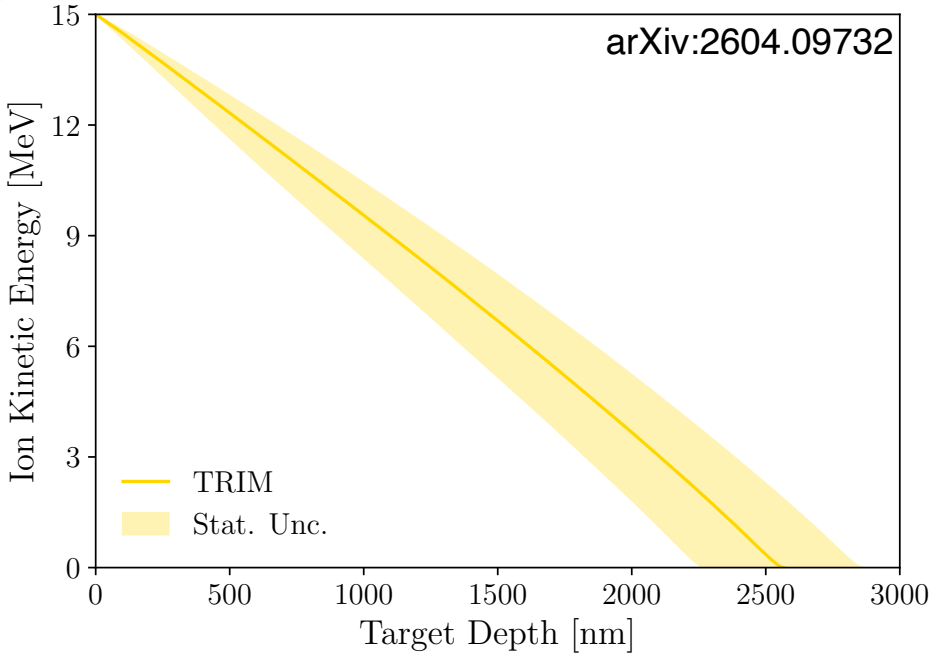
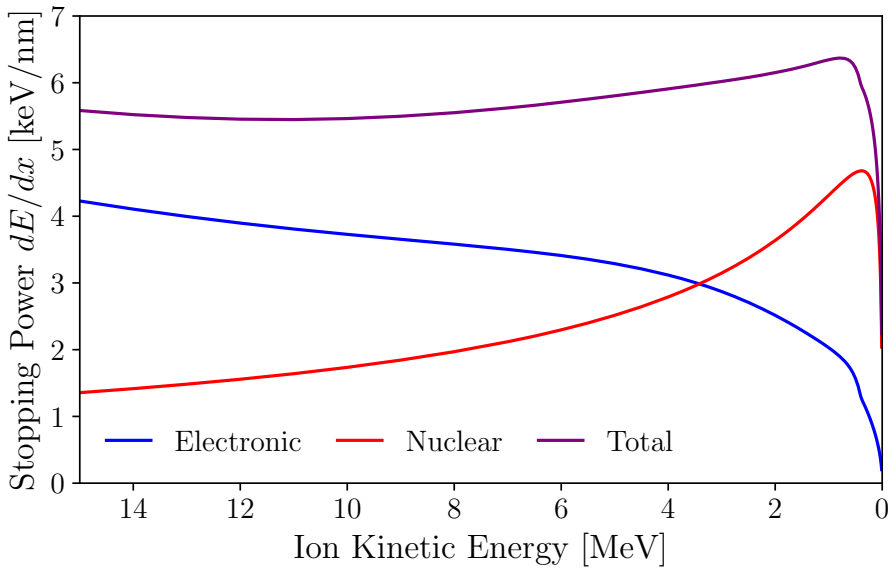


Image and simulate 15 MeV Au^{+5} tracks in natural Olivine





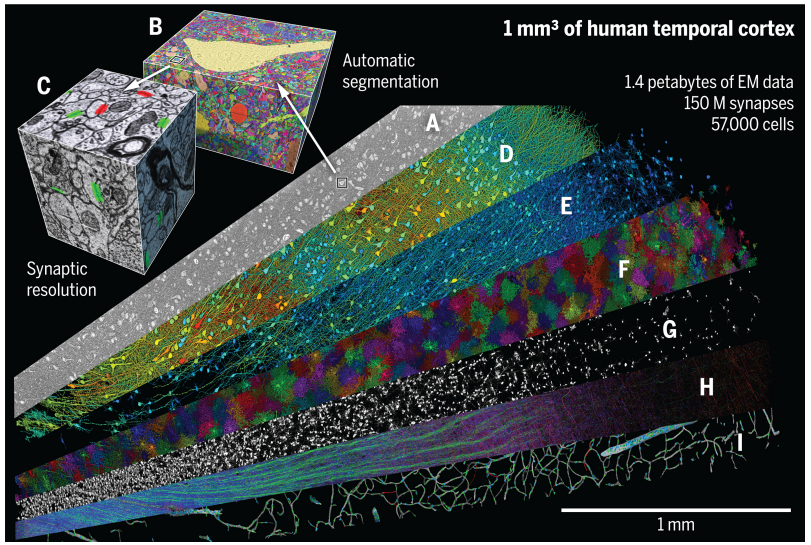


- No etching to enhance tracks
- 2D imaging of tracks at depth
- Track formation, morphology

Adapt techniques from biology and materials science

Readout scenarios for different x_T

- Petascale SEM could read out up to 10 mg with nm resolution
- SAXs at a synchrotron could resolve 15 nm in 3D for 100 g
- Combination with SPIM to zoom in on regions of interest



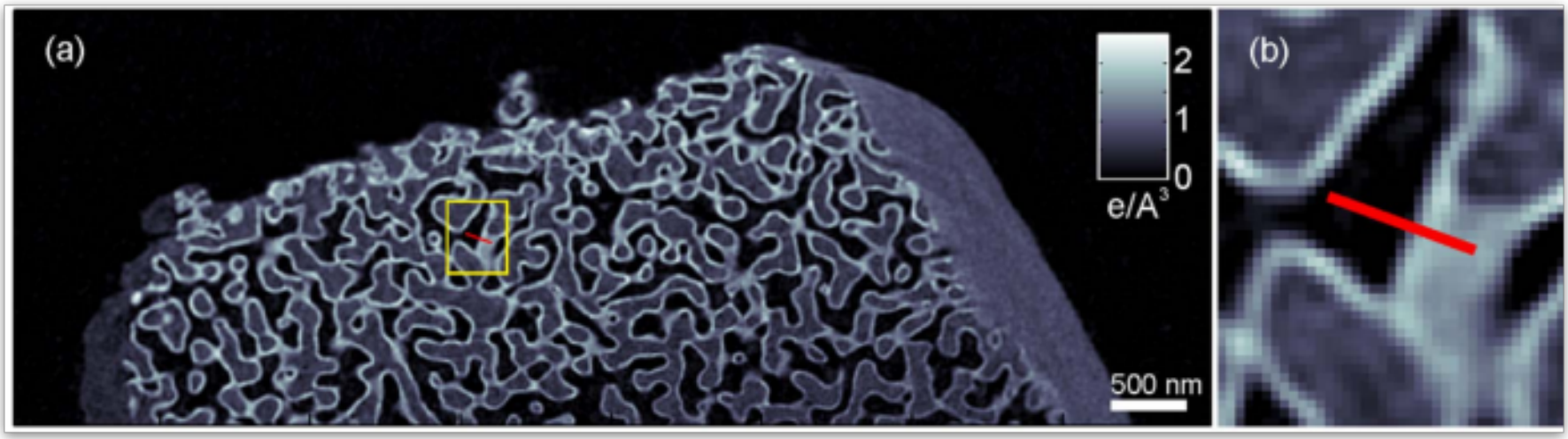
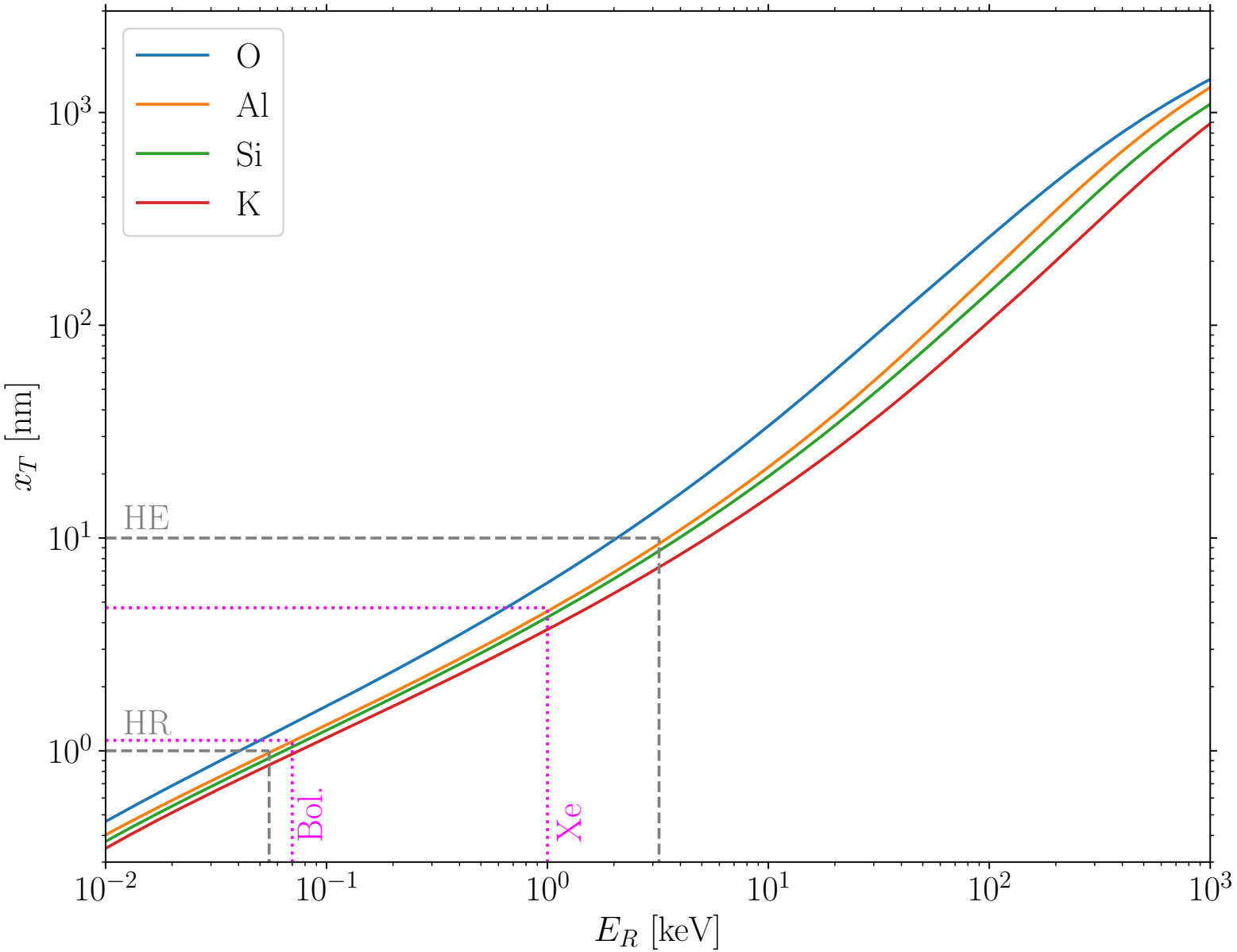


Figure: SEM human brain Shapson-Coe+ '24, SAXs nanoporous glass Holler+ '14

Integrate stopping power to estimate track length



Cosmogenic backgrounds suppressed in deep boreholes

Large exposure from small samples

$$1\,\mathrm{g}\cdot\mathrm{Gyr} = 1\,\mathrm{kton}\cdot\mathrm{yr}$$

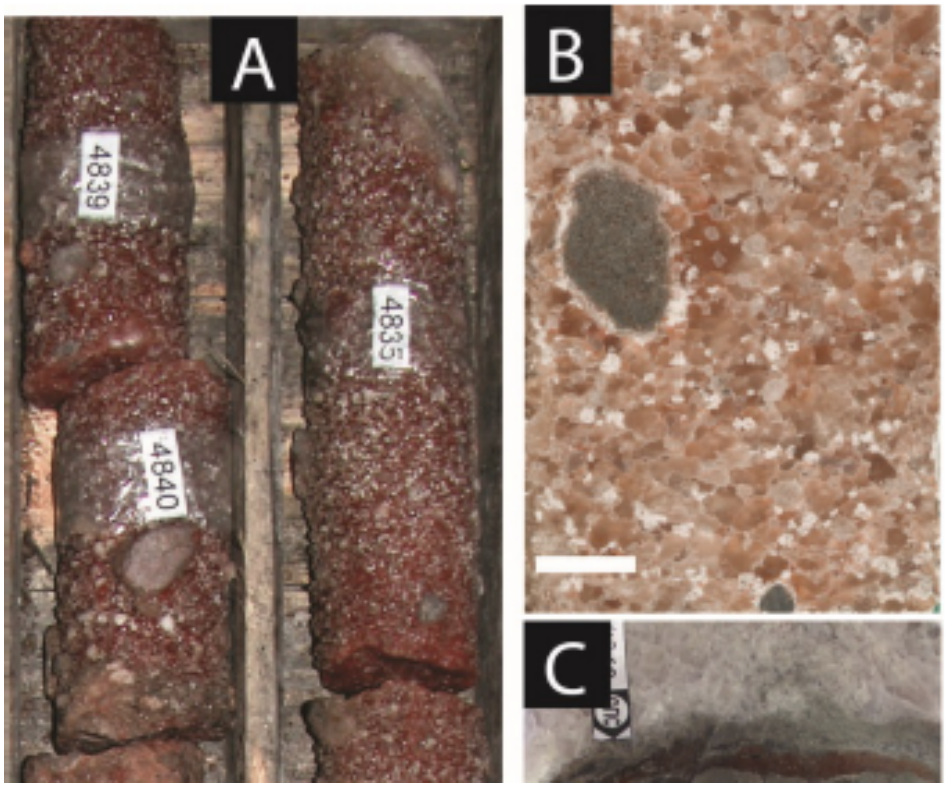


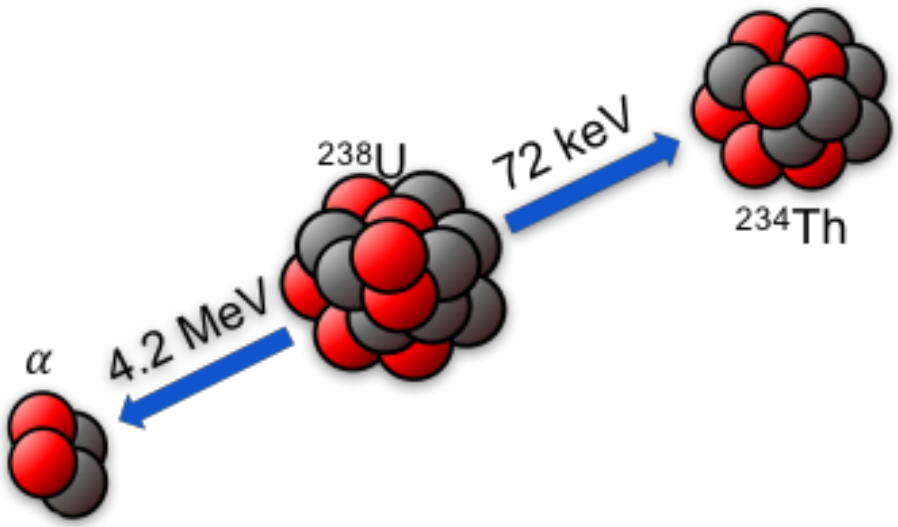
Figure: $\sim$ 2Gyr old Halite cores from $\sim$ 3km deep borehole, Blättler+ '18

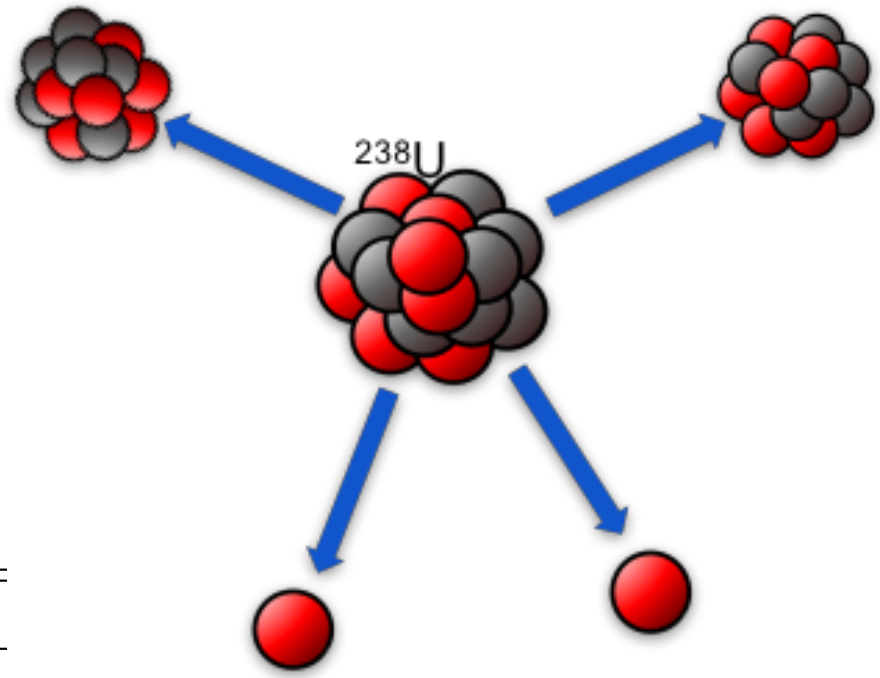
Depth	Neutron Flux
2 km	$10^6/\mathrm{cm}^2/\mathrm{Gyr}$
5 km	$10^2/\mathrm{cm}^2/\mathrm{Gyr}$
6 km	$10/\mathrm{cm}^2/\mathrm{Gyr}$
50 m	$70/\mathrm{cm}^2/\mathrm{yr}$
100 m	$30/\mathrm{cm}^2/\mathrm{yr}$
500 m	$2/\mathrm{cm}^2/\mathrm{yr}$

Need minerals with low ^{238}U

- Marine evaporites with $C^{238} \gtrsim 0.01\,\mathrm{ppb}$
- Ultra-basic rocks from mantle, $C^{238} \gtrsim 0.1\,\mathrm{ppb}$

Find α-recoils and model radiogenic neutron background





Nucleus	Decay mode	$T_{1/2}$
^{238}U	α	4.468×10^9 yr
	SF	8.2×10^{15} yr
^{234}Th	β^-	24.10 d
$^{234\mathrm{m}}$Pa	β^- (99.84 %)	1.159 min
	IT (0.16 %)	
^{234}Pa	β^-	6.70 d
^{234}U	α	2.455×10^5 yr

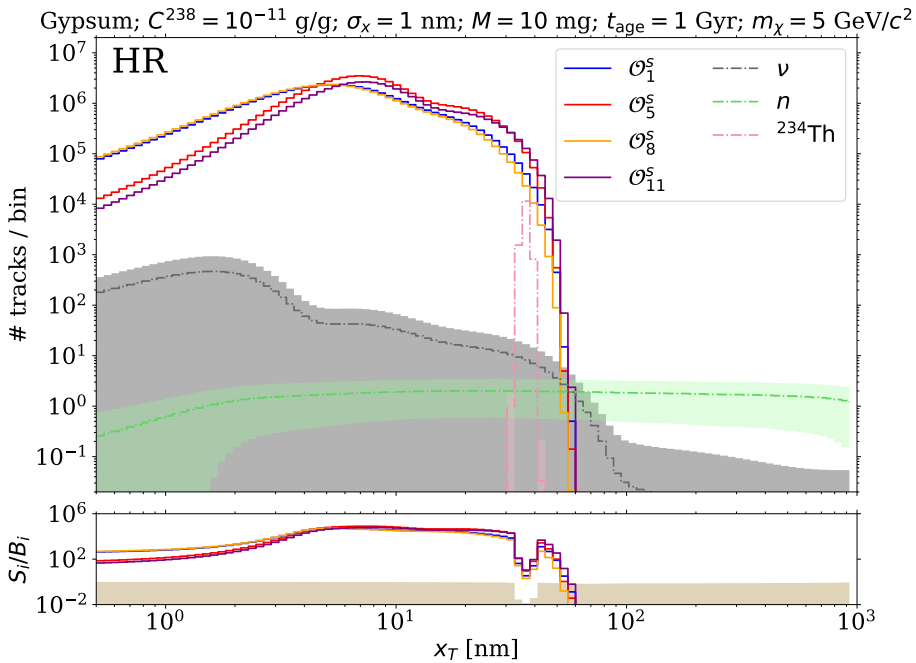
SF yields several $\sim$ MeV neutrons

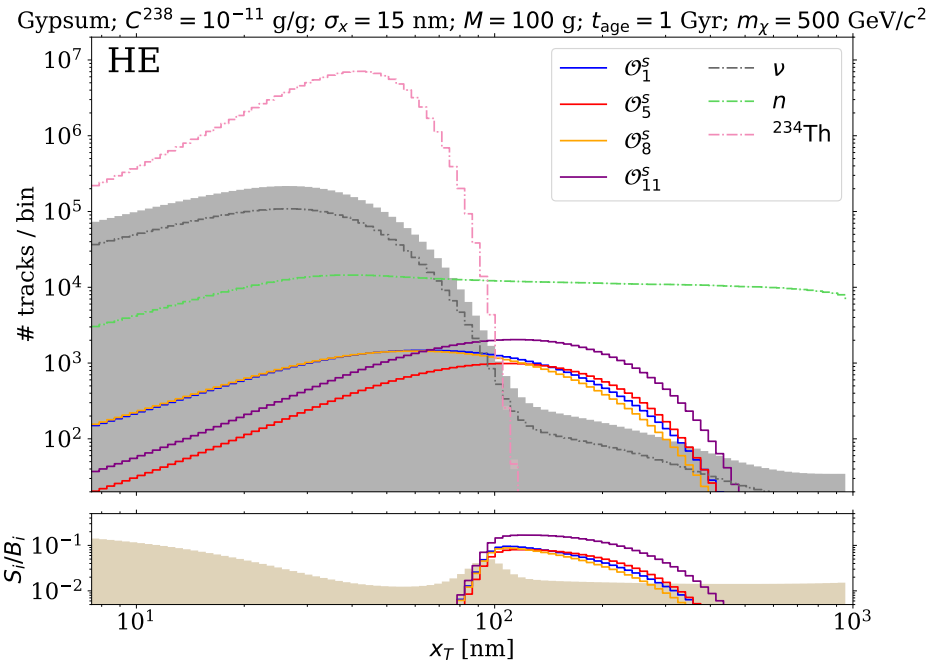
Each neutron will scatter elastically 10-1000 times before moderating

Non-relativistic effective field theory (NREFT) interactions

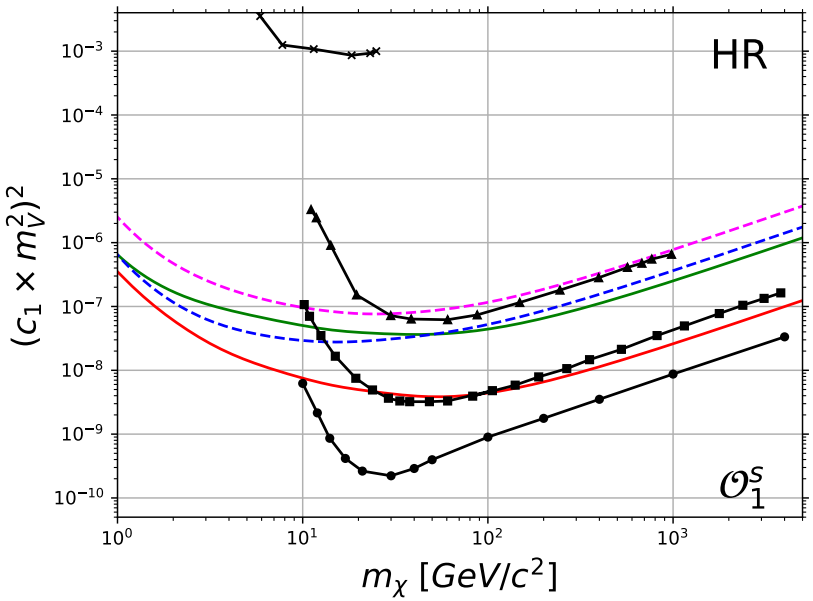
$$\mathcal{L}_{\rm int} = \sum_{N=n,p} \sum_{i} c_i^{(N)} \mathcal{O}_i \, \chi^+ \chi^- N^+ N^- \qquad \mathcal{O}_1 = 1_\chi 1_N \qquad \mathcal{O}_{11} = i \, \vec{S}_\chi \cdot \vec{q}/m_N$$

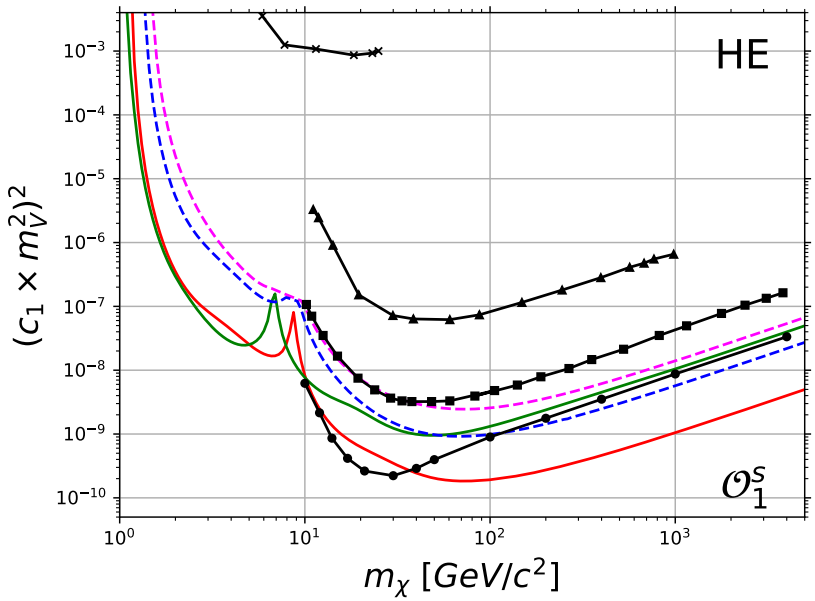
$$\left(\frac{dR}{dE_R} \right)_{(Z,A)} = N_T \frac{\rho_\chi m_T}{32\pi m_\chi^3 m_N^2} \left\langle \frac{1}{v} \sum_{ij} \sum_{N,N'=p,n} c_i^{(N)} c_j^{(N')} F_{ij,\,(Z,A)}^{(N,N')}(v^2, q^2) \right\rangle$$

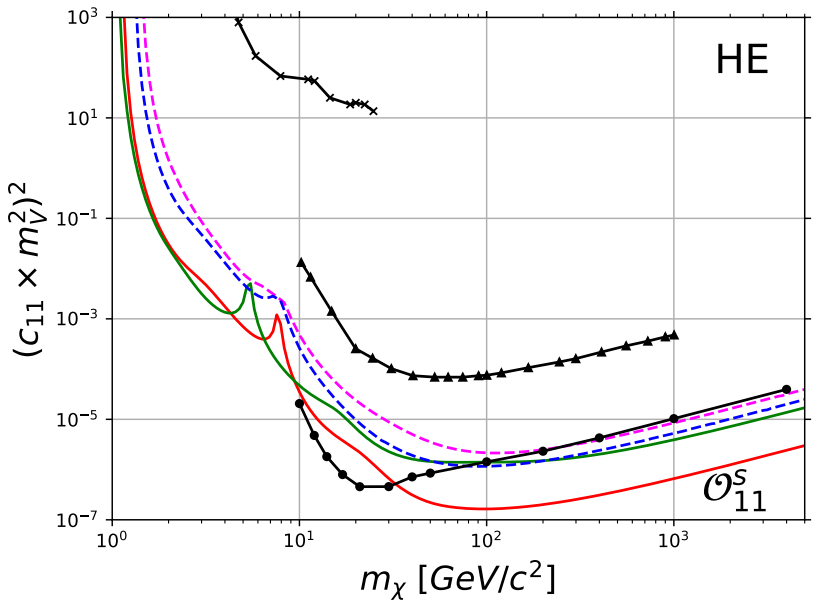




Projected sensitivity for variety of minerals and readouts



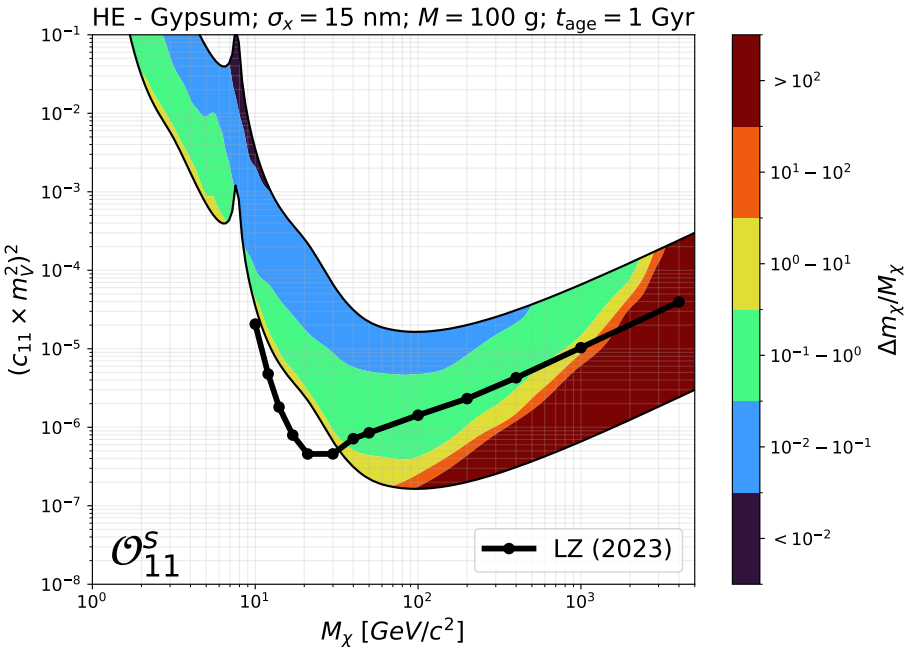


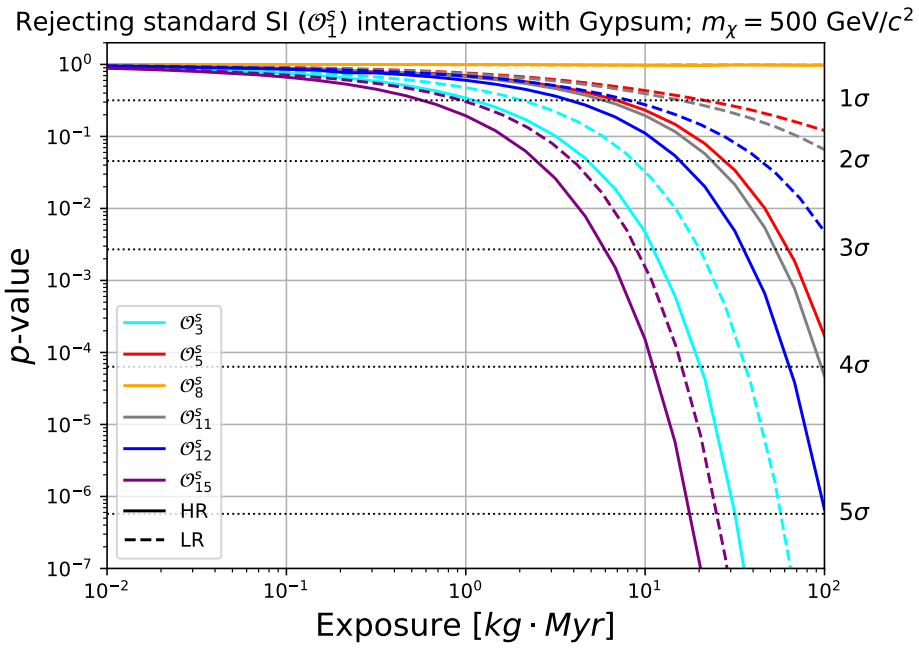


- Gypsum
- Halite
- Olivine
- Muscovite
- LZ (2023)
- XENON100 (2017)
- PandaX-II (2019)
- SuperCDMS (2022)

arXiv:2603.13629

Reconstruct dark matter mass and distinguish interactions





Fractional interval $\Delta m_\chi / M_\chi$

Δm_χ difference between the maximum and minimum masses m_χ not rejected at 2σ

$$\mathcal{O}_1 = 1_\chi 1_N \quad \mathcal{O}_3 = i\,\vec{S}_N \cdot (\vec{q}/m_N \times \vec{v}^\perp)$$
$$\mathcal{O}_5 = i\,\vec{S}_\chi \cdot (\vec{q}/m_N \times \vec{v}^\perp) \quad \mathcal{O}_8 = \vec{S}_\chi \cdot \vec{v}^\perp$$
$$\mathcal{O}_{11} = i\,\vec{S}_\chi \cdot \vec{q}/m_N \quad \mathcal{O}_{12} = \vec{S}_\chi \cdot (\vec{S}_N \times \vec{v}^\perp)$$
$$\mathcal{O}_{15} = -(\vec{S}_\chi \cdot \vec{q}/m_N)[(\vec{S}_N \times \vec{v}^\perp) \cdot \vec{q}/m_N]$$

arXiv:2608.10105

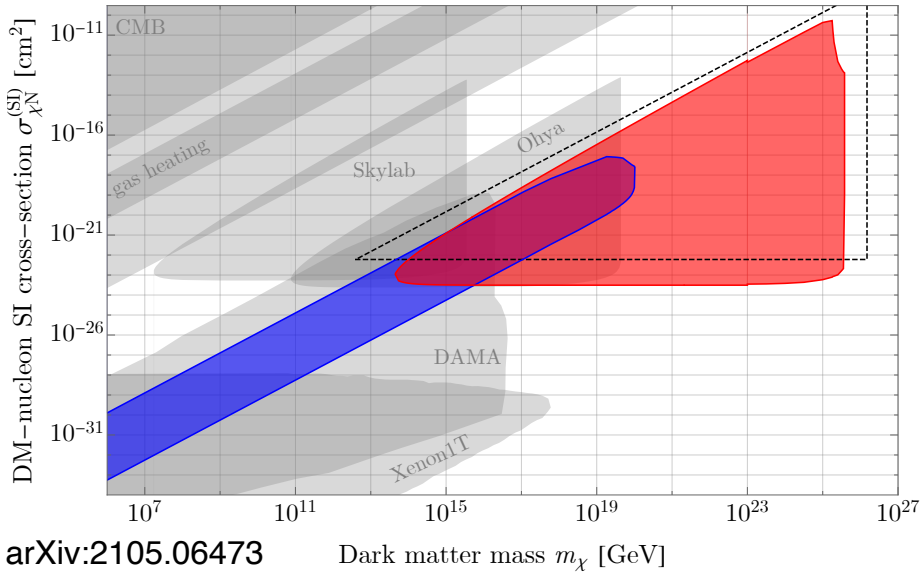
Mineral detectors could probe rare and/or previous events

Large exposure to BSM signals

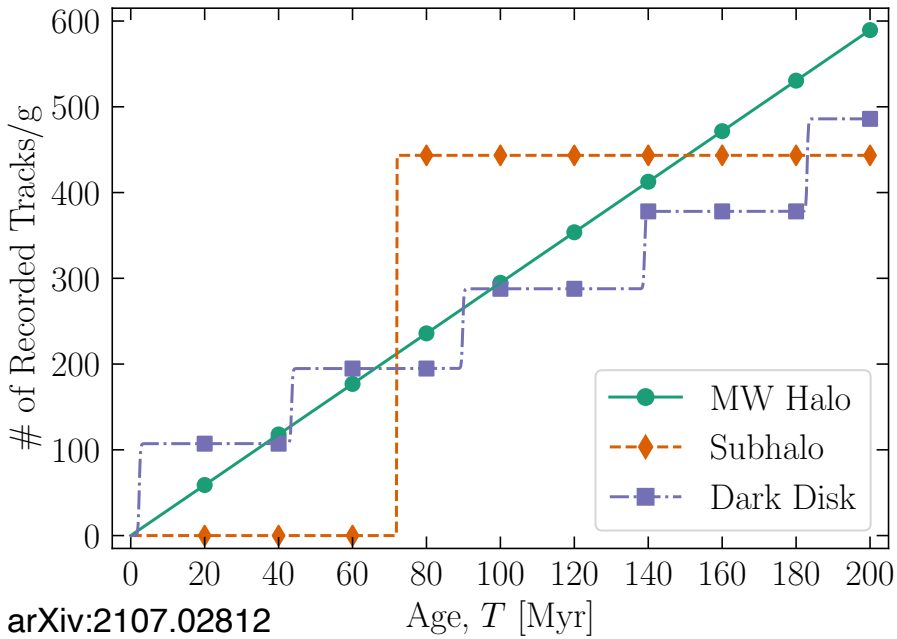
- Complement conventional dark matter direct detection
- Reconstruct dark matter mass and distinguish interactions
- Also heavy (ionizing) exotica
- Proton decay on the moon?

Evolution of neutrino and BSM physics over geological timescales

- Need geological history of rock
- Radiopure samples from depth
- Probe of stellar evolution and DM structure in Milky Way



arXiv:2105.06473

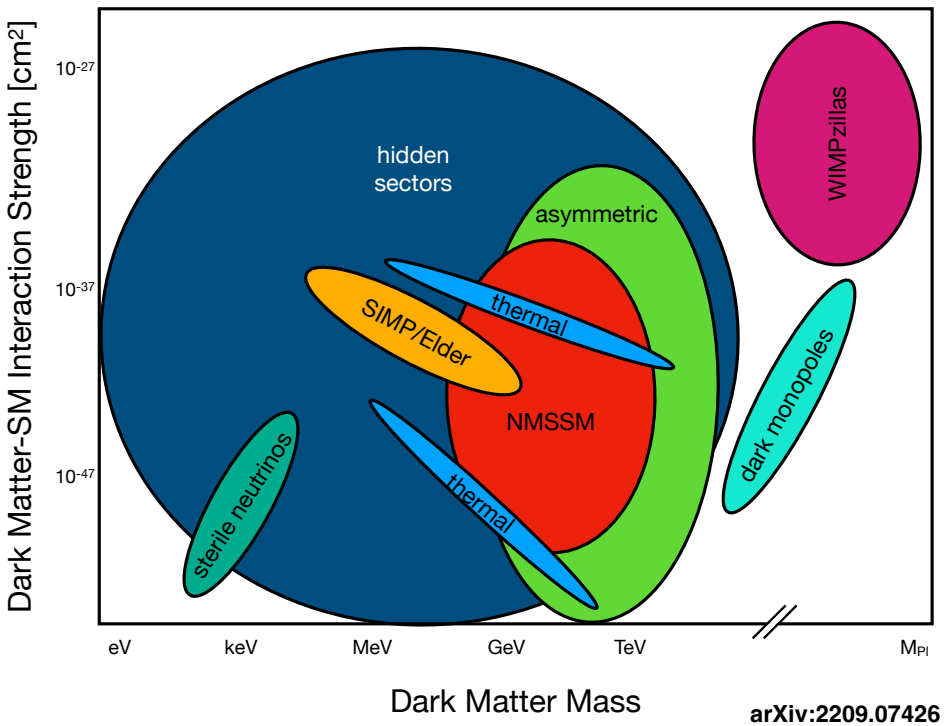


arXiv:2107.02812

What do we (not) know about dark matter?

What we (typically) assume

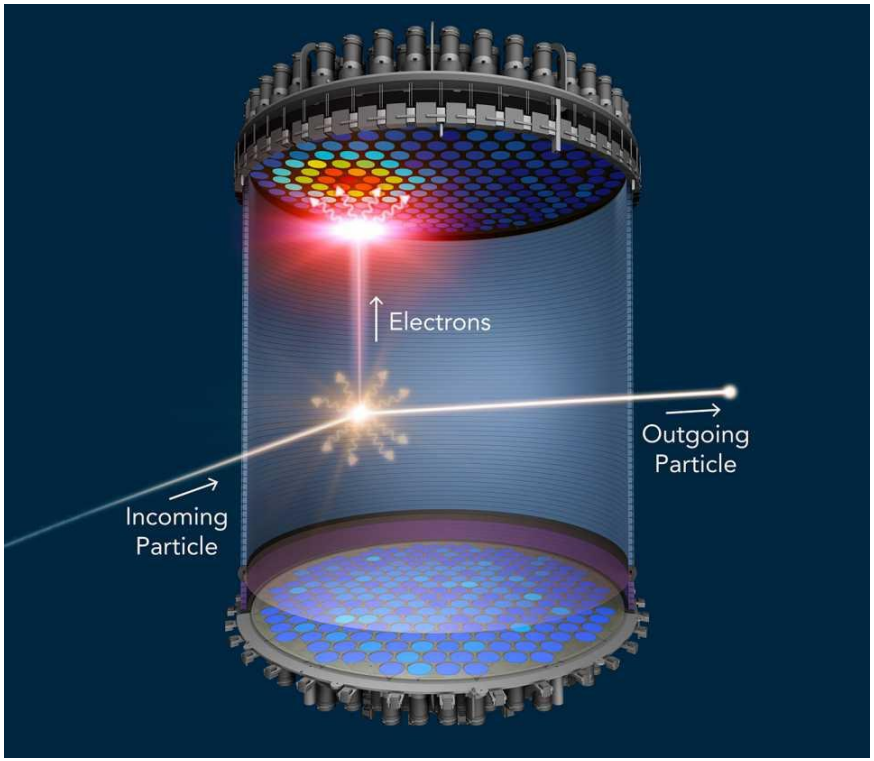
- No E&M interactions
- Must be cold and stable
- Not in the Standard Model

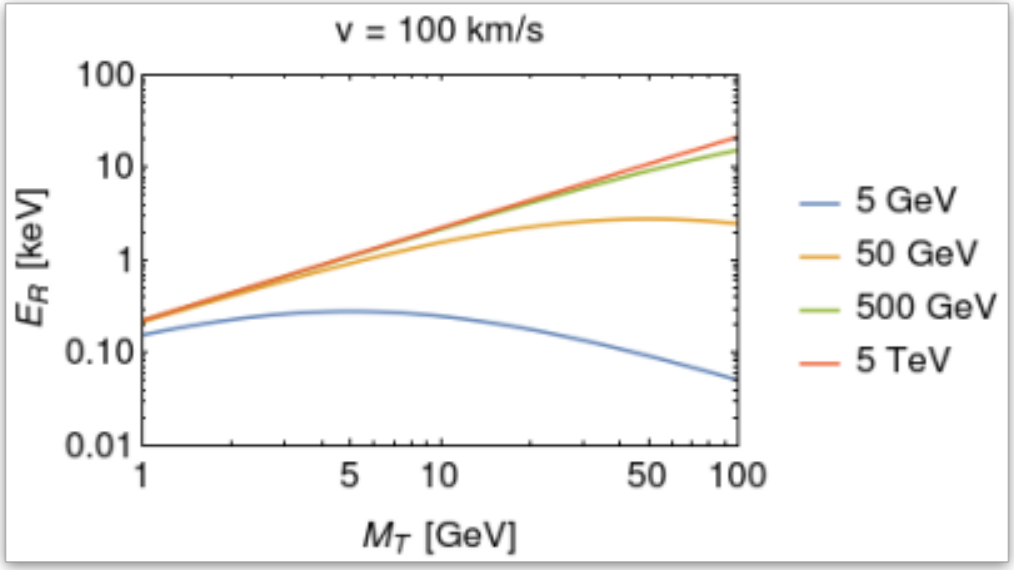


arXiv:2209.07426



Nuclear recoils induced by elastic WIMP-nucleus scattering





Rate per unit time per unit mass

$$\frac{dR}{dE_R} = \frac{n_X}{2} \frac{\sigma^{SI}_{Xp}}{\mu^2_{Xp}} A^2 F(q)^2 \eta(v_q)$$

Scattering kinematics $\Rightarrow$ event rate

- Account for finite size of nucleus
- Convolute with WIMP flux
- Write cross section in terms of WIMP-nucleon interaction

Rotation curves of spiral galaxies and the Bullet Cluster

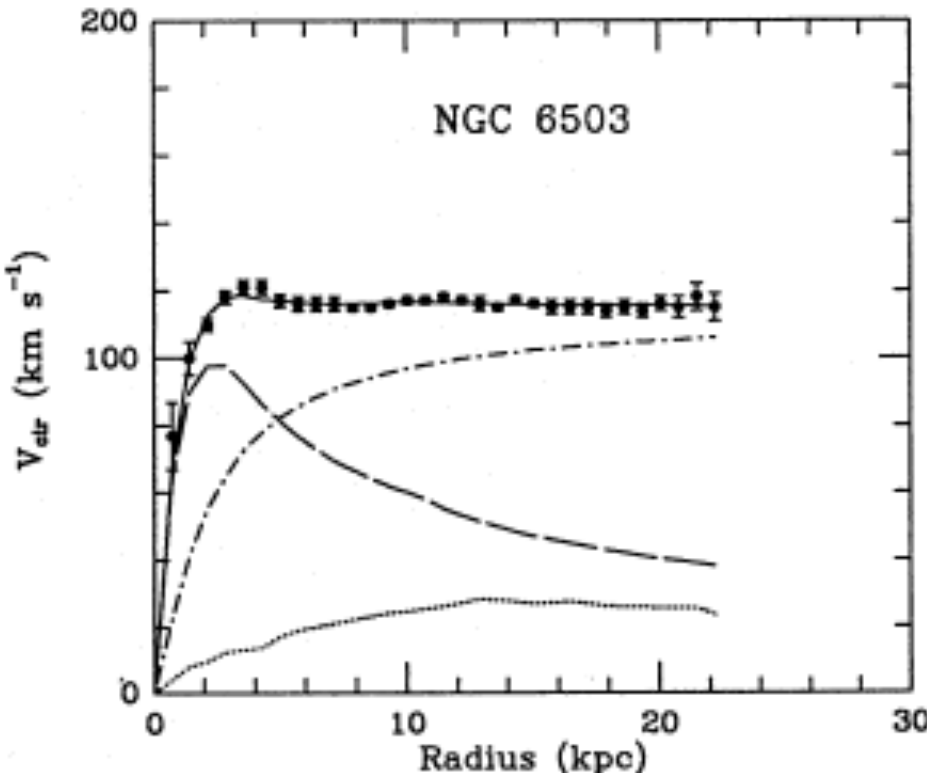


Figure: Begeman et al. (1991)

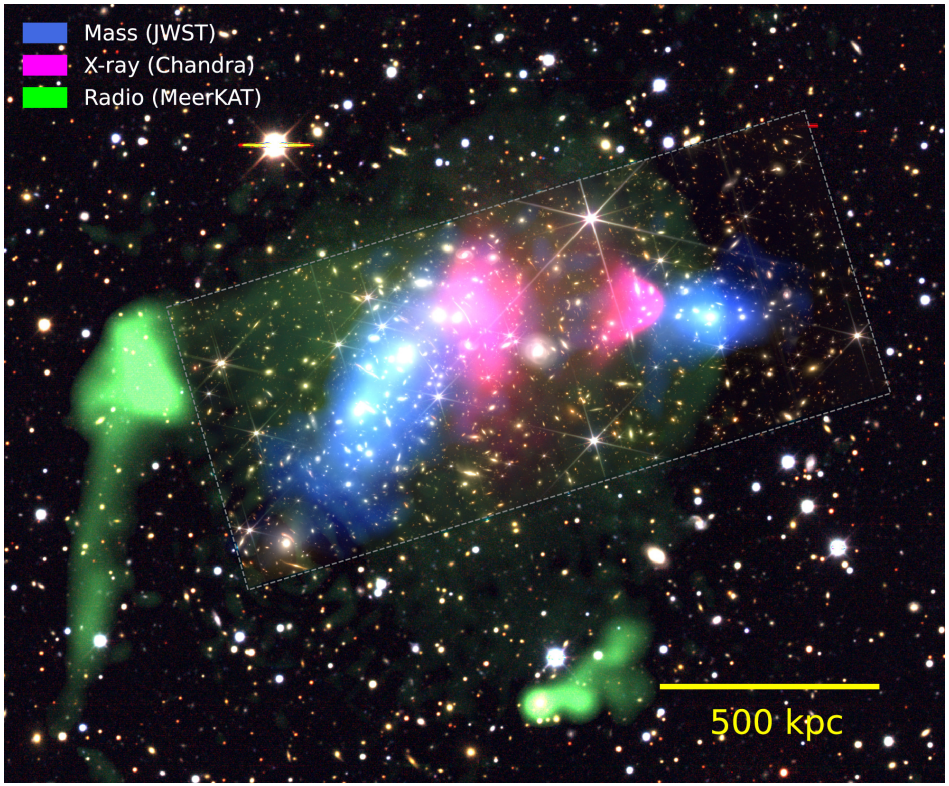


Figure: Cha et al. (2025)

Dark matter density in the galaxy

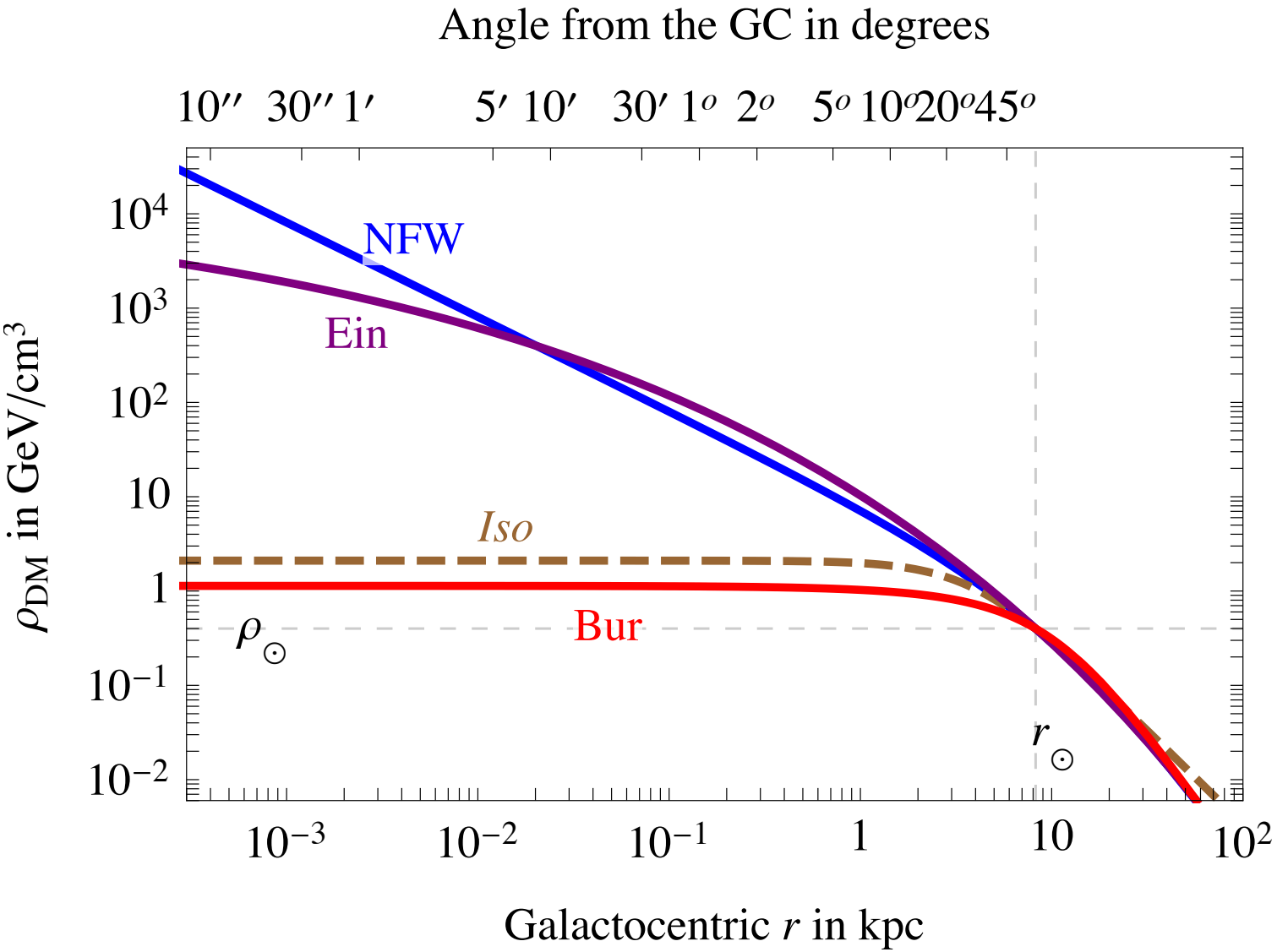
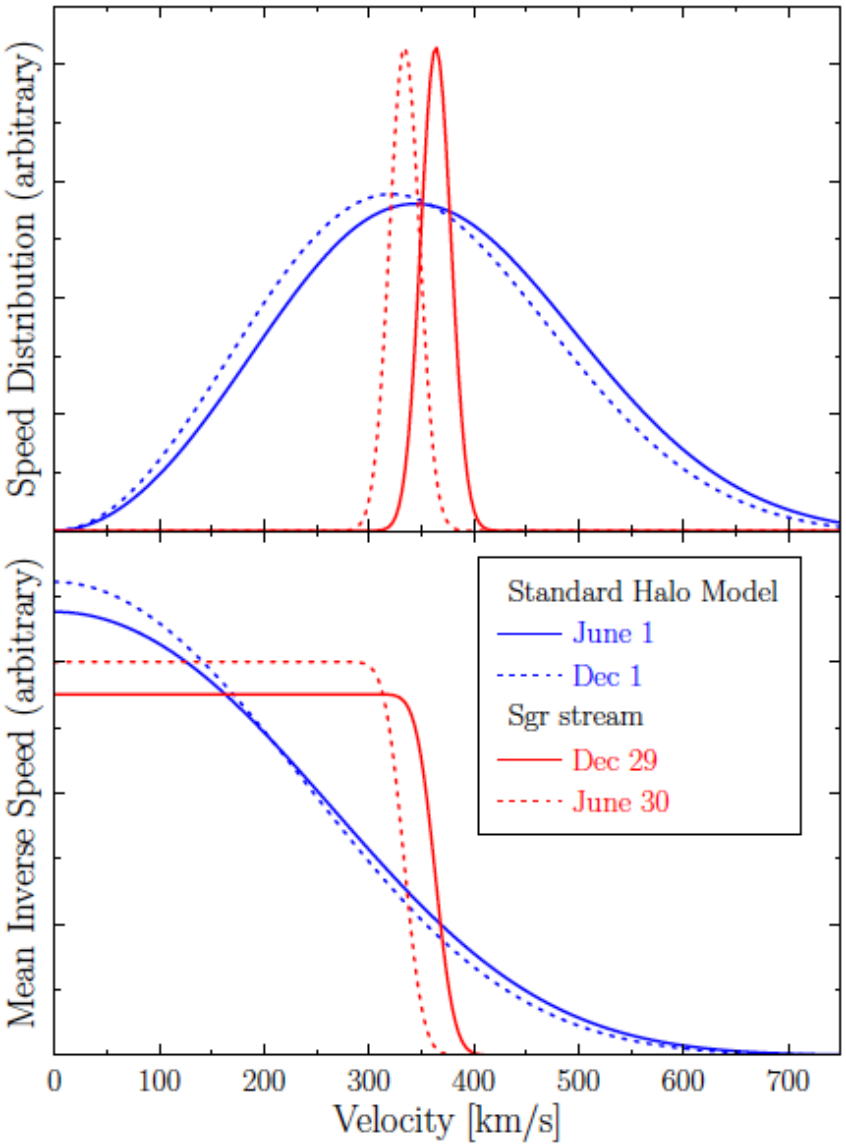


Figure: 2406.01705

WIMP velocity distribution and induced recoil spectra



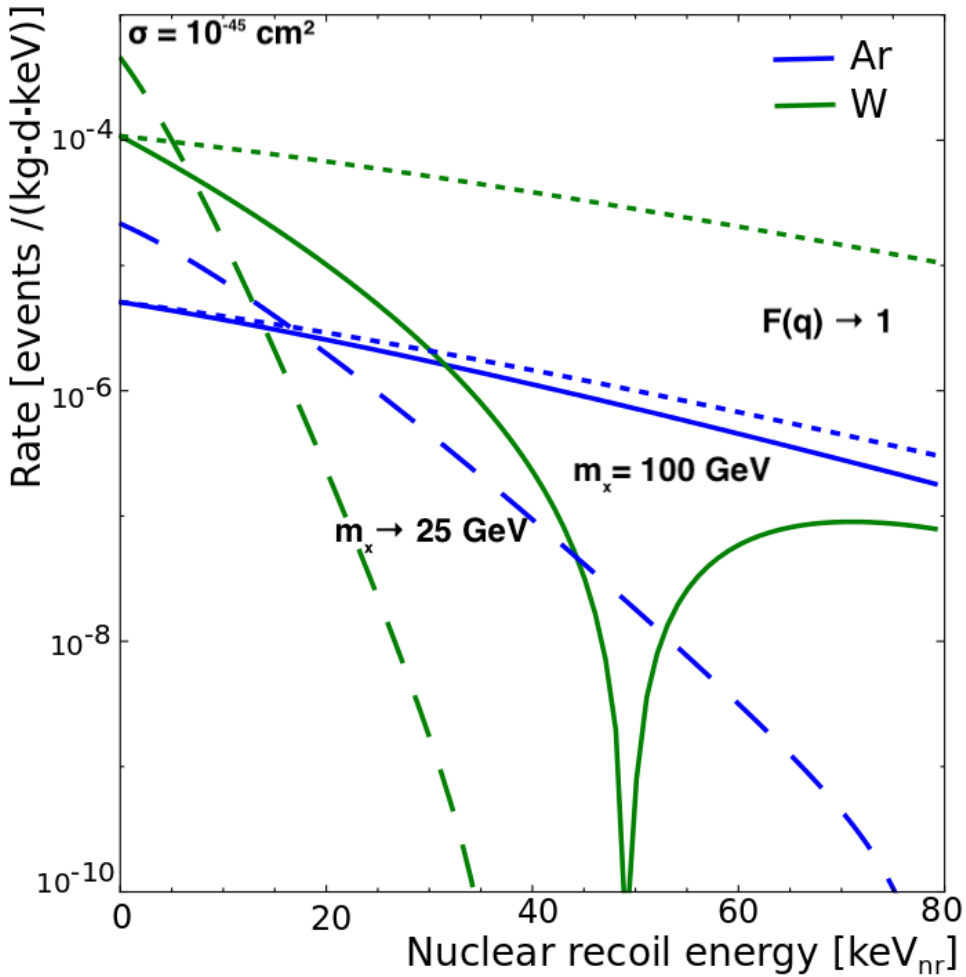
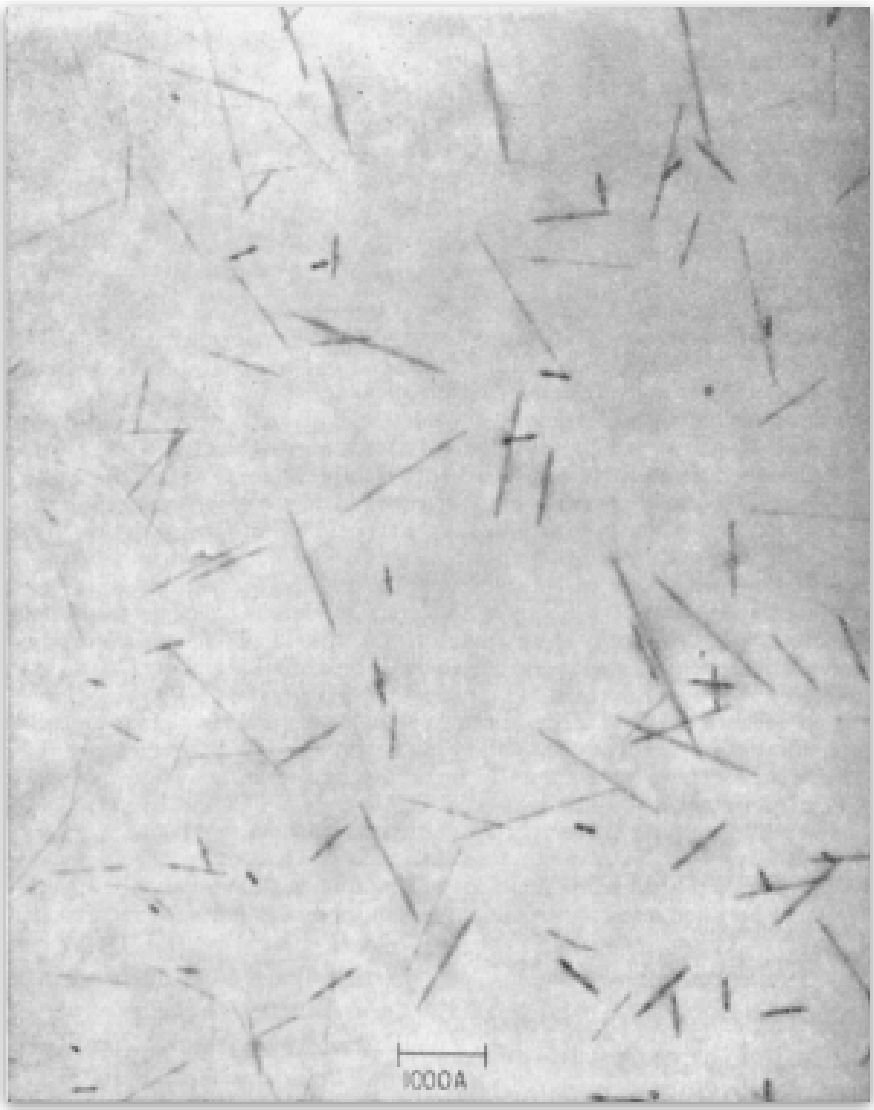


Figure: (left) 1209.3339 (right) 1509.08767

Fission fragments can be seen by TEM/optical microscopes



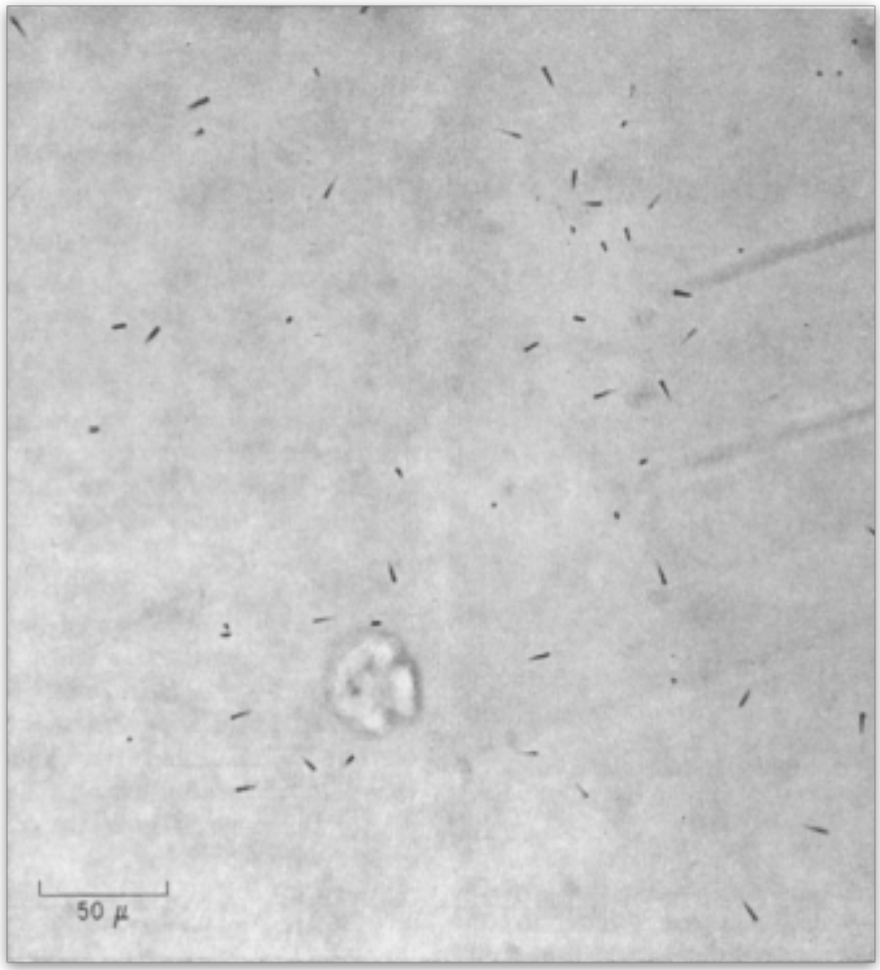
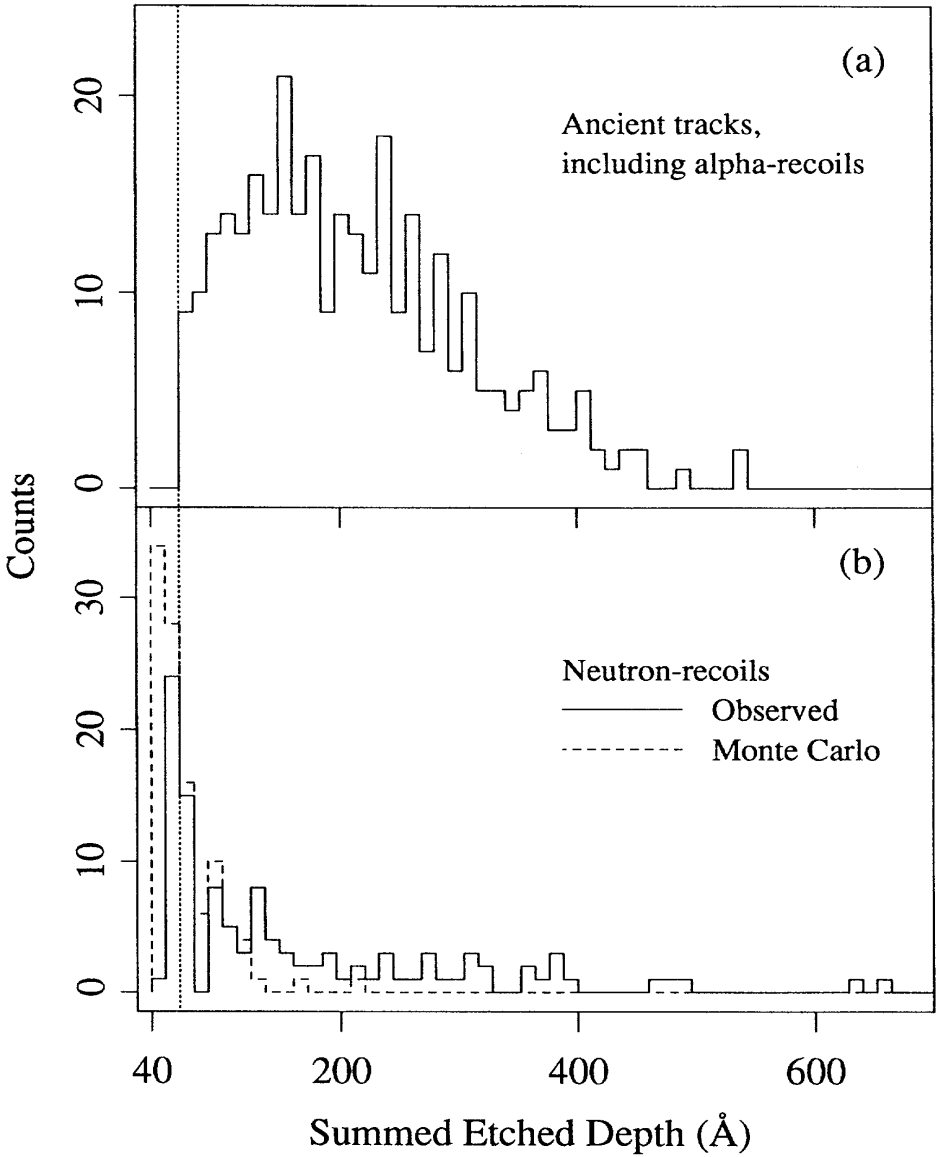


Figure: Price+Walker '63

Mineral detectors used to constrain WIMPs before



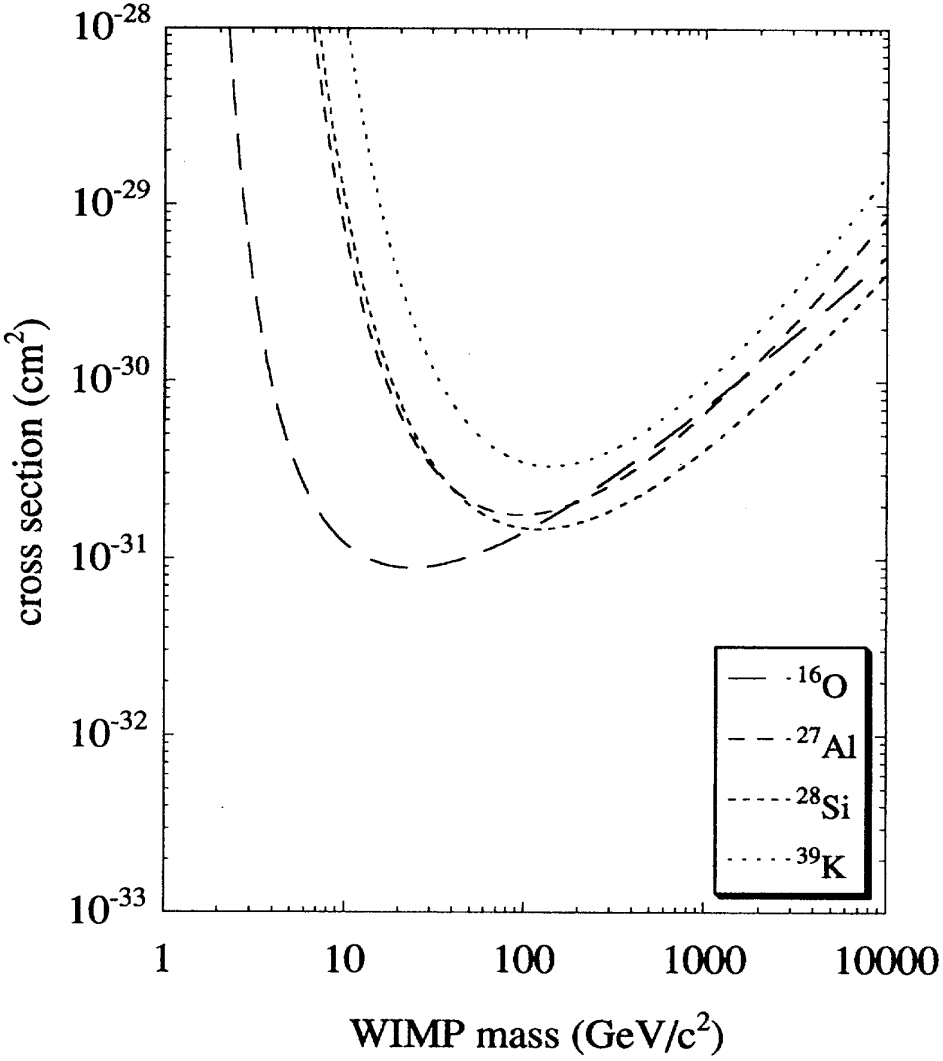
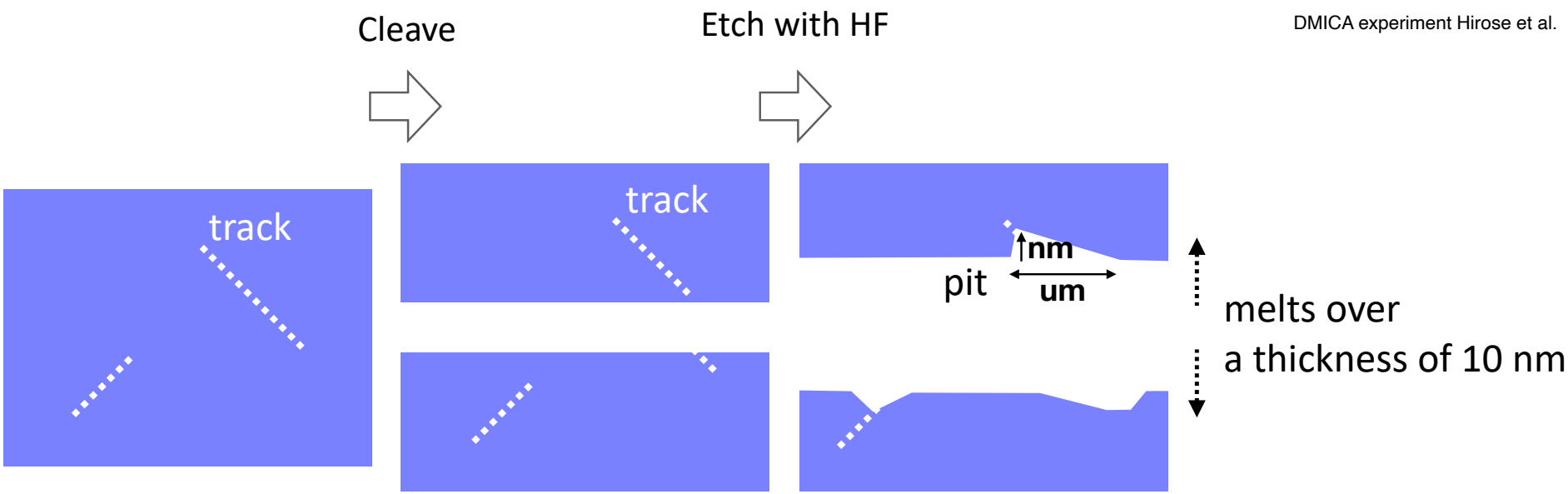
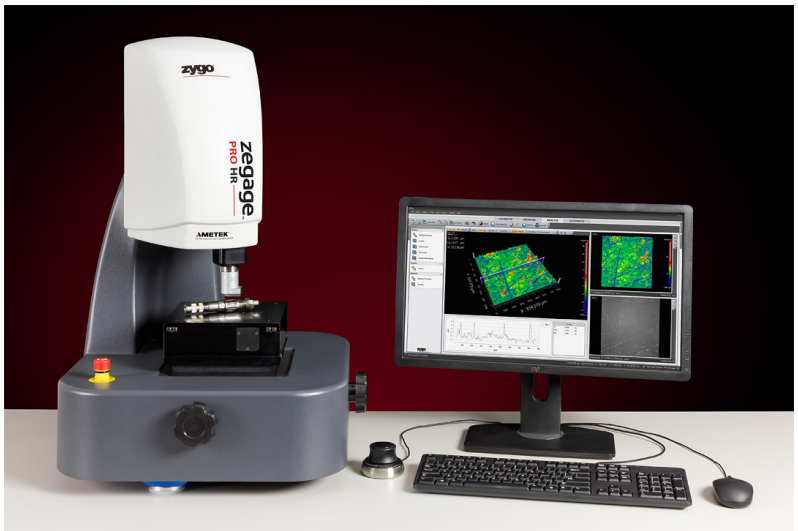
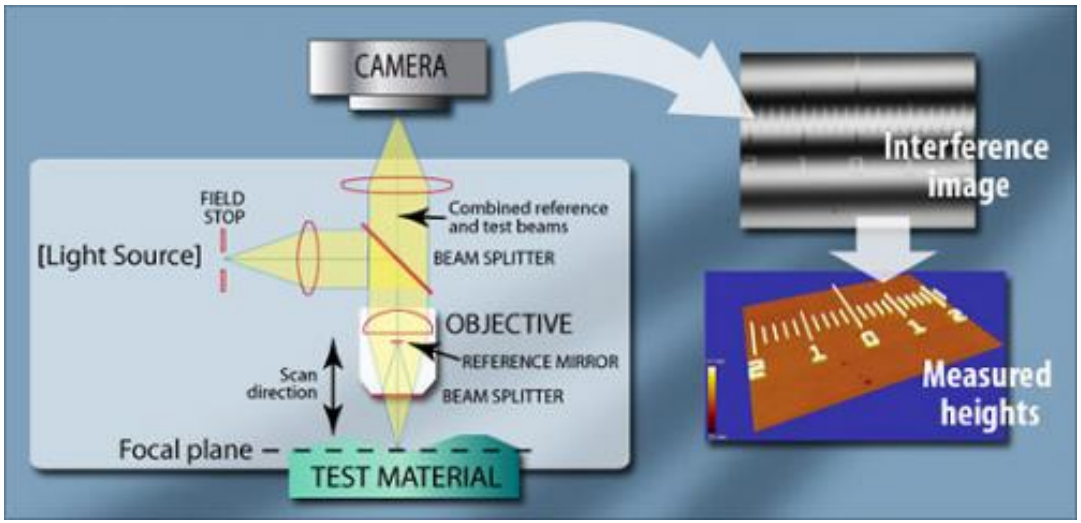


Figure: Snowden-Ifft et al. (1995)

New techniques allow for much larger readout capacity

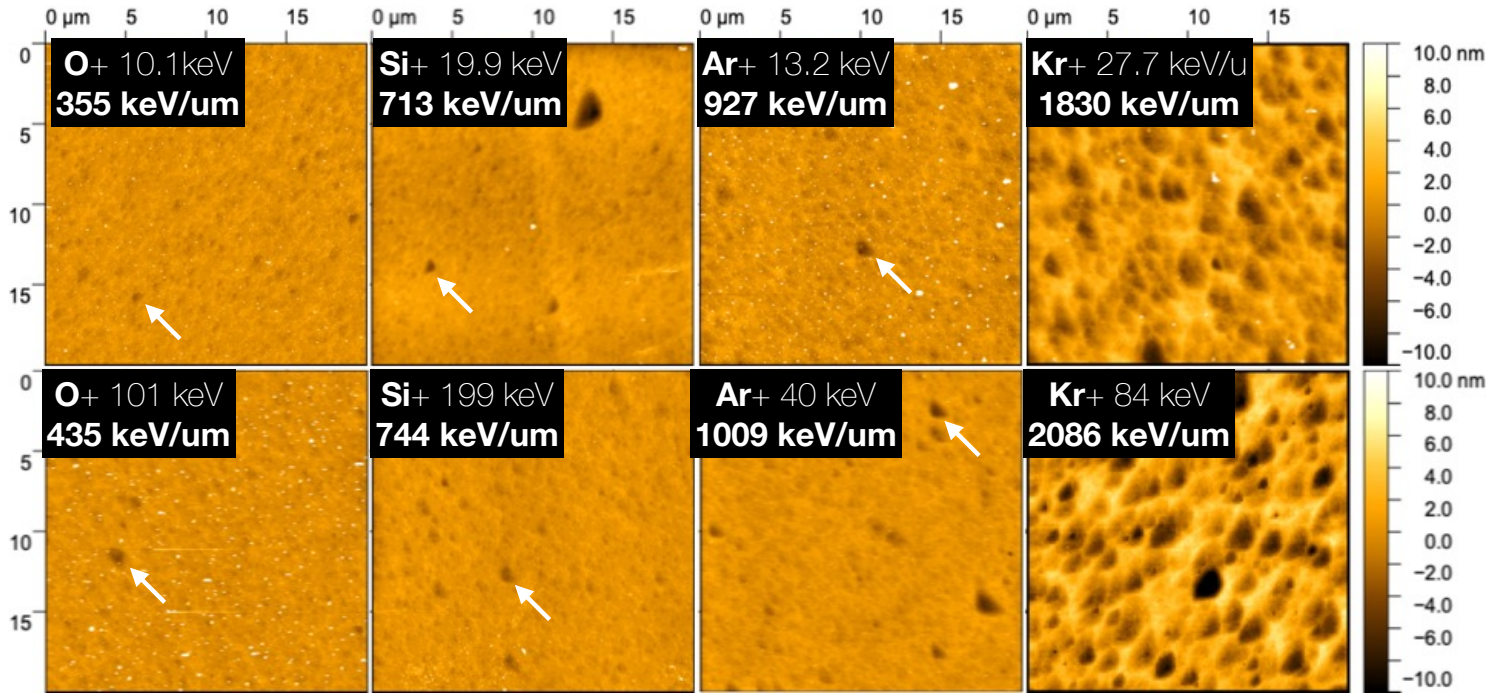






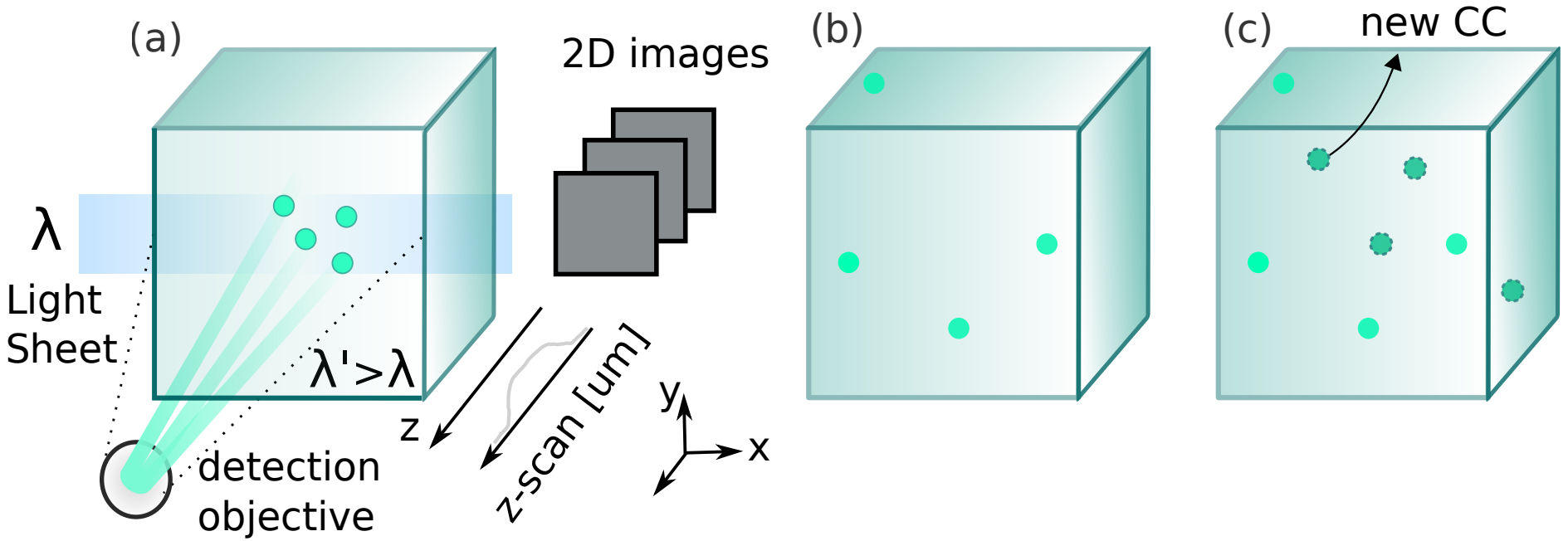
Increase throughput from AFM to optical profilometry

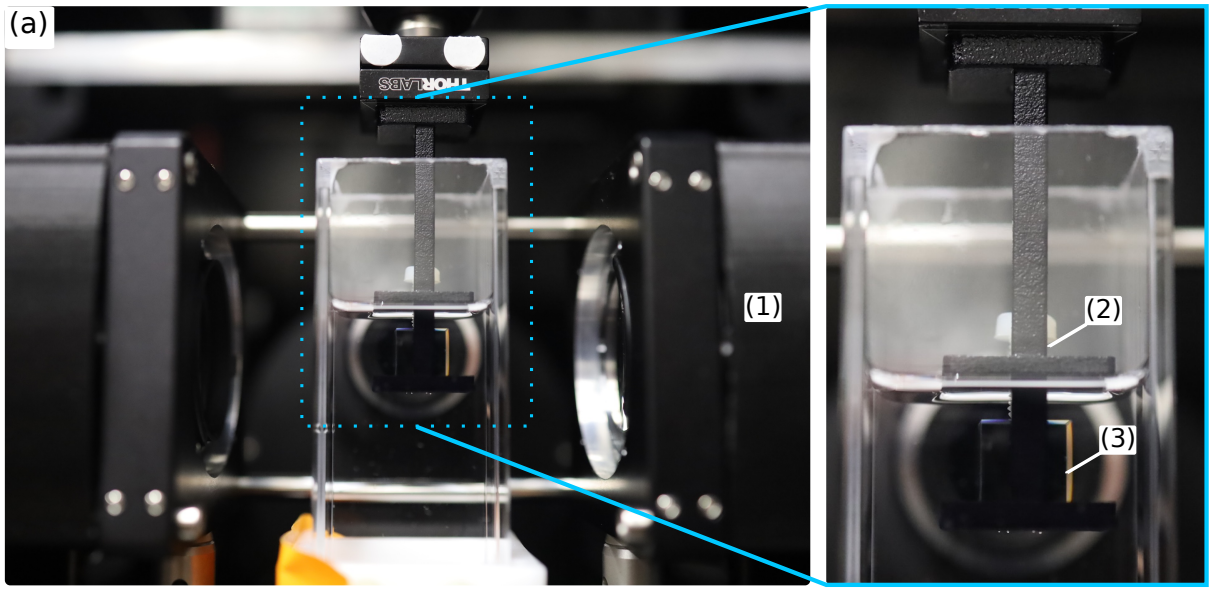
Irradiation dose is 80 ions per field of view (20umx20um).

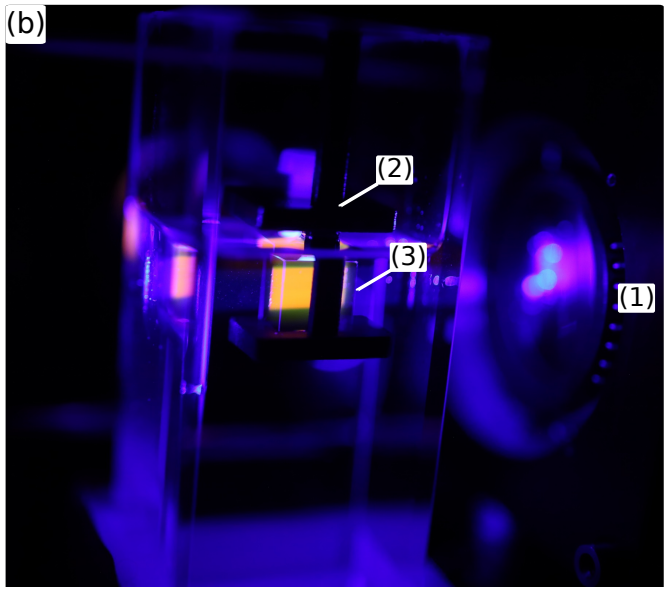


proxy	DM scattering	alpha recoils
pit formation efficiency	several to 10 %	~ 100%

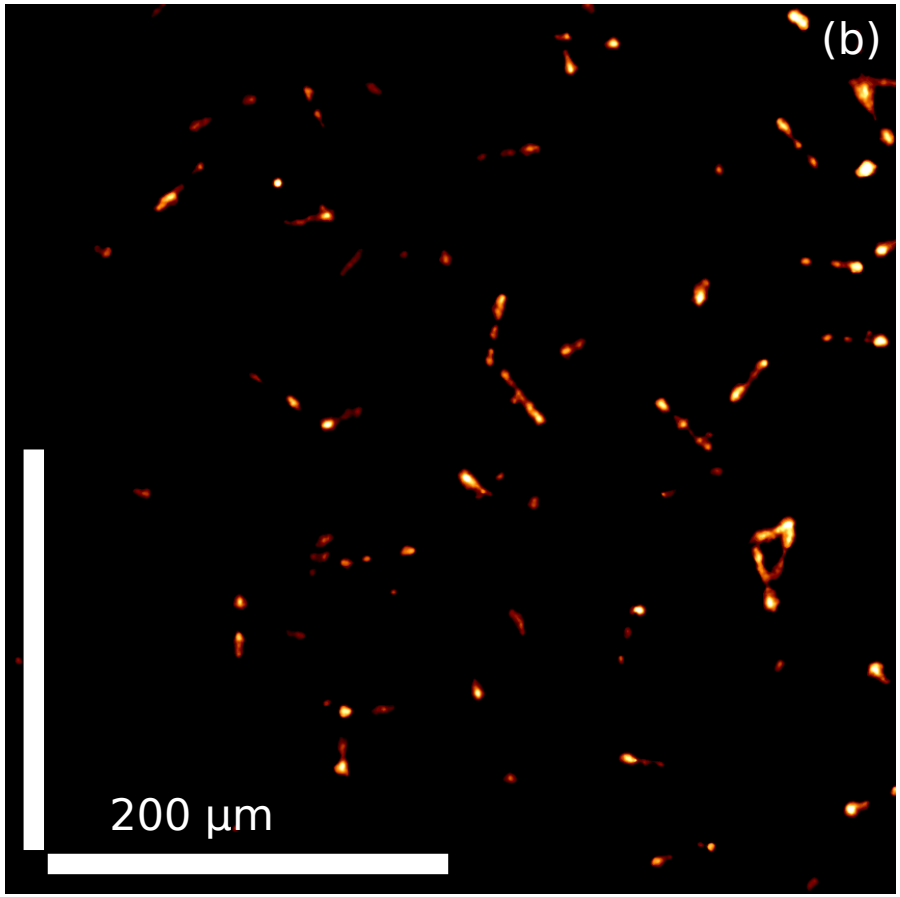
Selective plane illumination microscopy for color centers

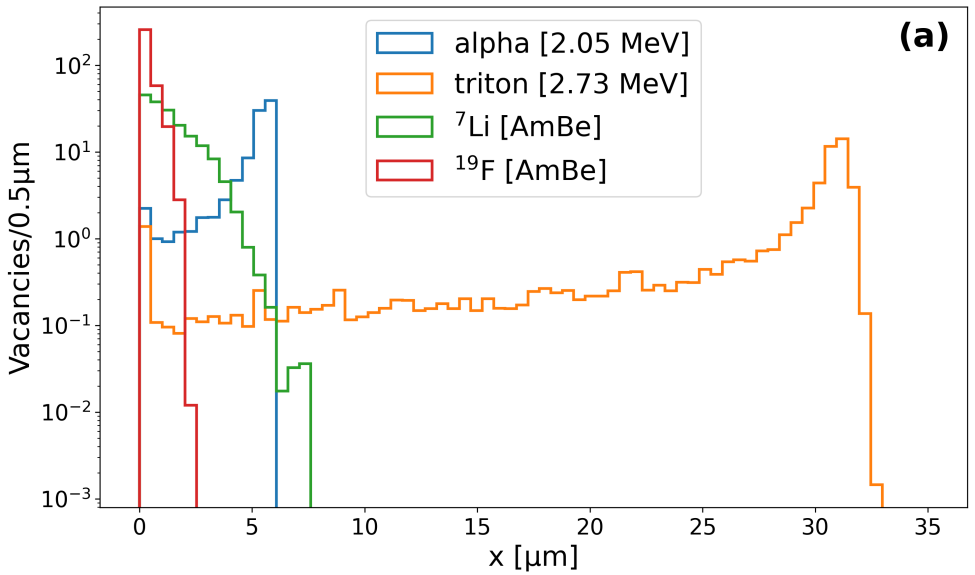


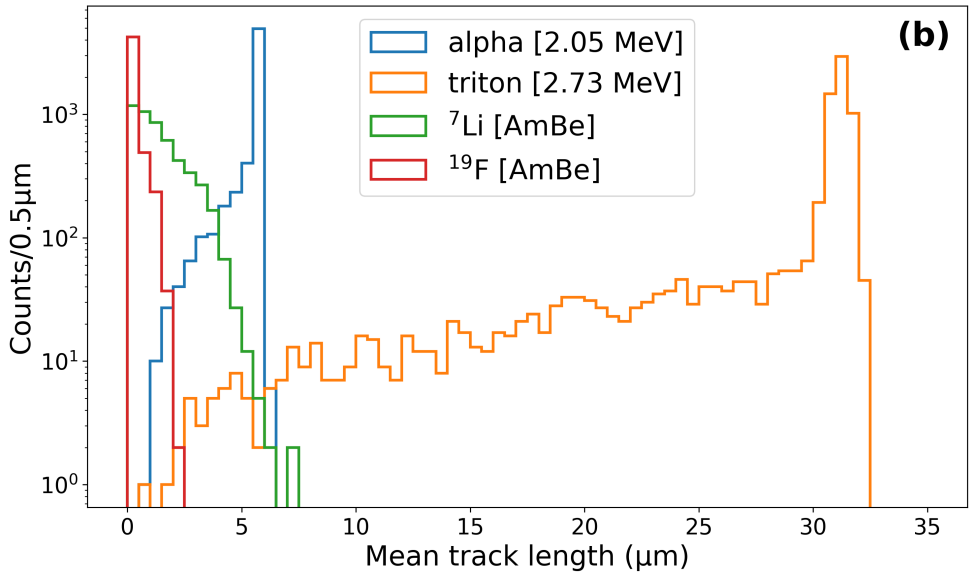




Compare SPIM data to TRIM simulations of nuclear recoils





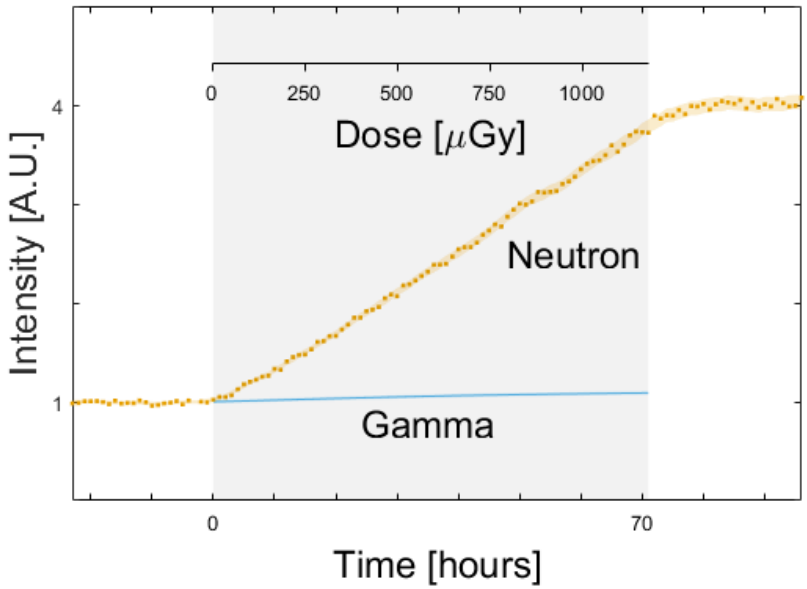


- 3D imaging of CCs in bulk
- Low ionizing CC tracks
- Could scan $\sim$cm^3 in hours

Crystal detectors alternative to conventional experiments

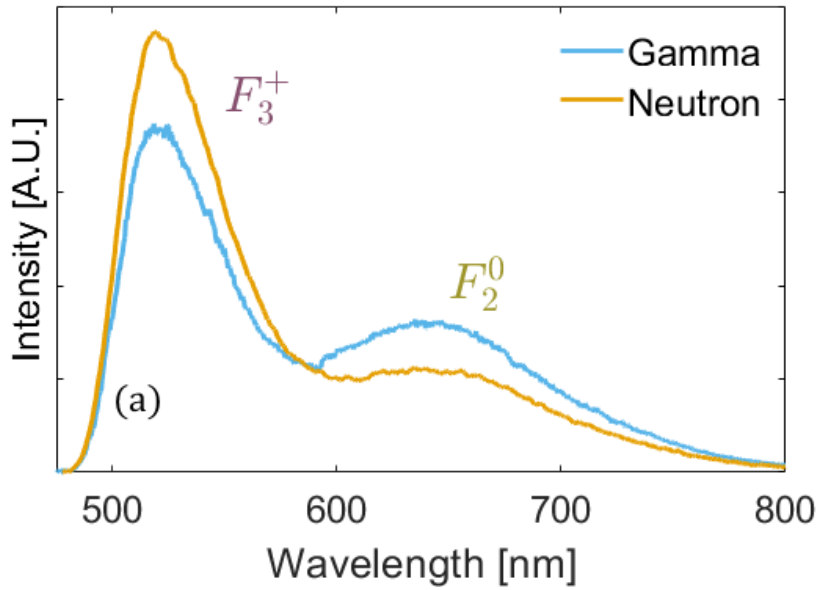
Irradiation of LiF samples

- Gammas from ^{60}Co for response to ionizing radiation
- Fast neutrons from AmBe for background calibration
- Thermal neutrons moderated by high-density polyethylene

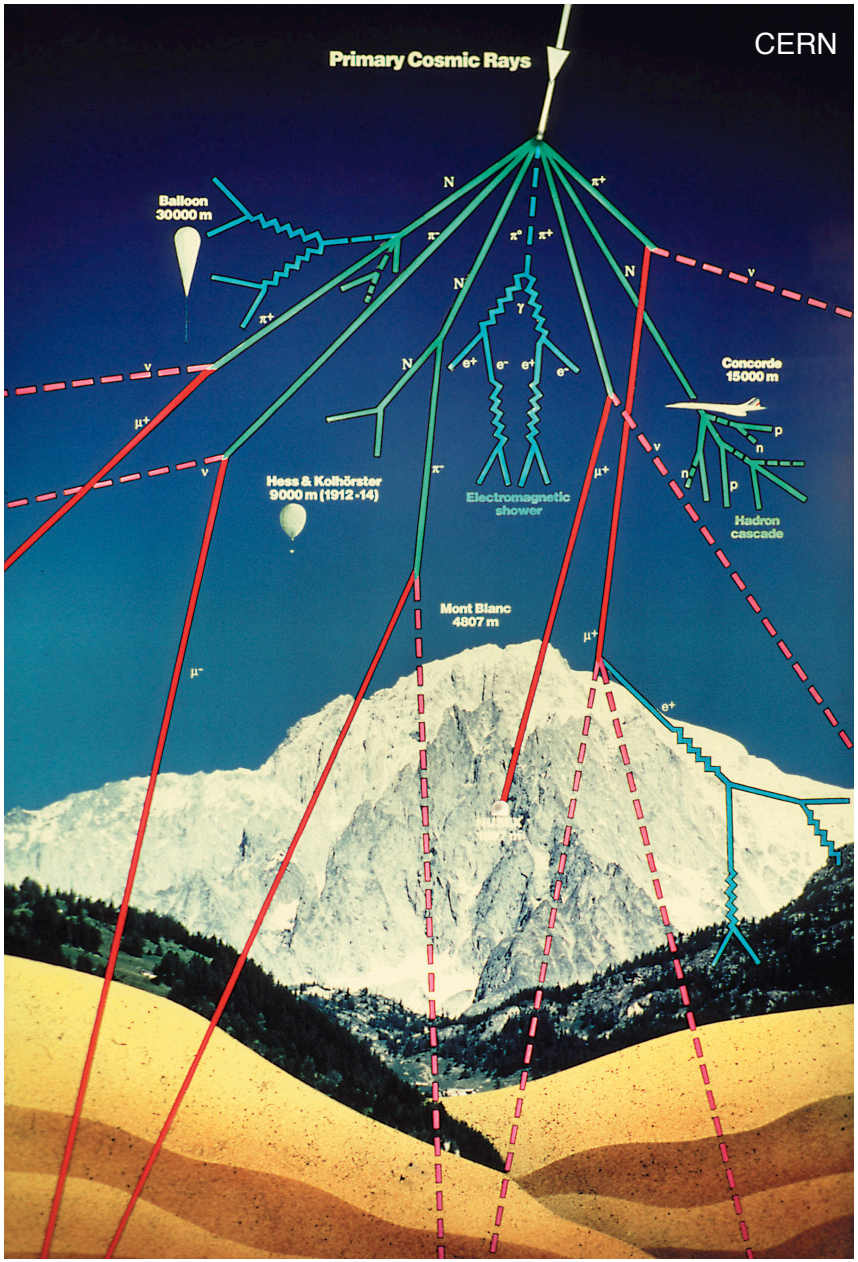


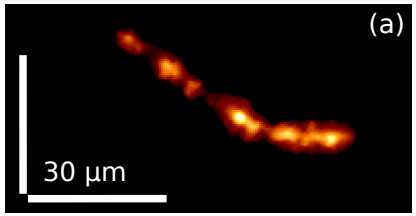
Imaging color centers in cm^3 samples

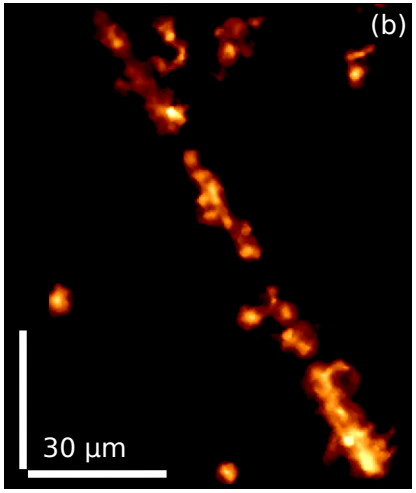
- Bulk florescence measurements at VT showed LiF ~50x more responsive to fast neutrons
- Localize color centers to $\sim \mu\mathrm{m}^3$ voxels using SPIM at UZH

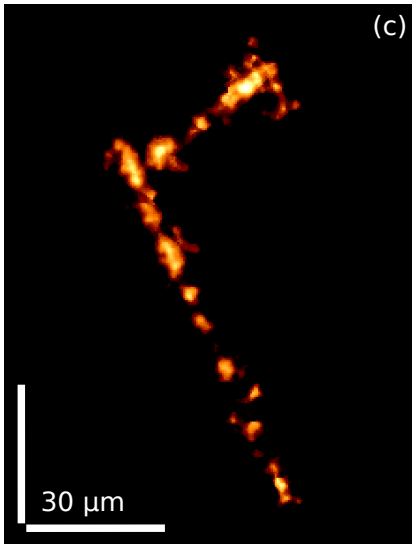


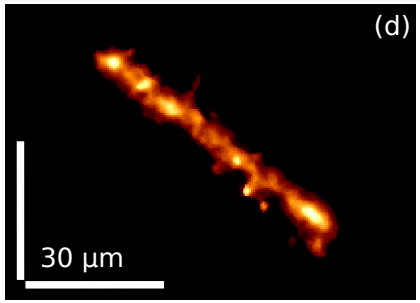
Spallation from cosmic ray muons interacting in samples

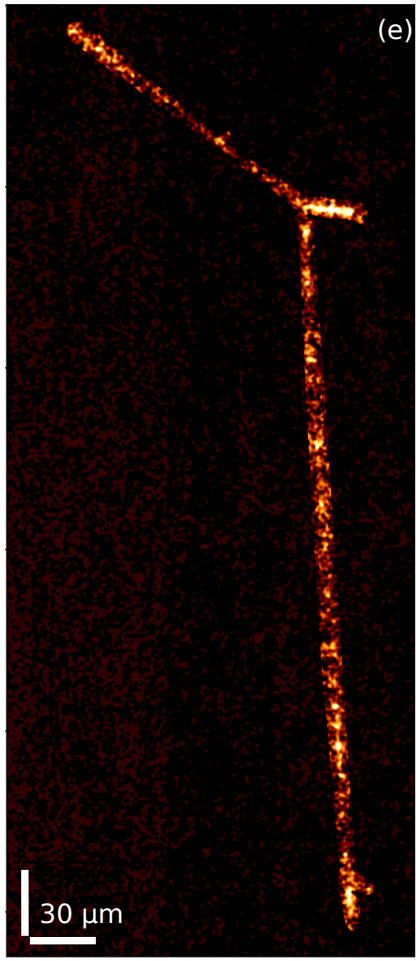




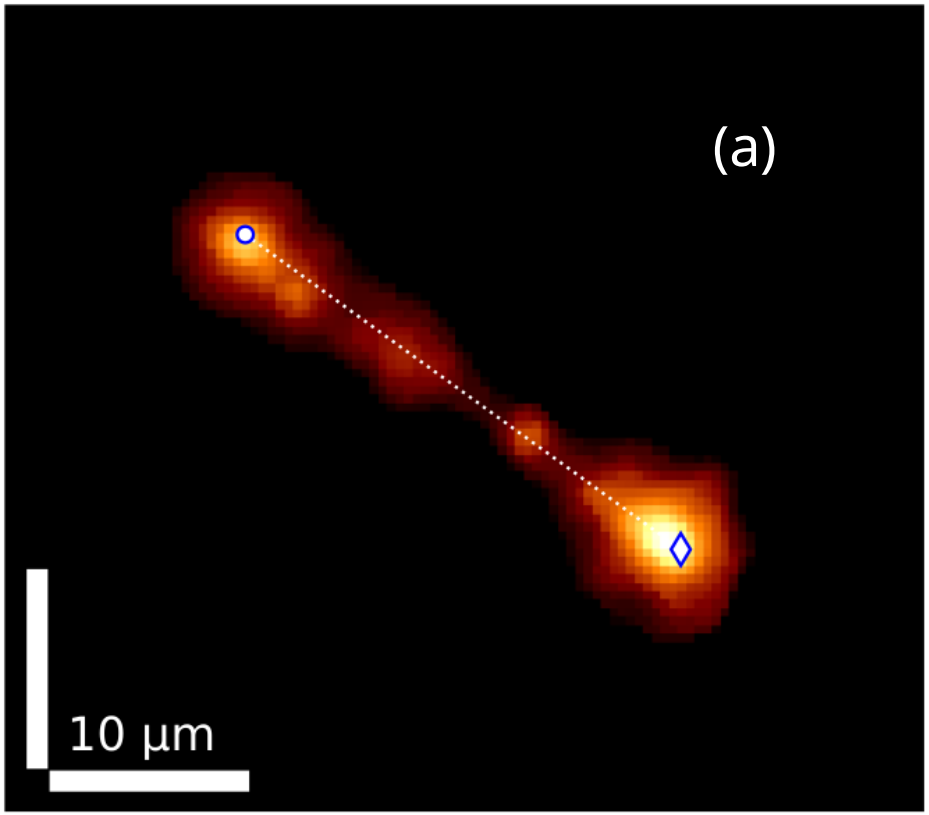


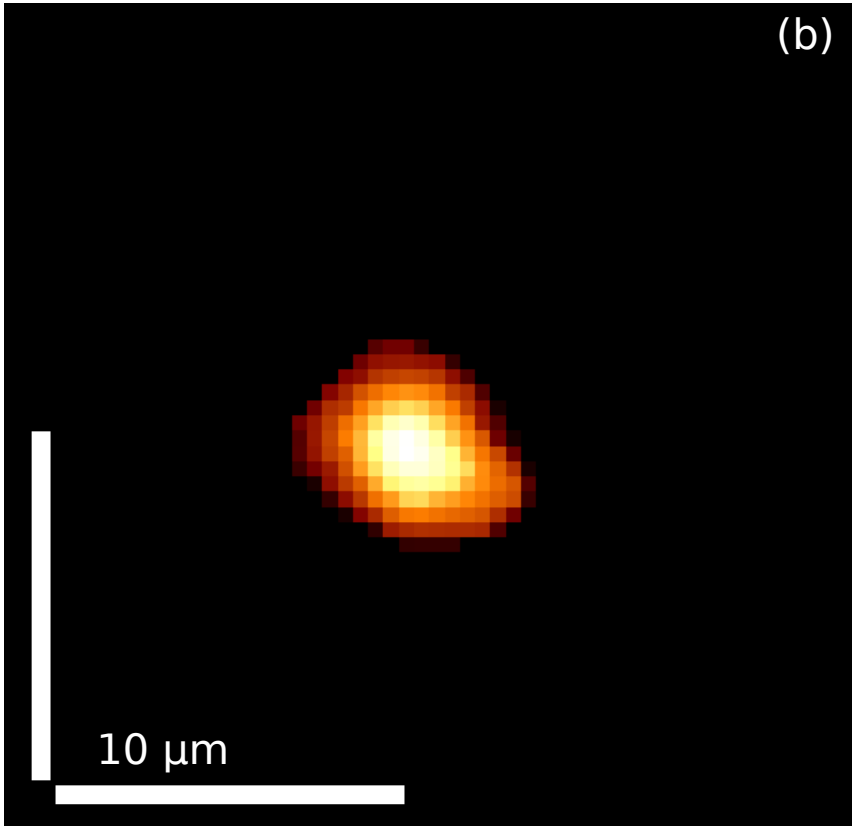






Color center tracks from irradiation of LiF with neutrons





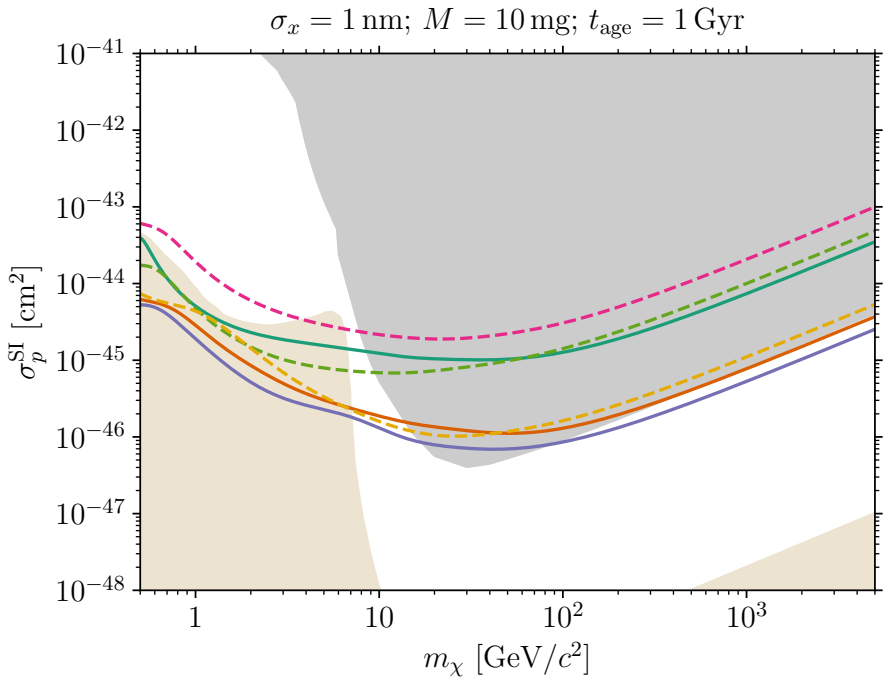
$^6\mathrm{Li} + n \rightarrow \alpha(2.1\mathrm{MeV}) + \mathrm{T}(2.7\mathrm{MeV})$

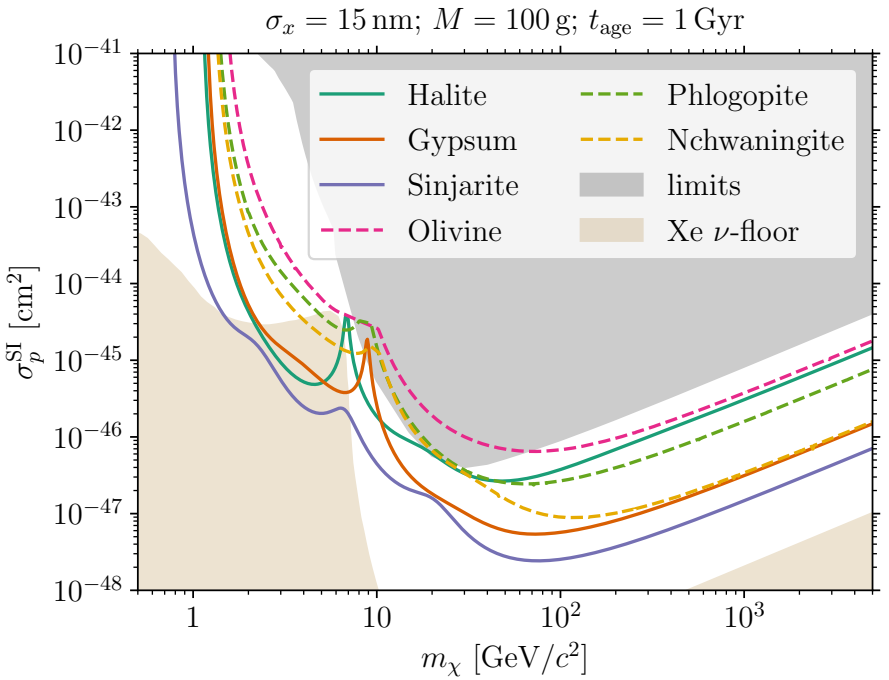
- Predict track length $30 - 35\mu$m
- Sparse CCs along track $\sim 4\mu\mathrm{m}^{-1}$
- Bragg peaks brighter at the ends

Elastic scattering of *n* off (Li,F)

- Calibrate LiF response with fast neutrons from AmBe
- Detect cosmogenic neutrons

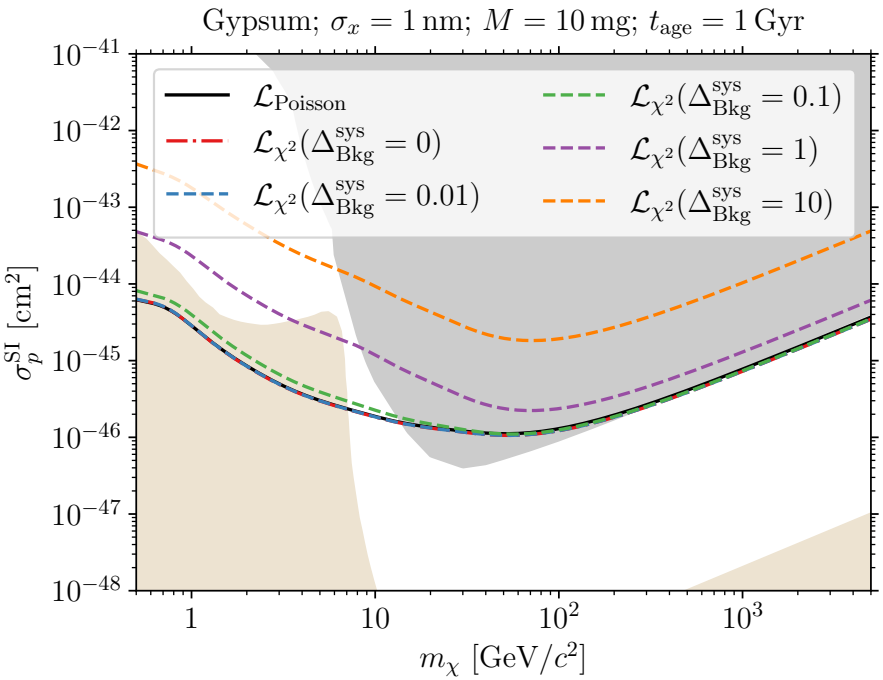
Sensitivity for different targets

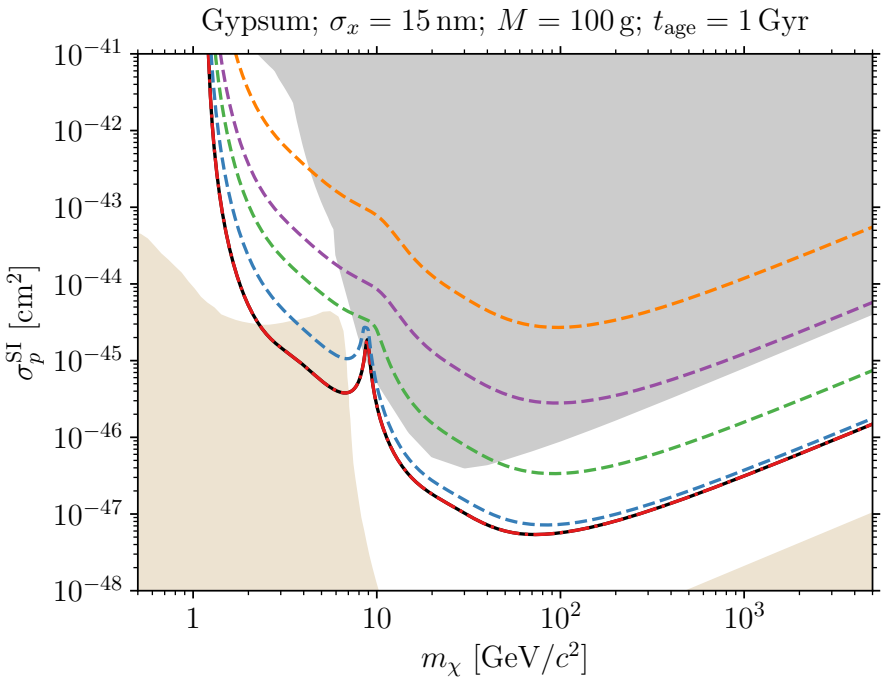




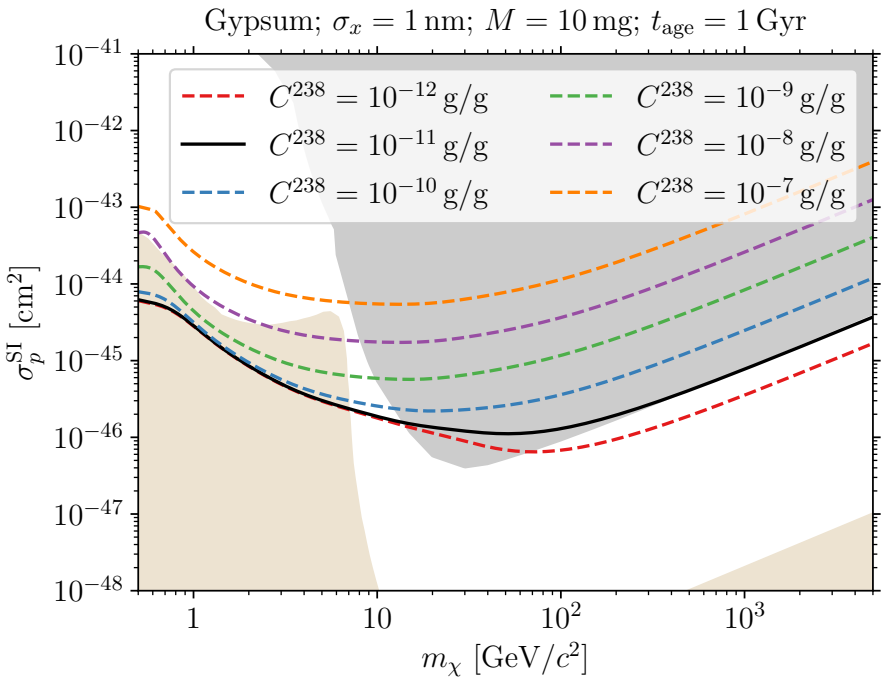
Halite	NaCl	$C^{238} = 10^{-11}$ g/g
Gypsum	$Ca(SO_4)\cdot 2(H_2O)$	$C^{238} = 10^{-11}$ g/g
Sinjarite	$CaCl_2\cdot 2(H_2O)$	$C^{238} = 10^{-11}$ g/g
Olivine	$Mg_{1.6}Fe^{2+}_{0.4}(SiO_4)$	$C^{238} = 10^{-10}$ g/g
Phlogopite	$KMg_3AlSi_3O_{10}F(OH)$	$C^{238} = 10^{-10}$ g/g
Nchwaningite	$Mn^{2+}_2SiO_3(OH)_2\cdot(H_2O)$	$C^{238} = 10^{-10}$ g/g

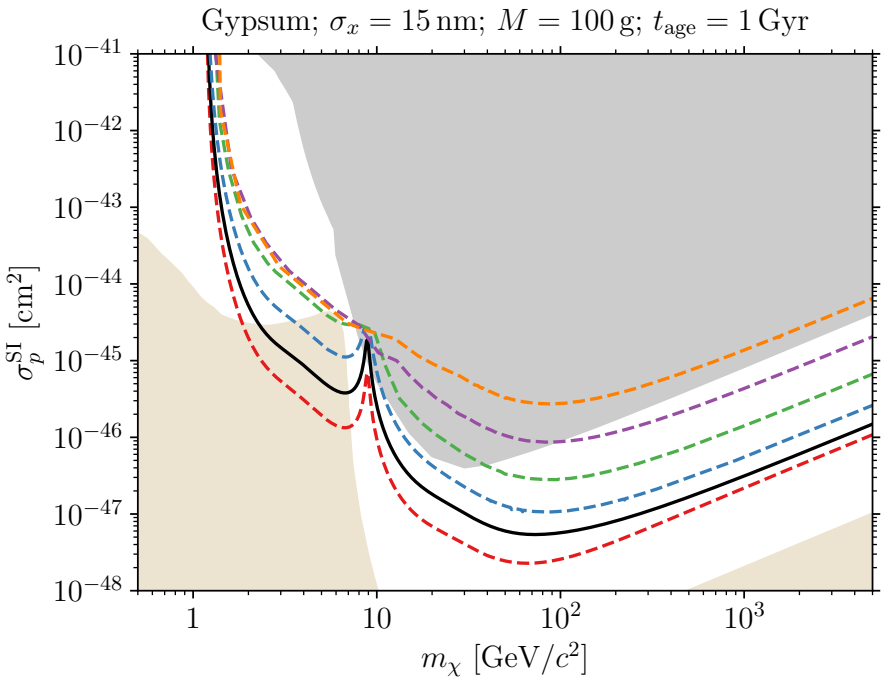
Effects of background shape systematics



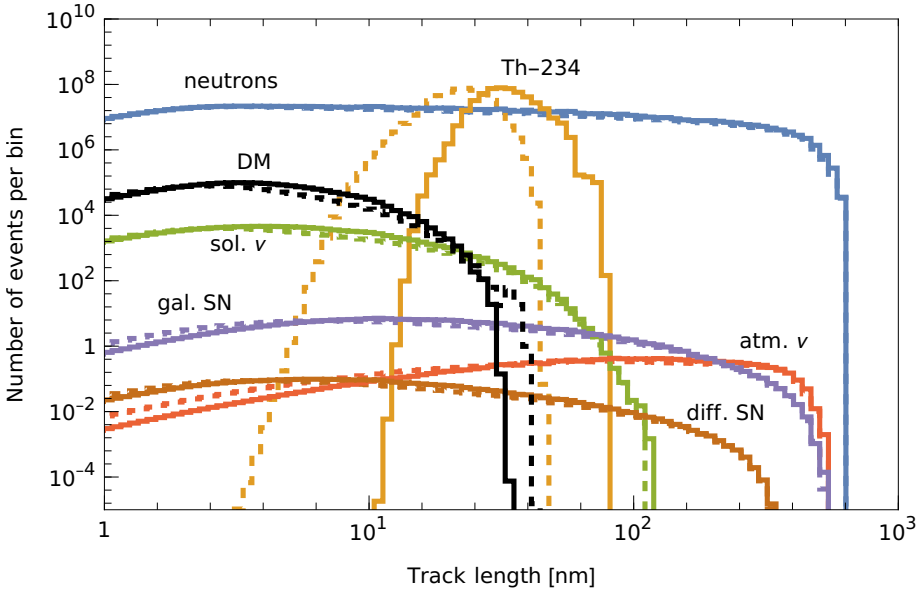


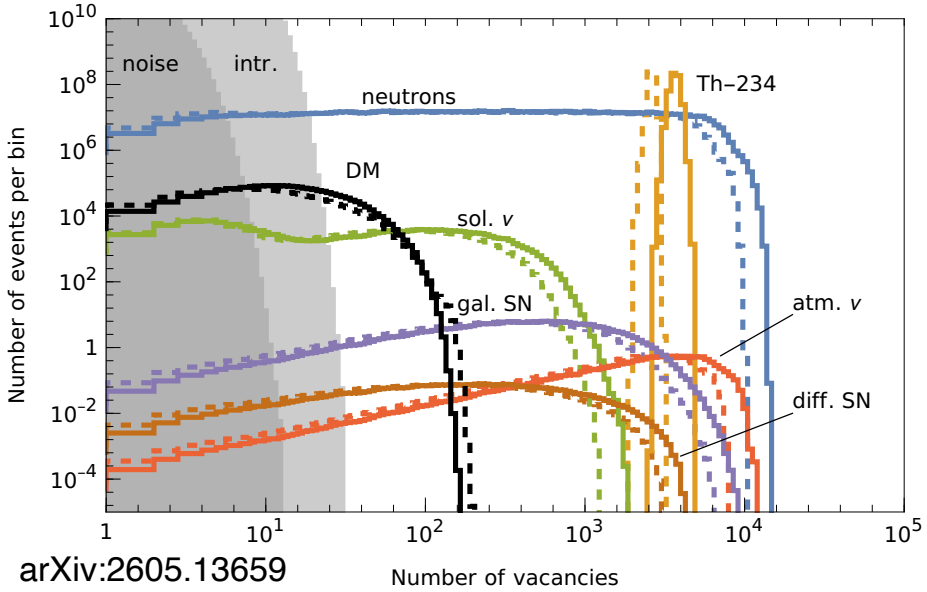
Sensitivity for different ^{238}U concentrations





Improved simulations of recoil tracks and vacancies





arXiv:2605.13659

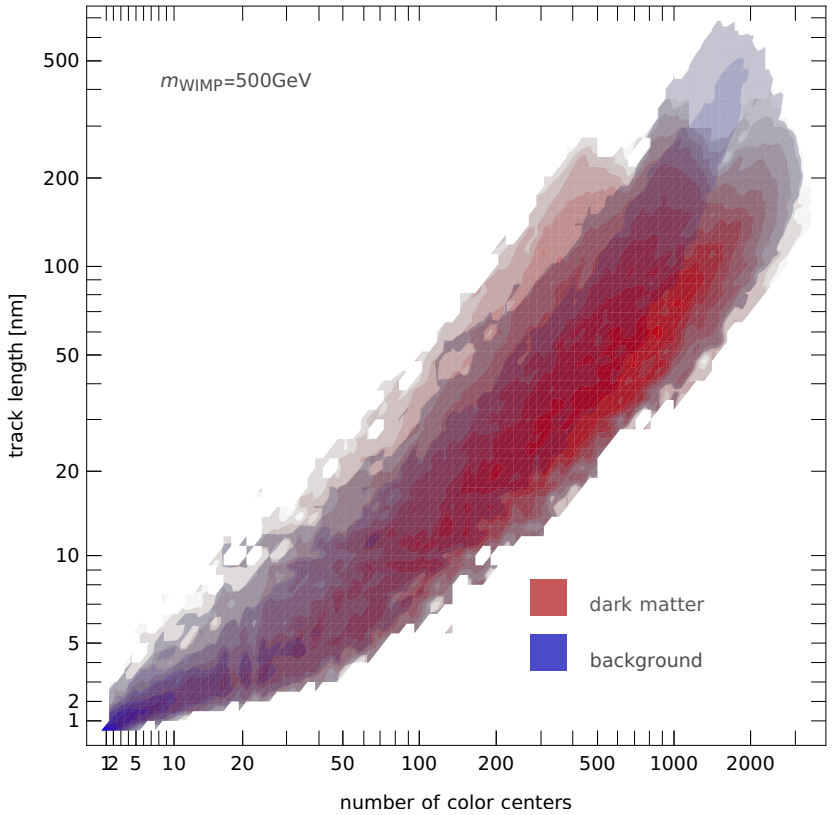
Binary collision approximation of recoils in $100\,\mathrm{g} \times 1\,\mathrm{Gyr}$ Olivine

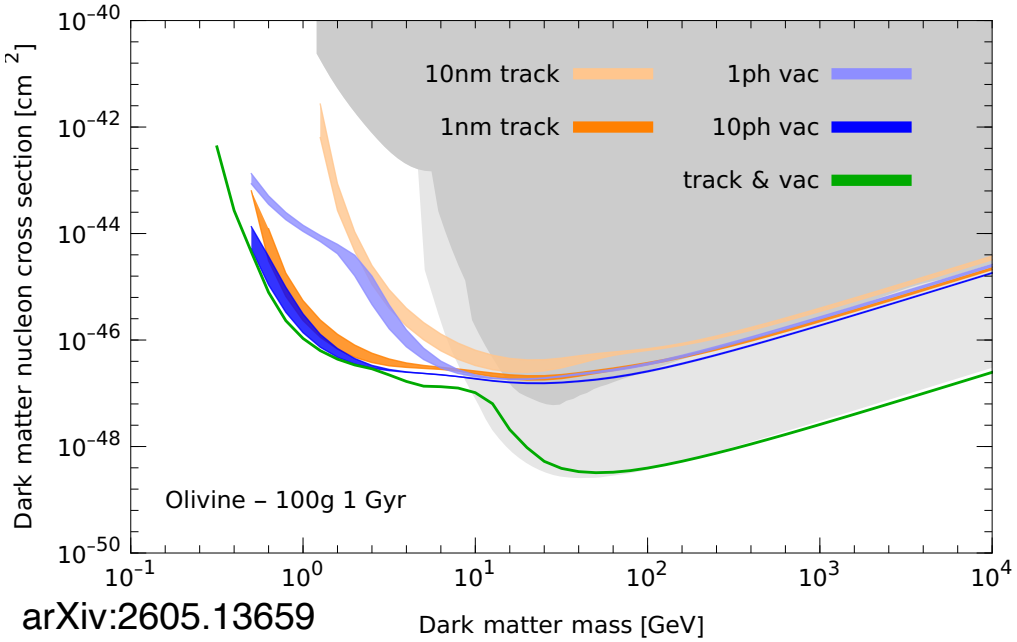
- Deterministic electronic stopping between scatters
- Pairwise stochastic nuclear stopping in amorphous material

Pick out peaking signal spectra for 5 GeV WIMP with $\sigma_{\chi p} = 10^{-45}\mathrm{cm}^2$

- Flat radiogenic backgrounds dominant for $C^{238} = 0.1\,\mathrm{ppb}$
- Peaking CEνNS backgrounds from astrophysical neutrinos

Combined read-out of recoil tracks and vacancies

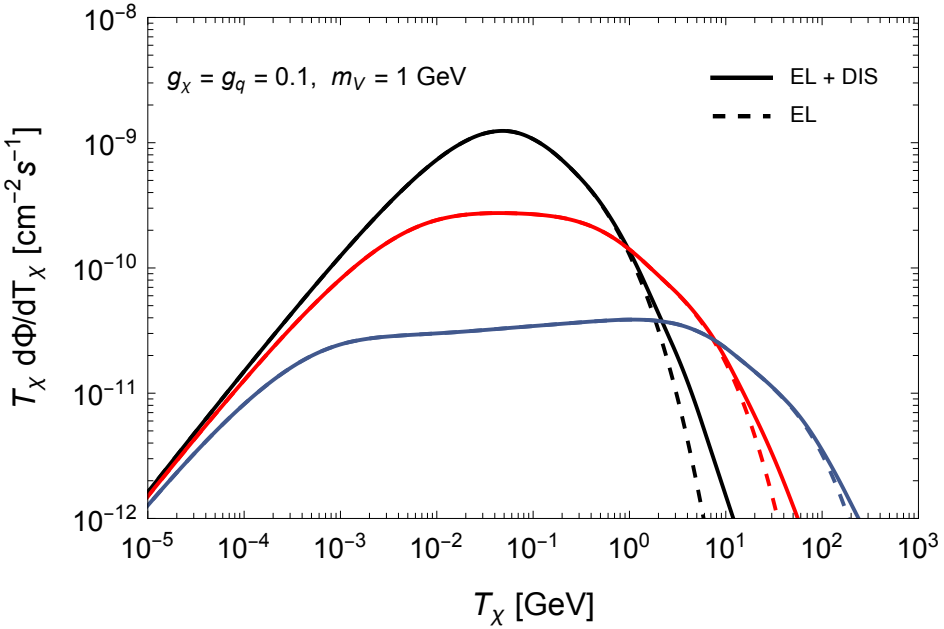


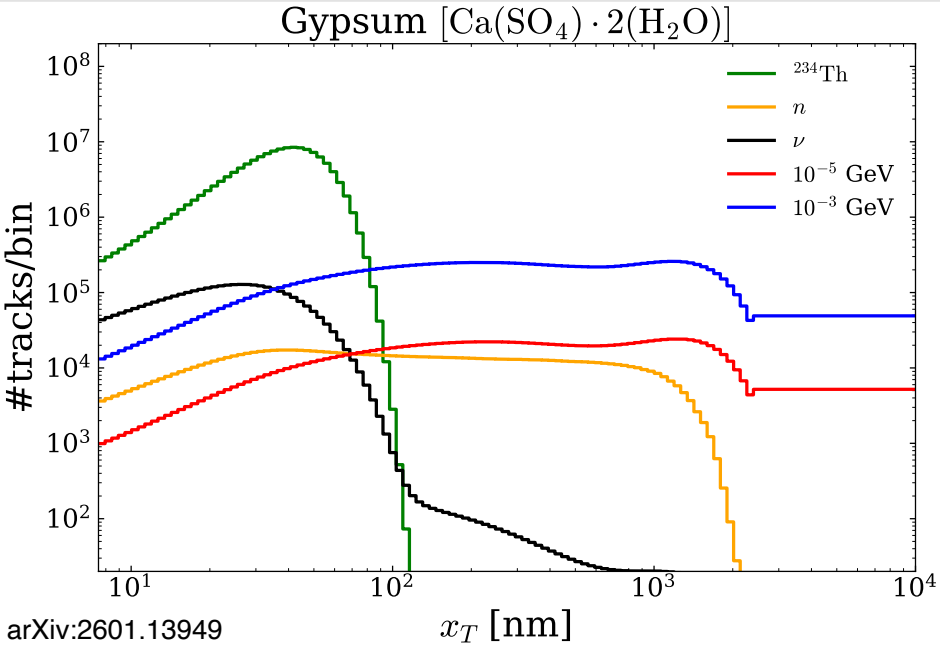


- Combination provides powerful neutron rejection
- Makes data rates and track analysis more feasible

- Track resolution and light yield important for masses $\lesssim 10\,\mathrm{GeV}$
- 1D tracks and vacancies similar sensitivity for masses $\gtrsim 10\,\mathrm{GeV}$
- 2D combined read-out increases sensitivity competitive with XLZD

Halo dark matter upscattered by galactic cosmic rays

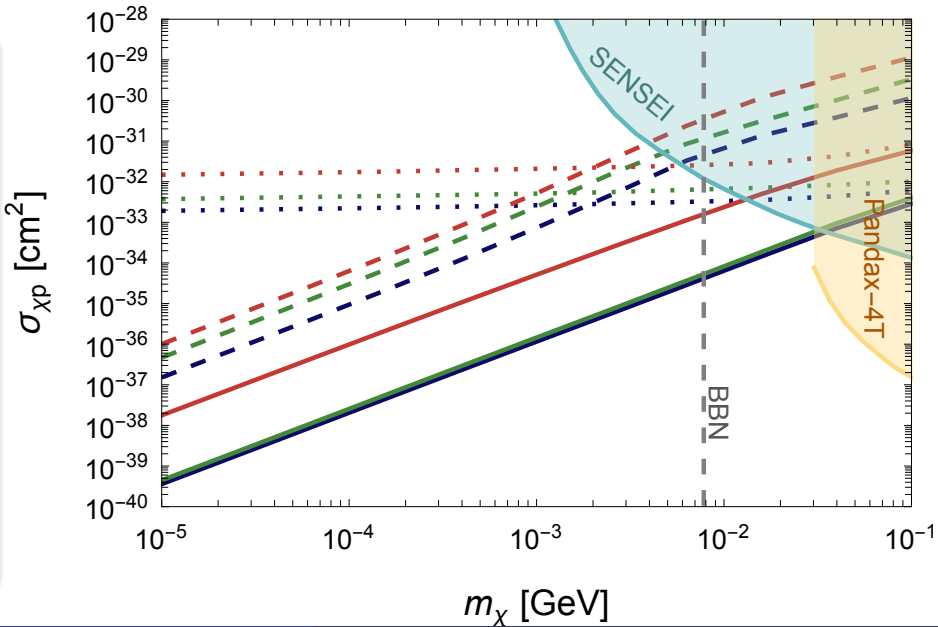




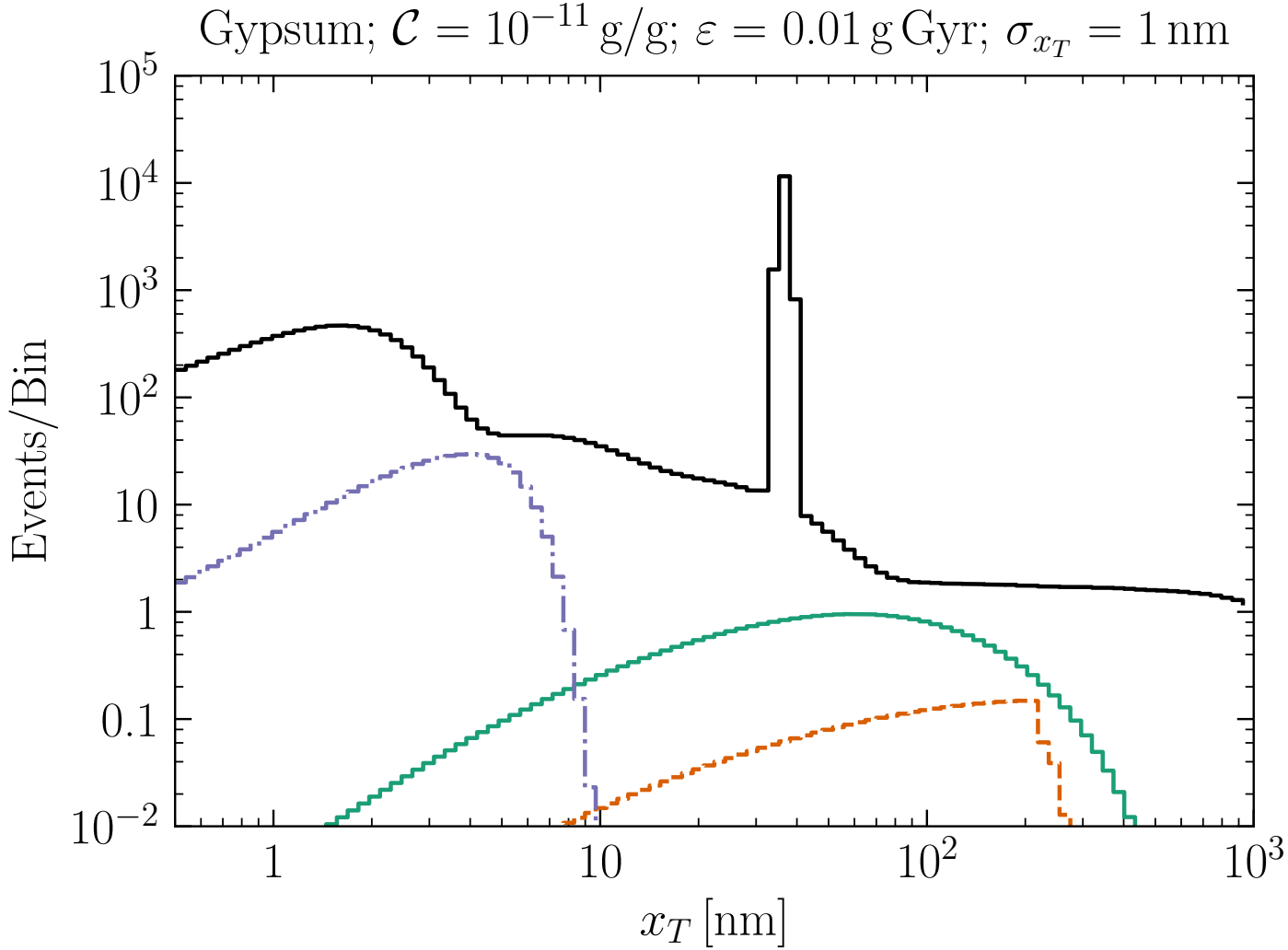
arXiv:2601.13949

CRDM with light vector mediator

- Fluxes for $m_\chi = 1, 10, \mathbf{100}$ MeV
- Track length spectra with $g_\chi = g_q = 0.7, m_V = 1$ GeV
- Constraints for Gypsum, Olivine with constant $\sigma_{\chi p}$ (dotted), $m_V = 10$ MeV (dashed), 1 GeV

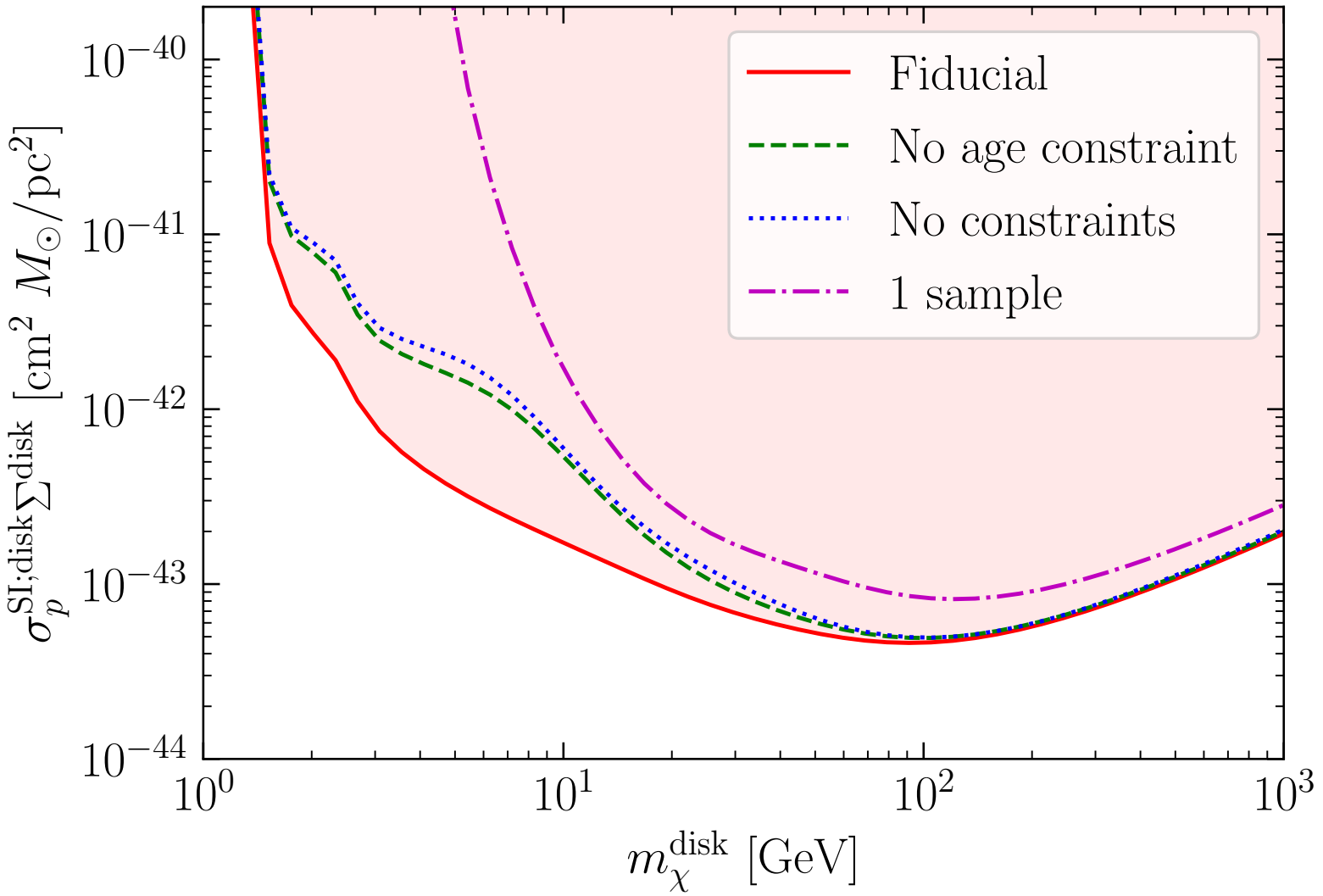


Multiple samples to detect dark disk transit every $\sim 45\,\mathrm{Myr}$



$m_X^{\mathrm{disk}} = 100\,\mathrm{GeV}$ $\sigma_{Xp}^{\mathrm{disk}} = 10^{-43}\,\mathrm{cm}^2$ $m_X = 500\,\mathrm{GeV}$ $\sigma_{Xp} = 5 \times 10^{-46}\,\mathrm{cm}^2$

Distinguish from halo with 20, 40, 60, 80, 100 Myr samples



Systematic uncertainties $\Delta_t = 5\%$ $\Delta_M = 0.1\%$ $\Delta_C = 10\%$ $\Delta_\Phi = 100\%$

Grand Unified Theories (GUTs)

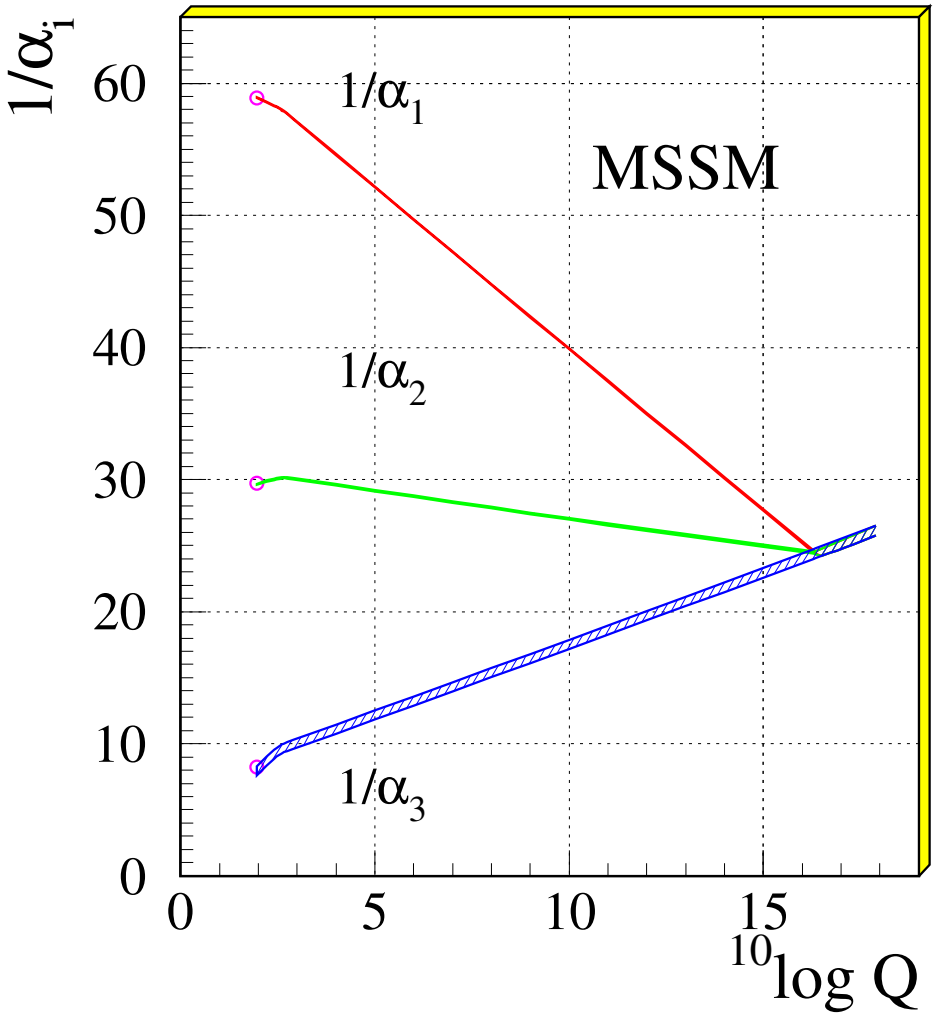


Figure: arXiv:hep-ph/0012288

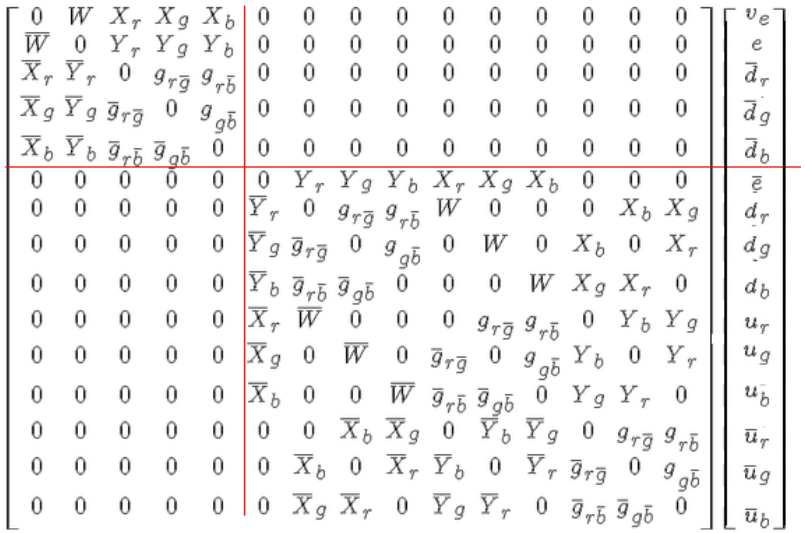


Figure: Paul Bird (2011)

Relevant characteristics of GUTs

- Gauge coupling unification
- SM quarks and leptons in the same **gauge multiplets**

GUTs generically predict proton decay

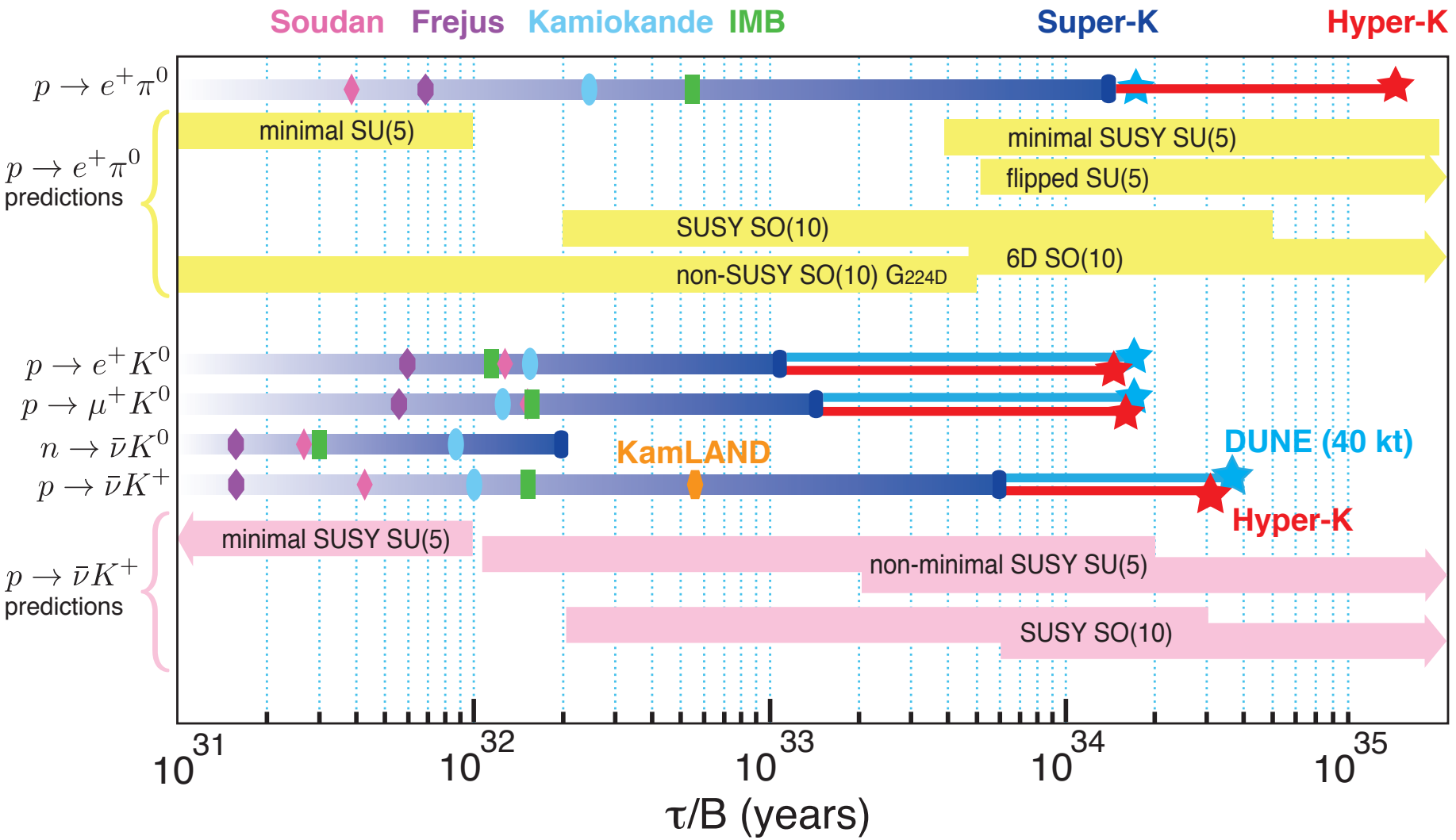
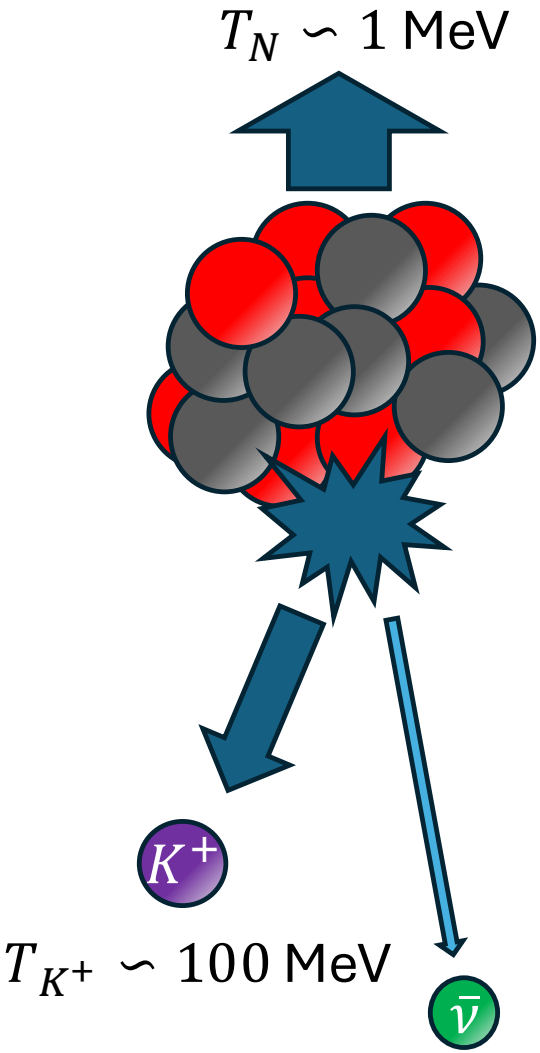
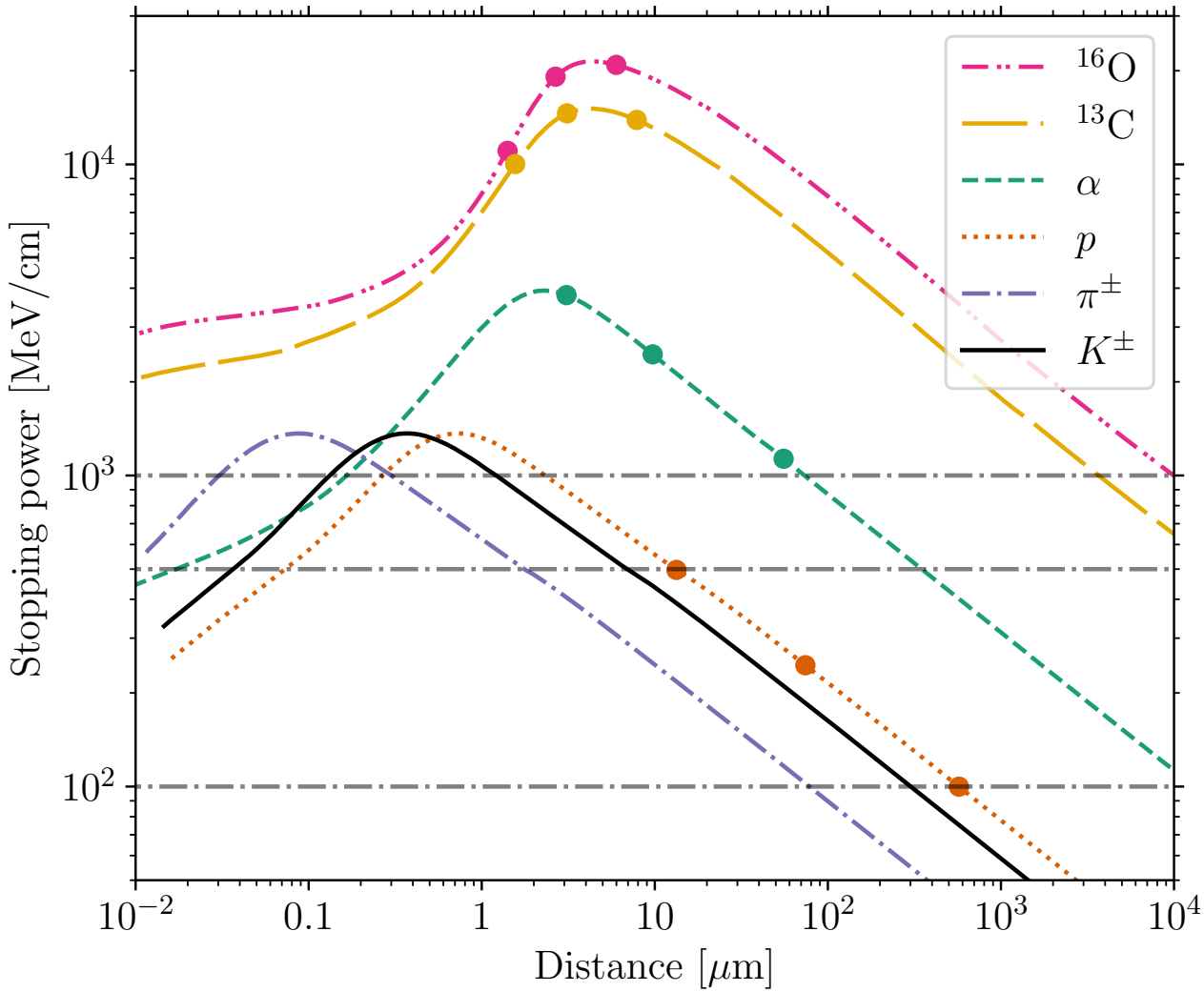


Figure: arXiv:1805.04163

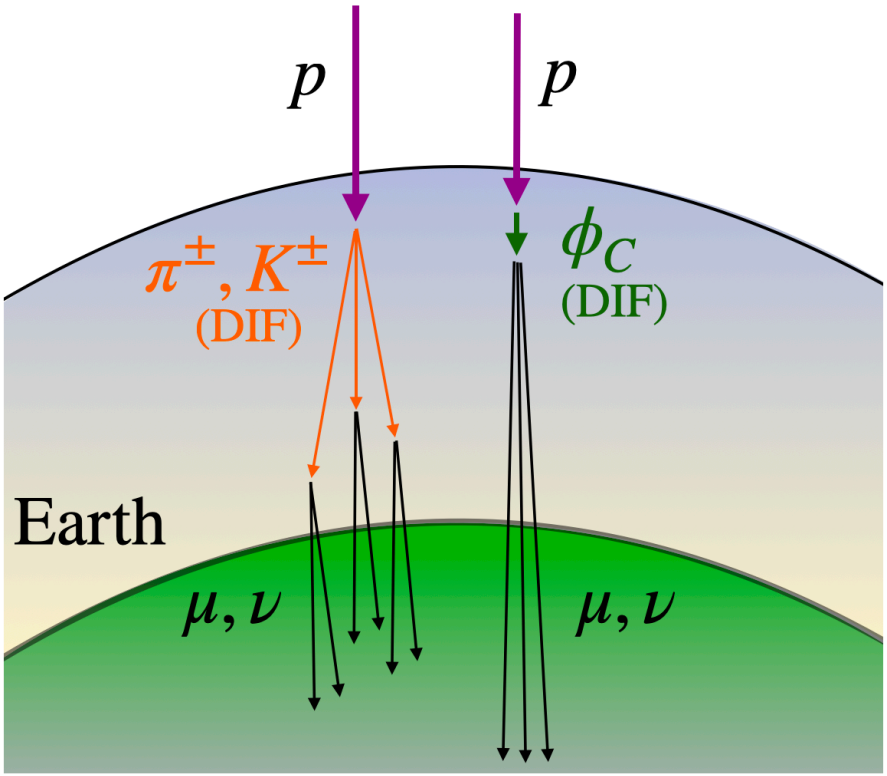
Proton decay remnants could be detected by color centers

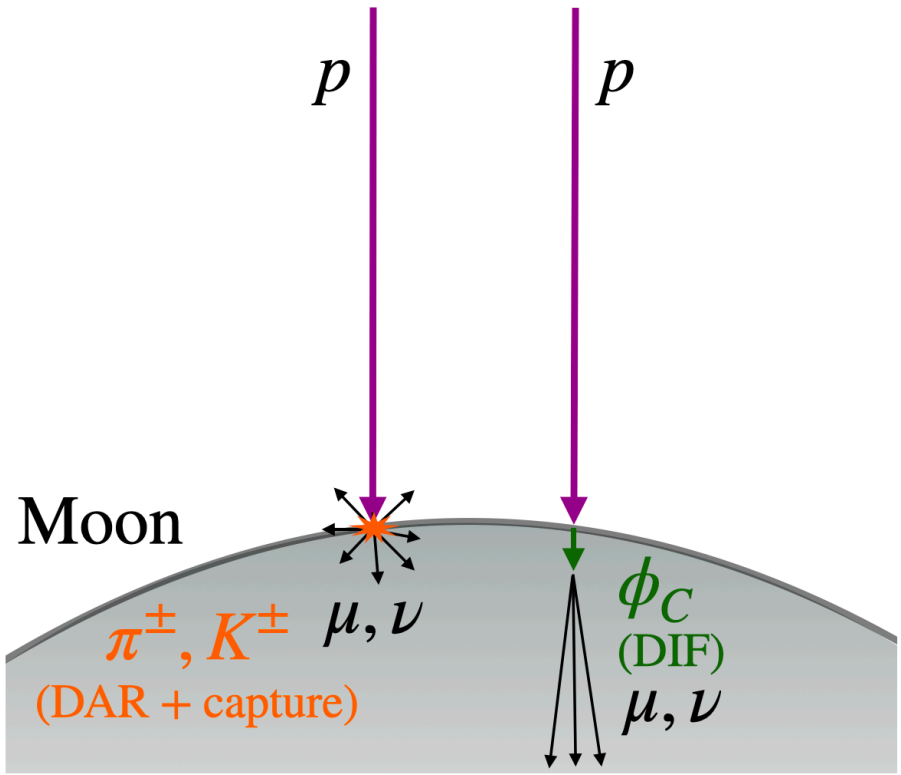




arXiv:2405.15845

Atmospheric neutrinos induce $\mathcal{O}(100)\, K^+/100\,\mathrm{g/Gyr}$





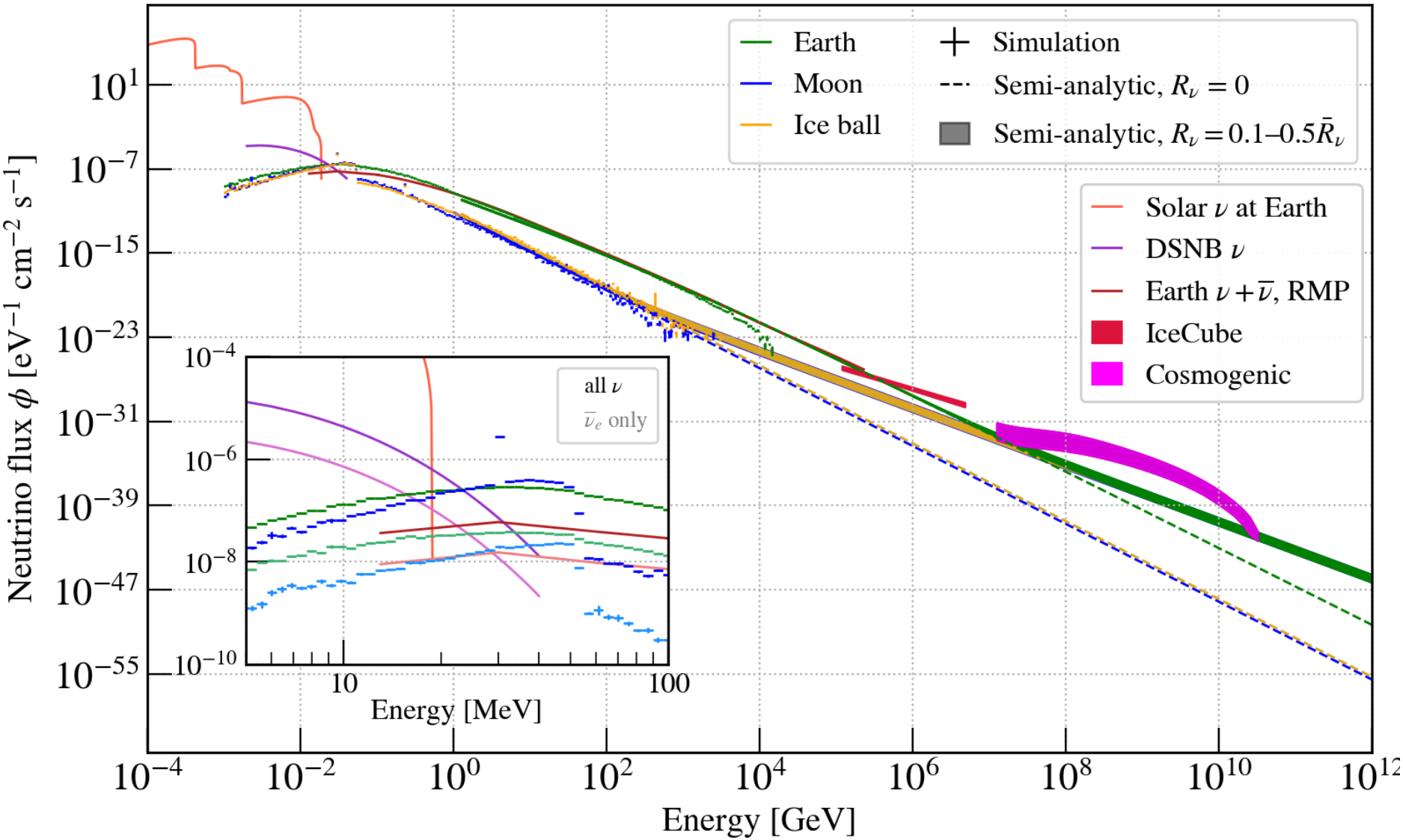
Figures from arXiv:2411.09634

- Conventional secondary mesons **decay in flight** on Earth
- Prompt fluxes from short-lived mesons decaying in flight

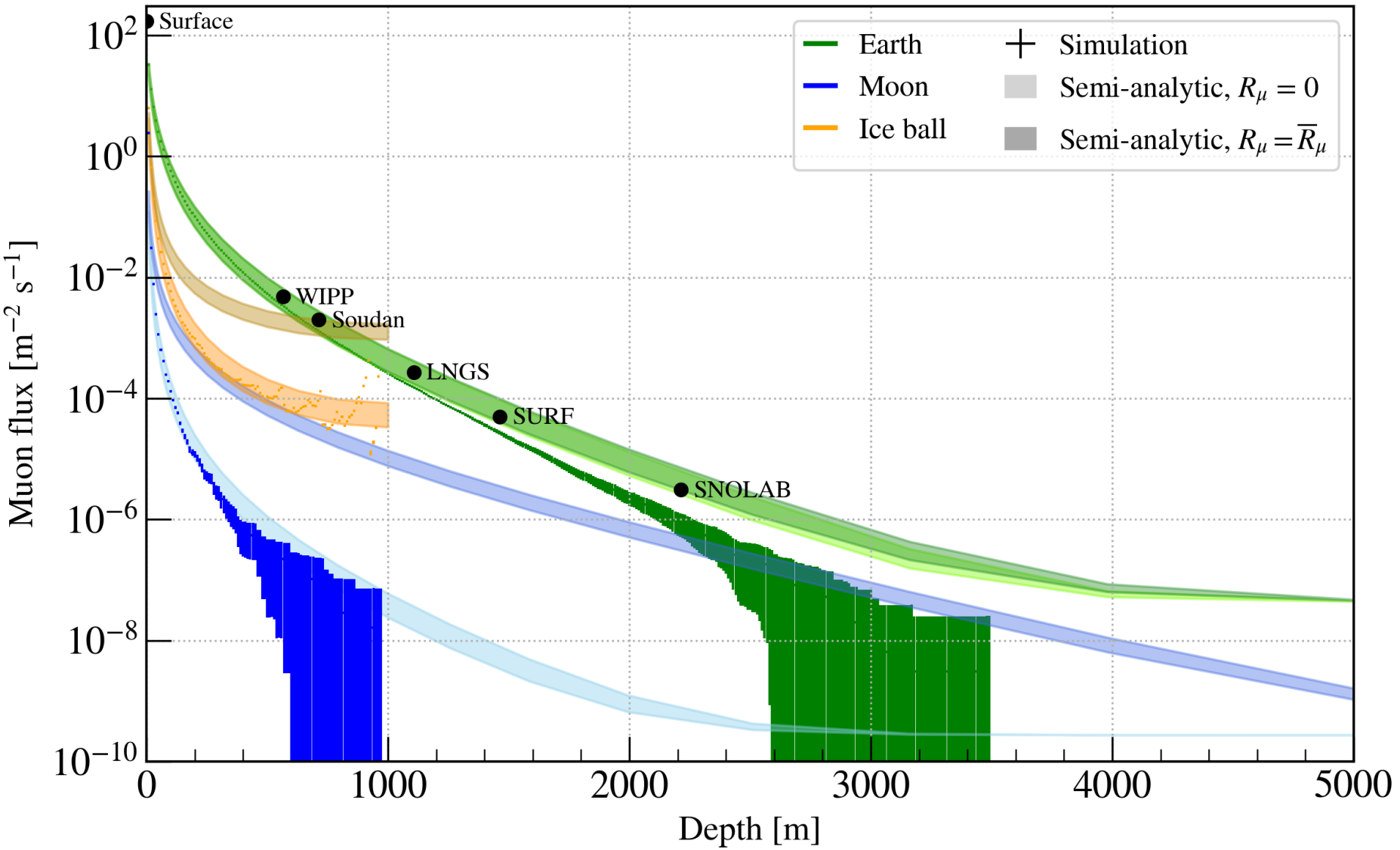
Suppression of lunar μ and ν fluxes

- Conventional secondary mesons **decay at rest** on the Moon
- Less suppression of short-lived mesons decaying in flight

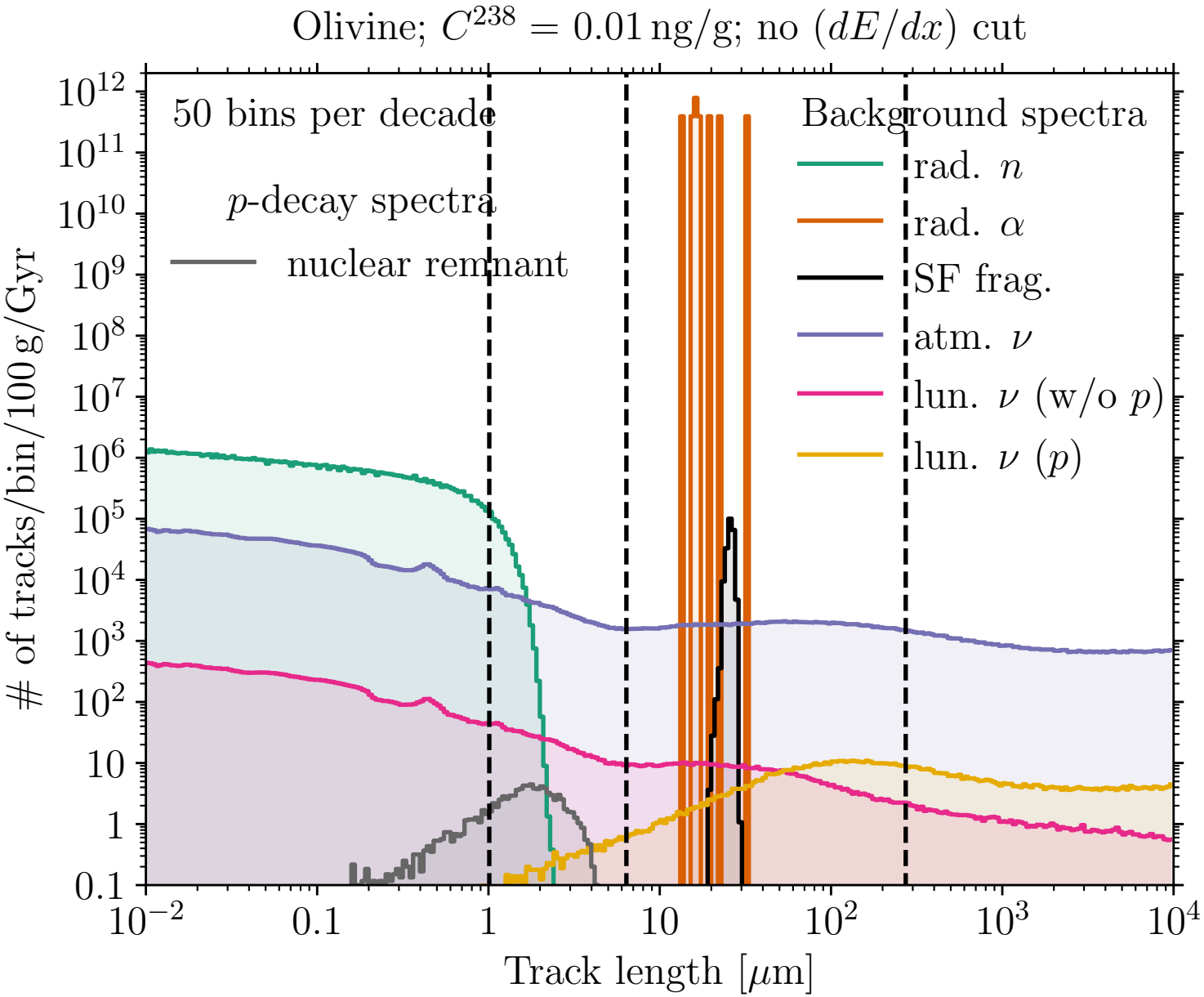
Lunar neutrinos induce $\sim 0.5\, K^+/100\,\mathrm{g}/\mathrm{Gyr}$ in Olivine



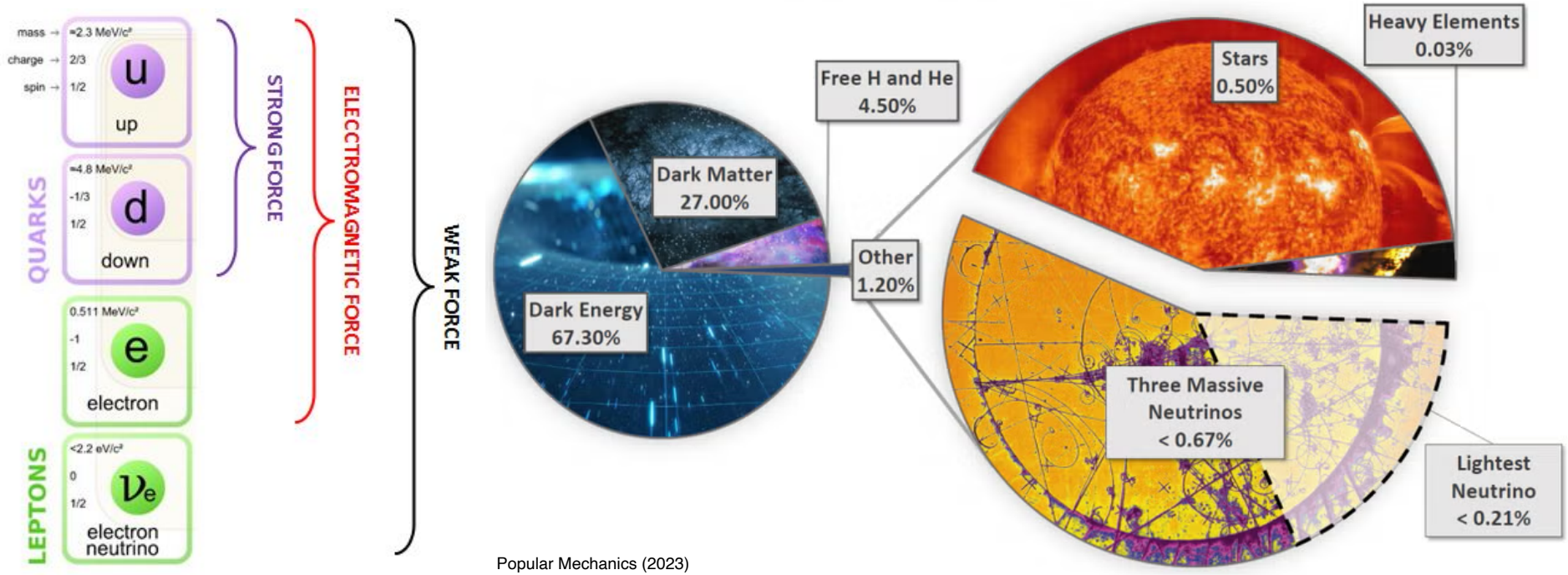
Lunar muons induce $\sim 0.1\, K^+/100\,\mathrm{g/Gyr}$ at $\sim 5\,\mathrm{km}$ depth



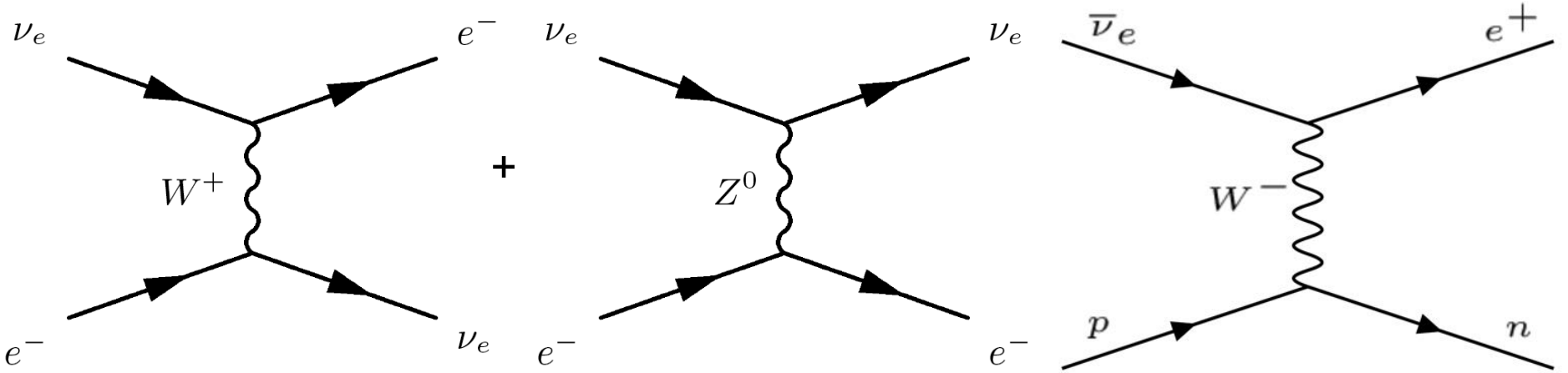
Expect $\lesssim 6\, K^+/100\,\mathrm{g}/\mathrm{Gyr}$ for $\tau(p \to \bar{\nu} K^+) > 5.9 \times 10^{33}\,\mathrm{yr}$



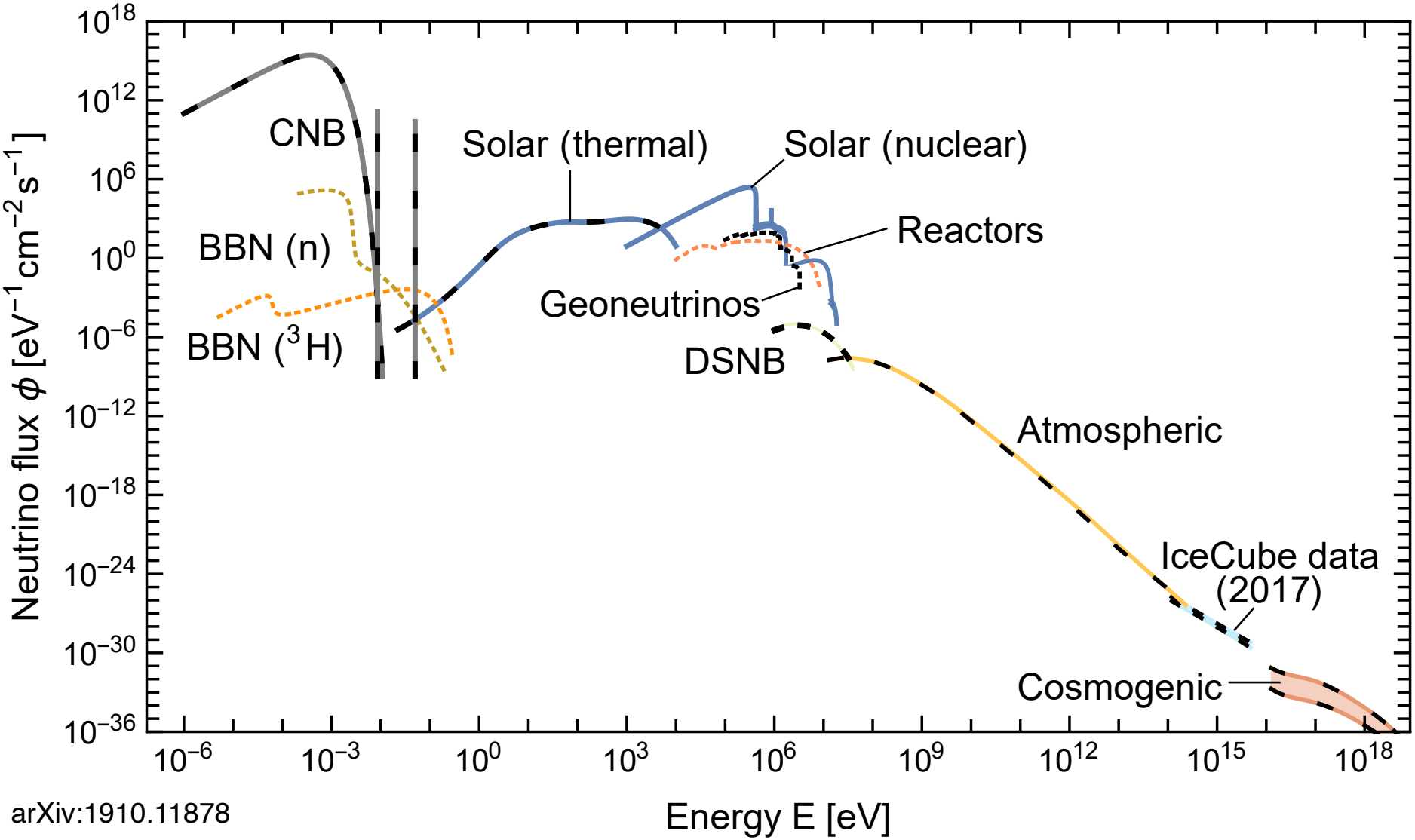
Weakly interacting nearly massless particles



Popular Mechanics (2023)

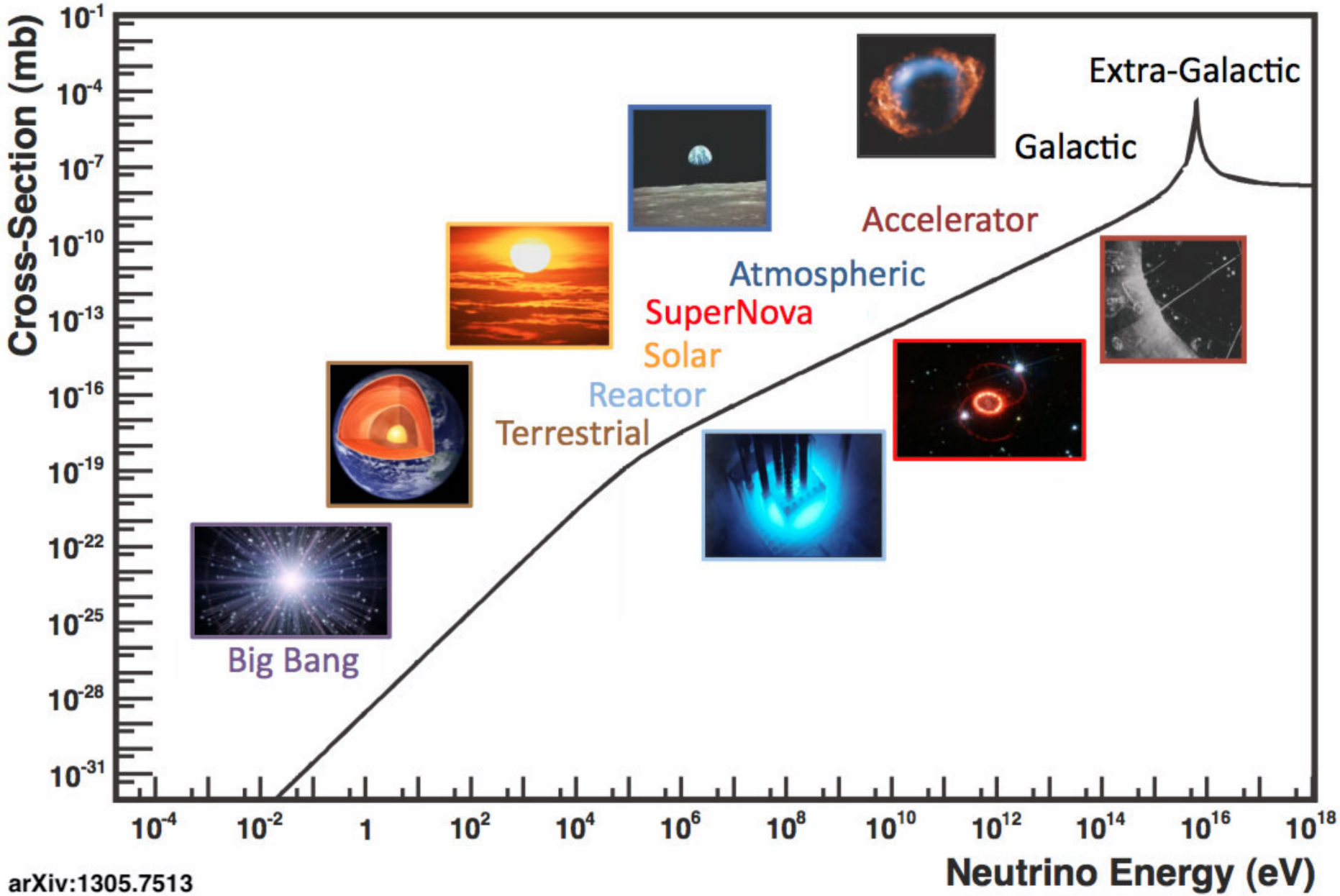


Grand Unified Neutrino Spectrum (GUNS)



arXiv:1910.11878

Interaction cross sections depend on neutrino energy



Nuclear recoil spectrum convolutes flux and cross section

$$\frac{dR}{dE_R} = \frac{1}{m_T} \int dE_\nu \frac{d\sigma}{dE_R} \frac{d\phi}{dE_\nu}$$

- Quasi-elastic for $E_\nu \gtrsim 100\,\text{MeV}$
- Resonant π production at $E_\nu \sim \text{GeV}$
- Deep inelastic for $E_\nu \gtrsim 10\,\text{GeV}$

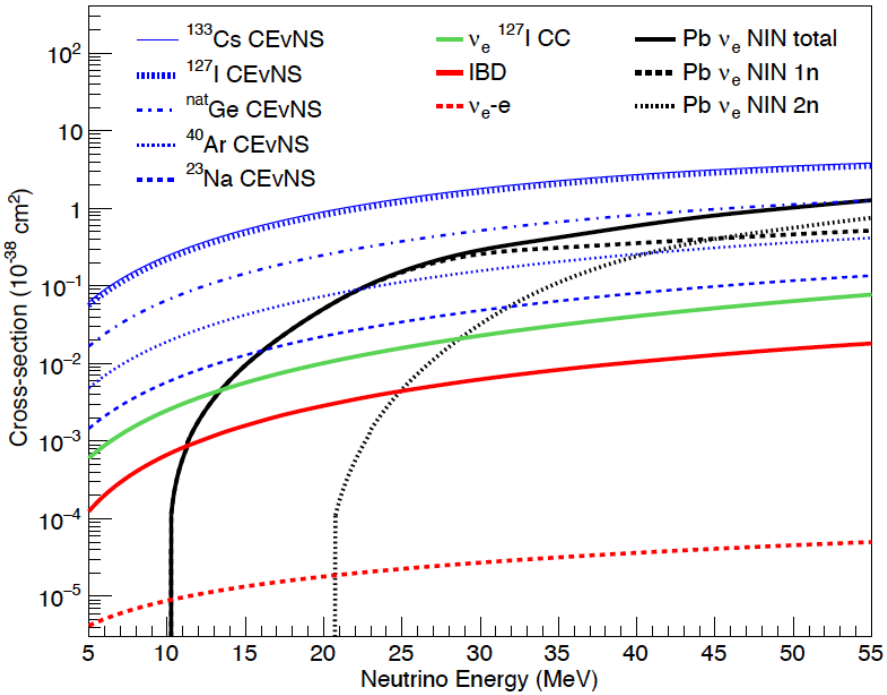


Figure: COHERENT, 1803.09183

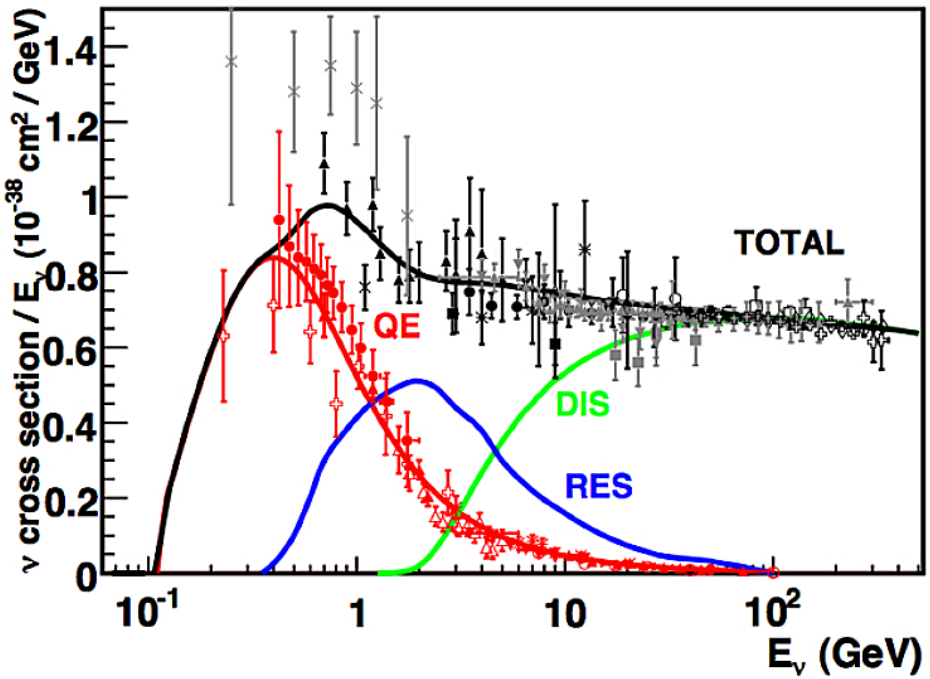
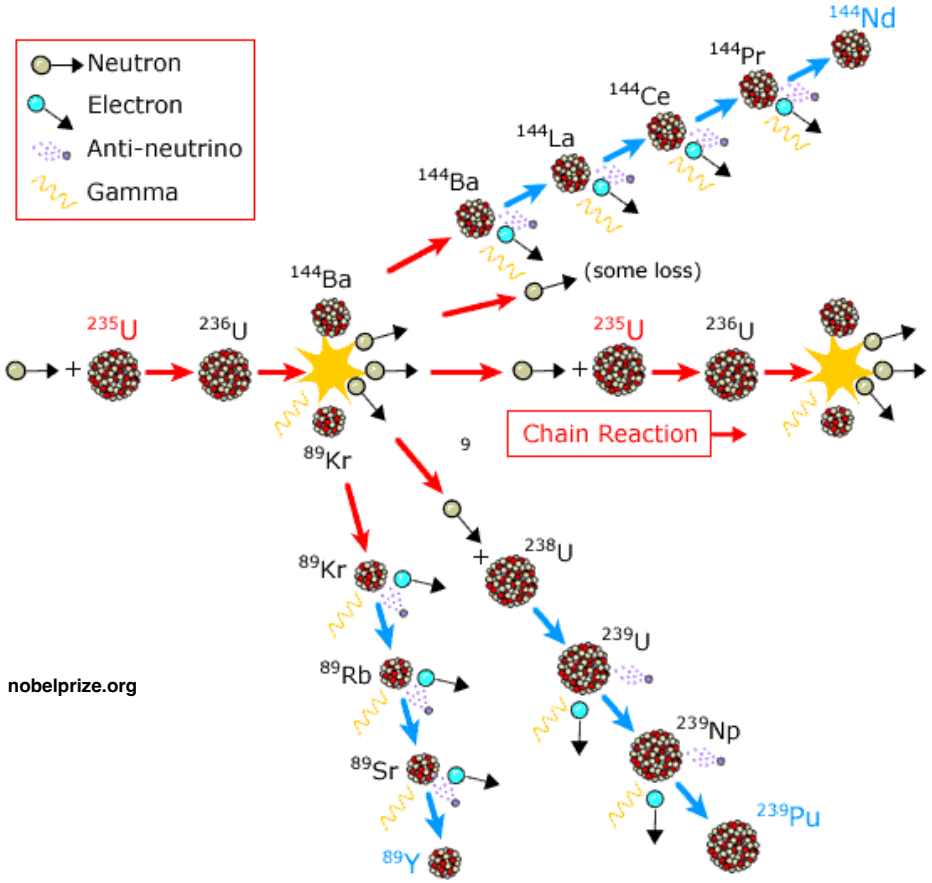


Figure: Inclusive CC $\sigma_{\nu N}$, 1305.7513

Reactor ν's produced in β decays of fission fragments



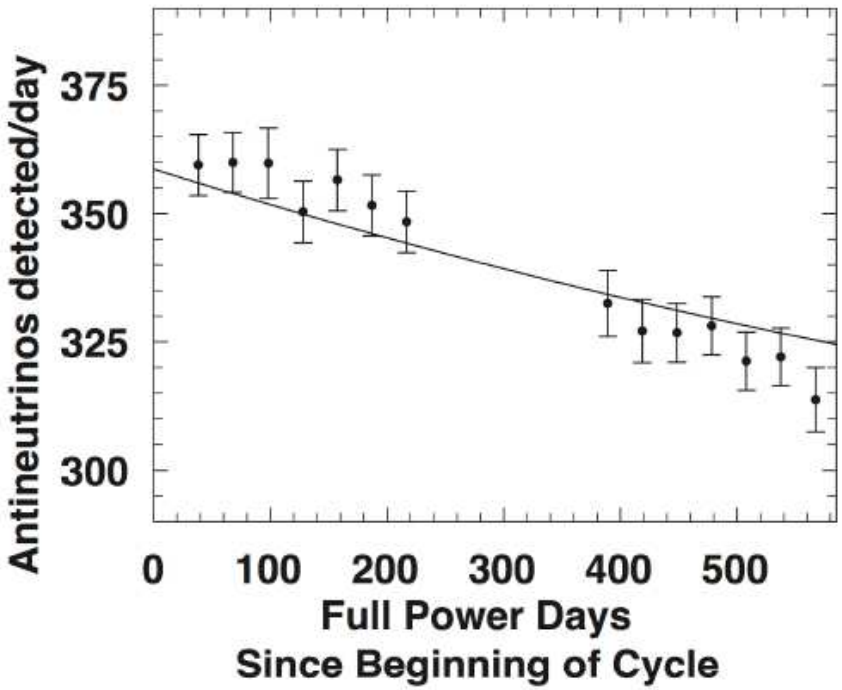


Figure: Processes yielding reactor ν's and time dependence over the course of reactor fuel cycle for $^{239}\mathrm{Pu}$ (1605.02047)

Nuclear safety and non-proliferation

- Measure soft nuclear recoils
- Passive and robust detectors operable at room temperature

First measurement of nuclear reactor CEνNS by CONUS+

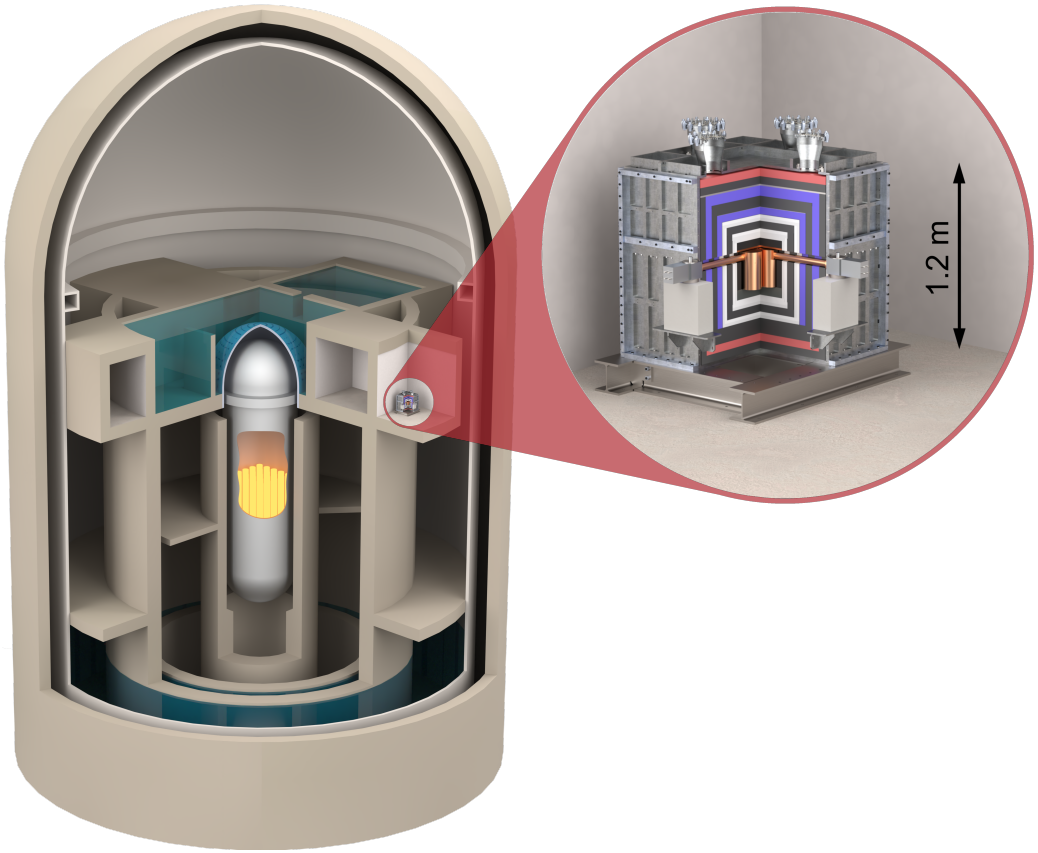
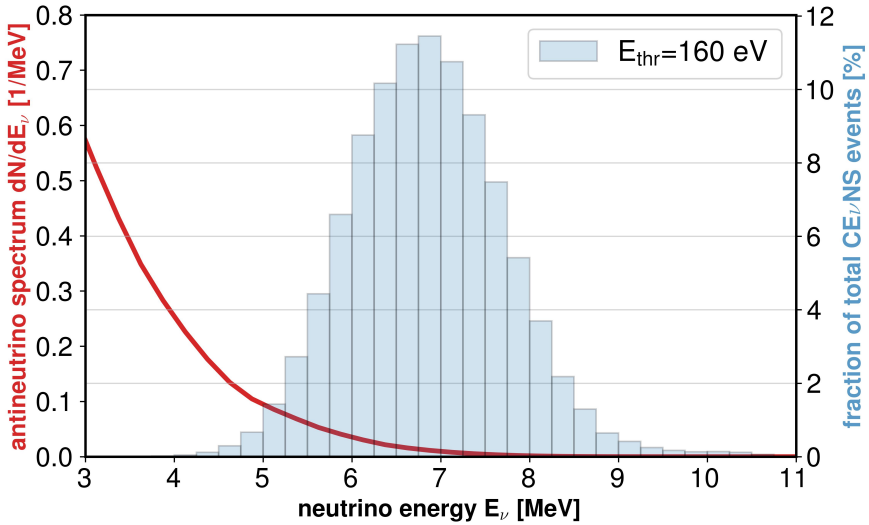
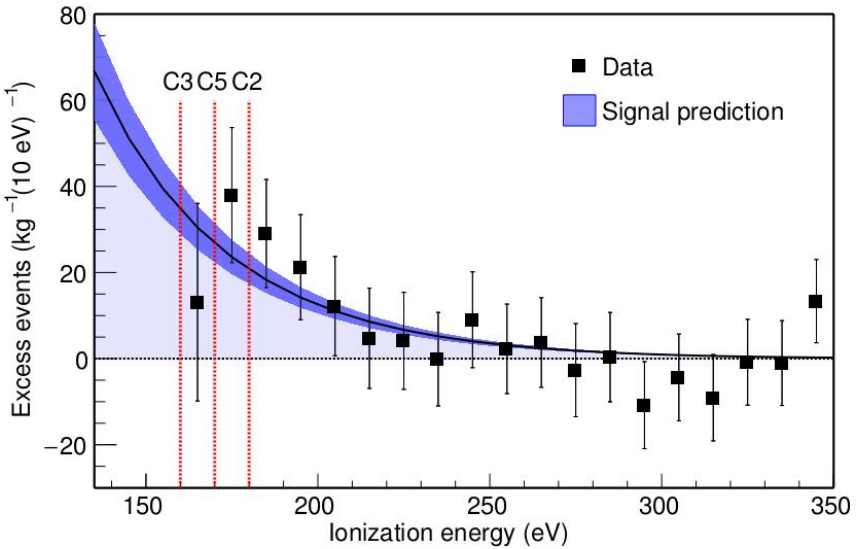
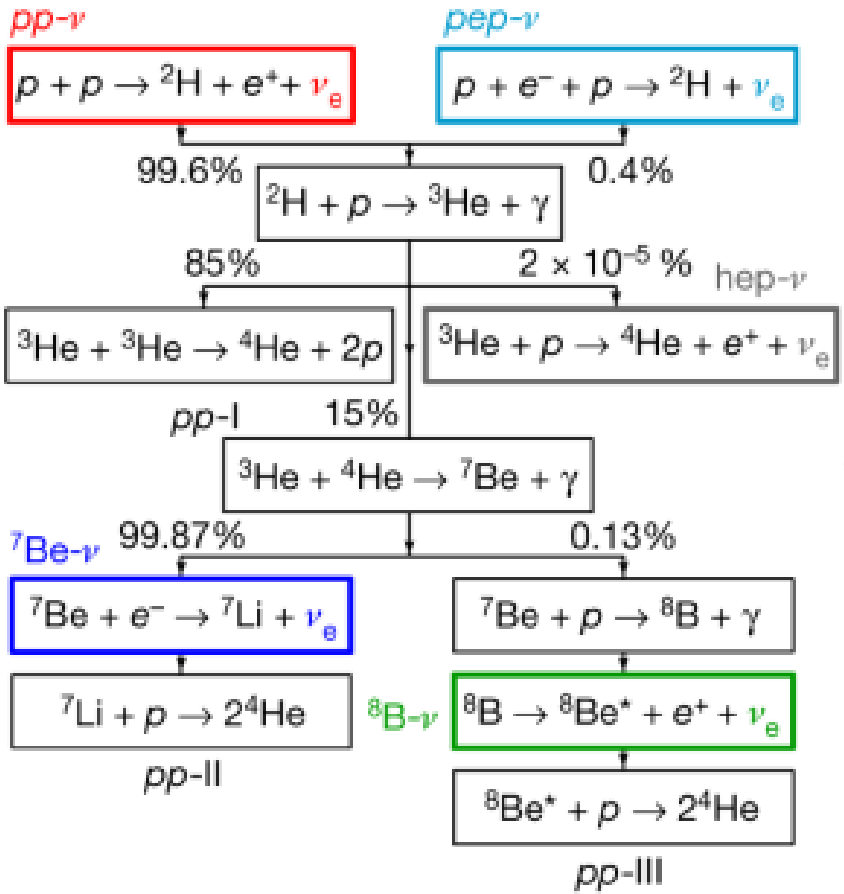


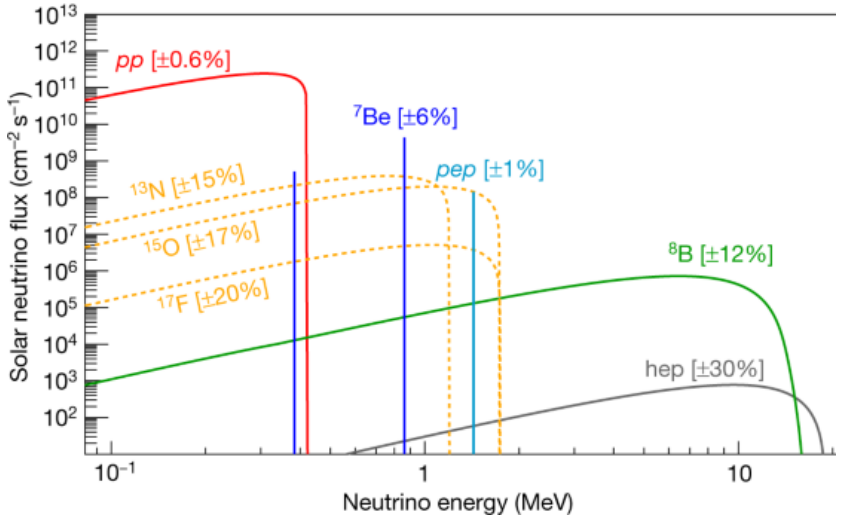
Figure: CONUS+ HPGe detector and shielding at KKL power plant, 2501.05206





Solar ν's produced in fusion chains from H to He





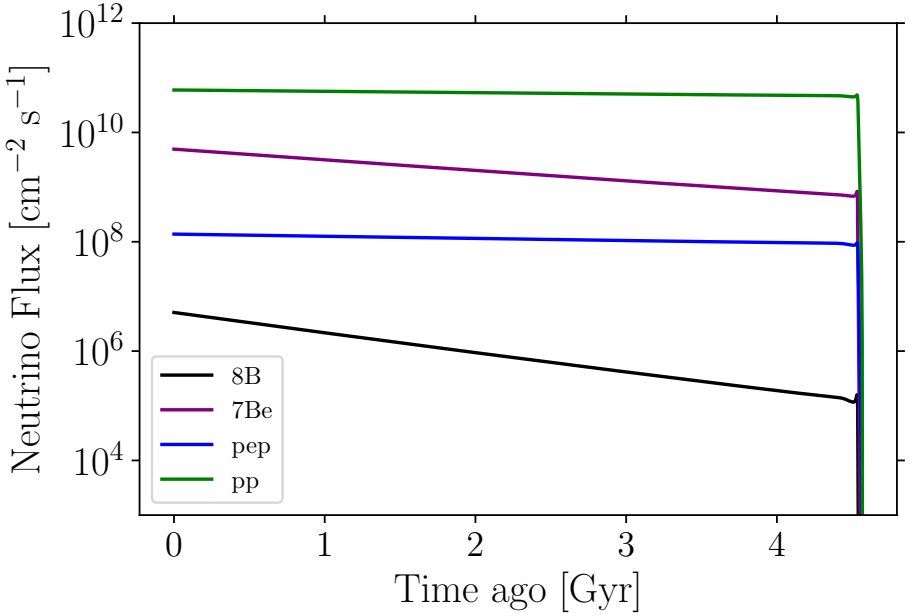
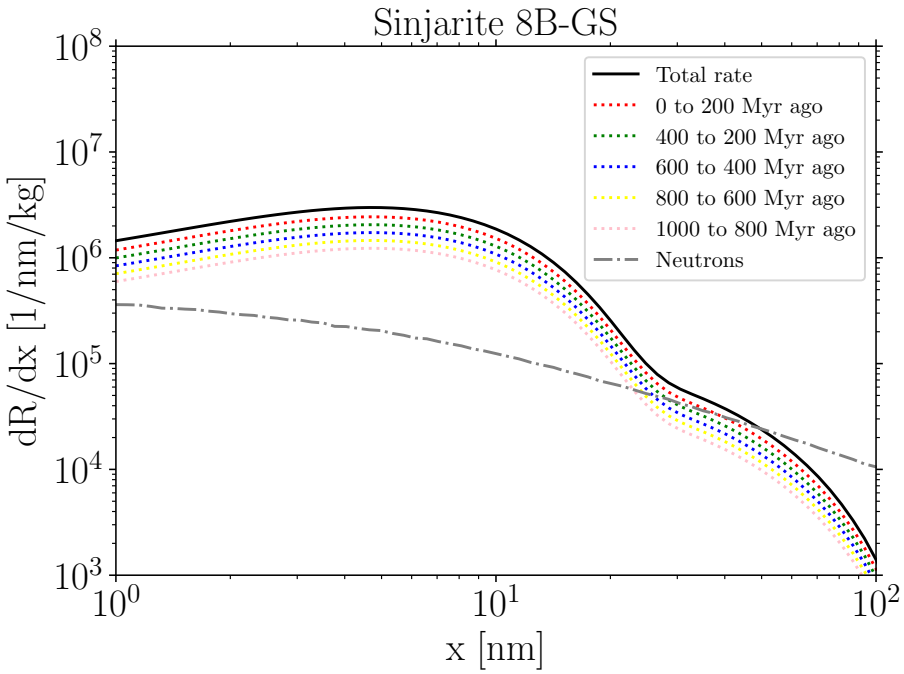
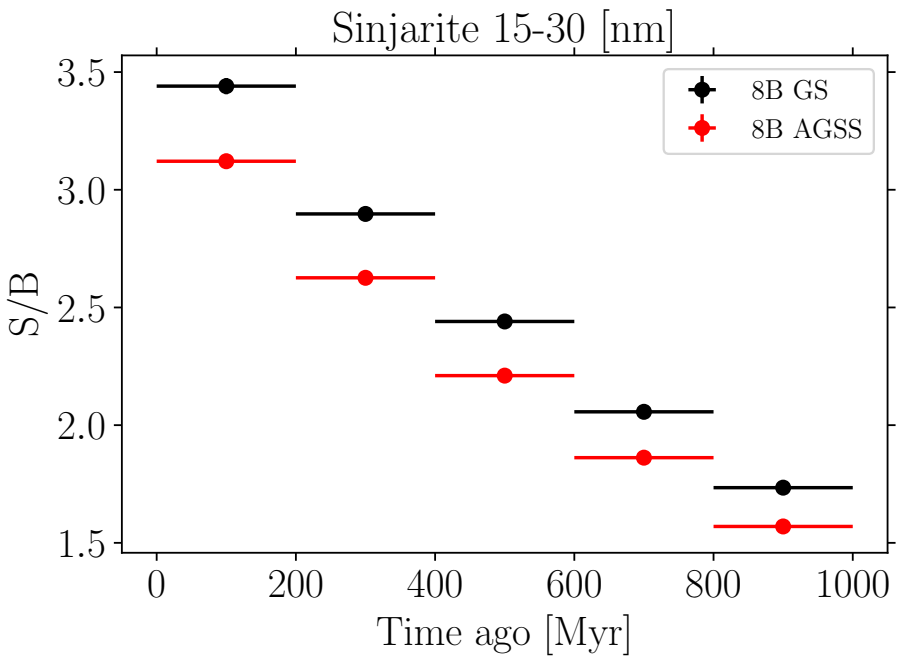


Figure: Today's flux at Borexino (Nature, 2018) and time dependence of GS metallicity model, 2102.01755

Could use large exposure to differentiate between scenarios





Could measure ^8B flux over time

- Higher $E_\nu \Rightarrow$ longer tracks
- Highly dependent on solar core temperature with flux $\propto T^{24}$
- Sensitive to metallicity model

100 g samples with 15 nm resolution

- Look in single bin $15 - 30$ nm
- Assume $\Delta_t \sim 10\%$, $\Delta_C = 10\%$
- $N_{\text{tot}}^{\text{GS}} \sim (1.63 \pm 0.05) \times 10^6$
  $N_{\text{tot}}^{\text{AGSS}} \sim (1.52 \pm 0.05) \times 10^6$

Galactic contribution to ν flux over geological timescales

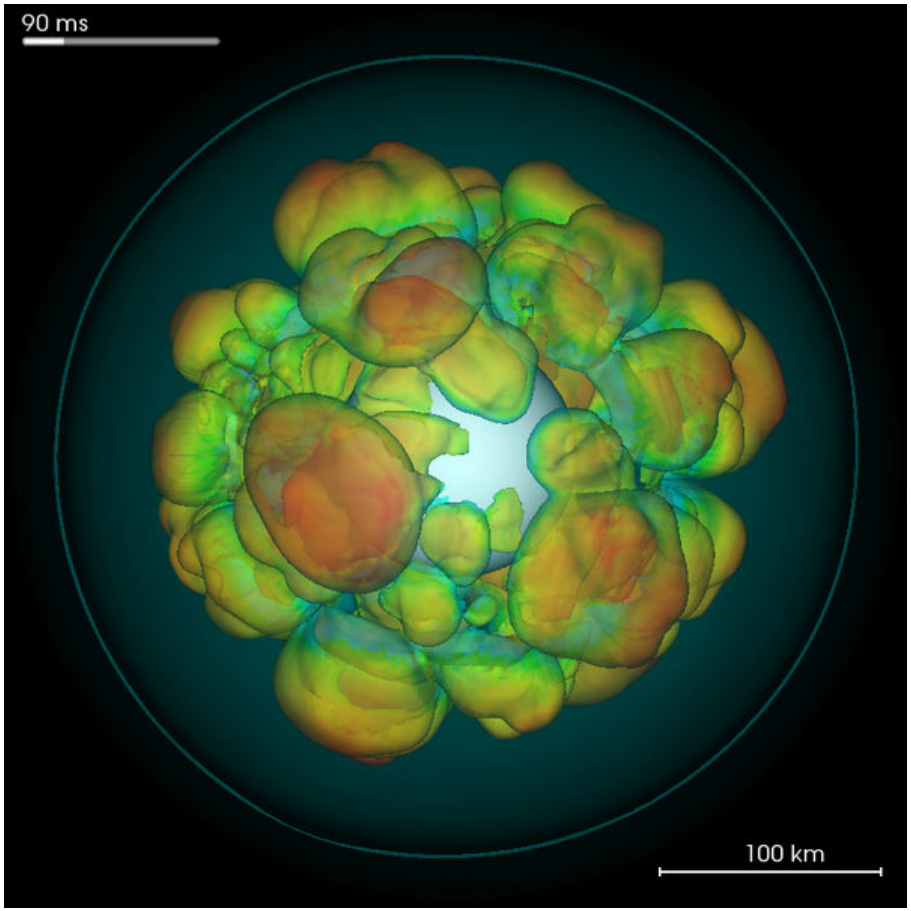


Figure: Supernova simulation after CC

Only $\sim$ 2 SN 1987A events/century

- Measure galactic CC SN rate
- Traces star formation history

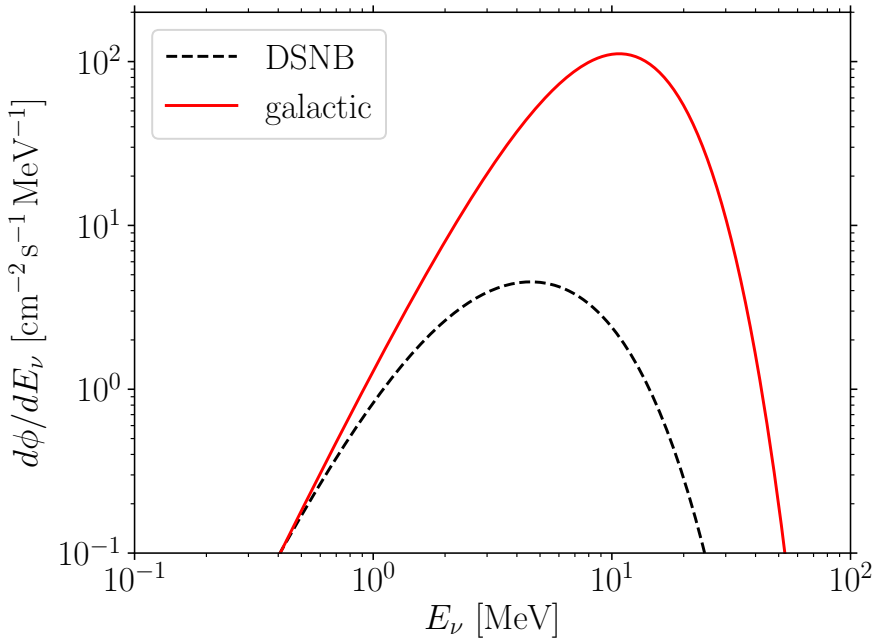
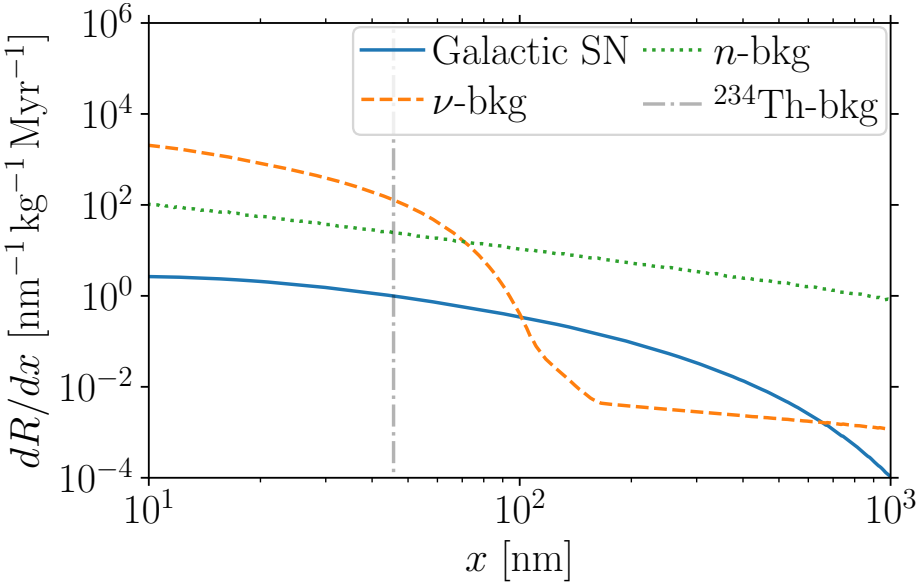


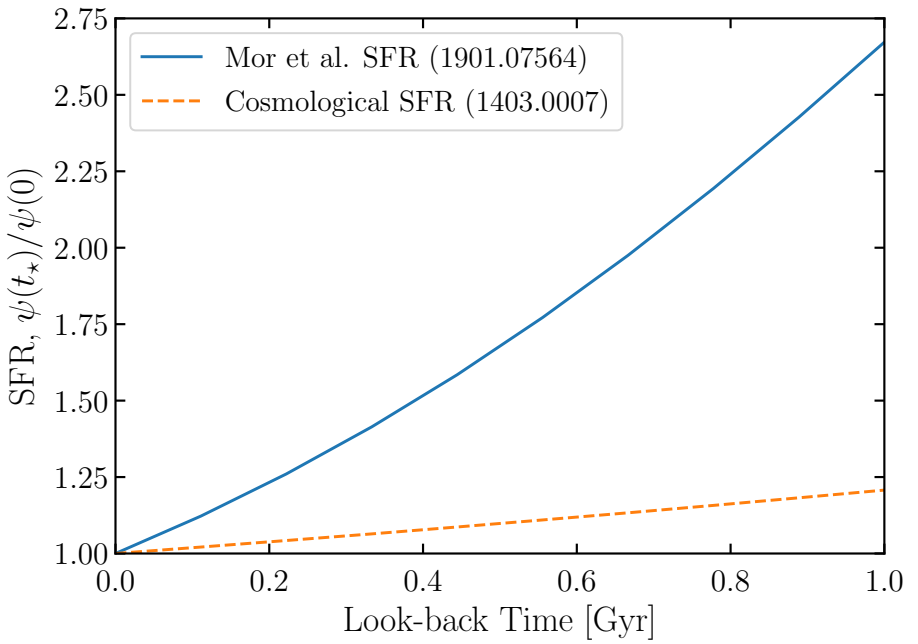
Figure: CC SN neutrino flux over geological timescales, arXiv:1906.05800

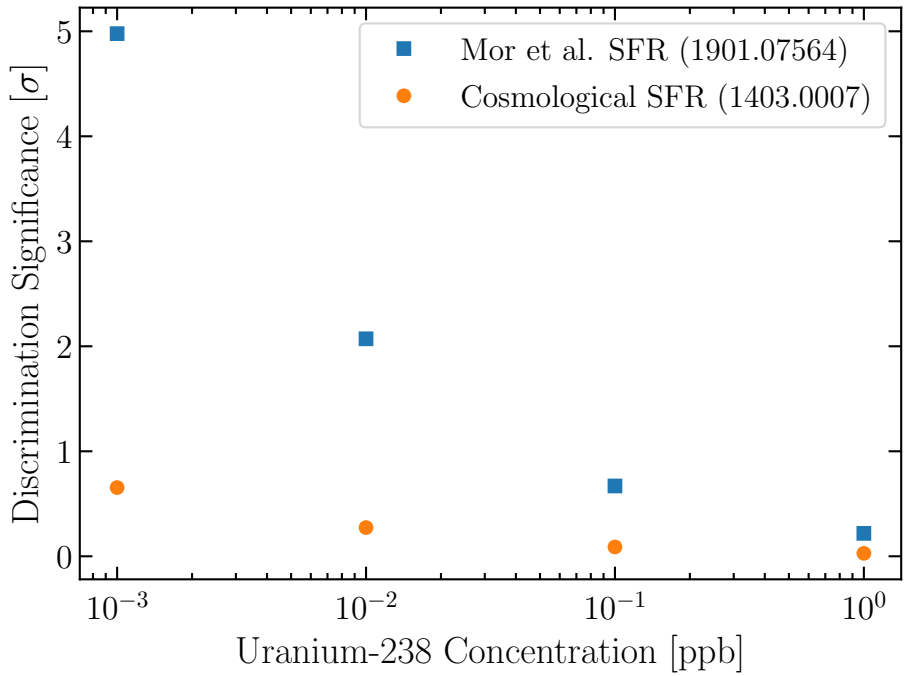
Difficult to pick out time evolution of galactic CC SN rate



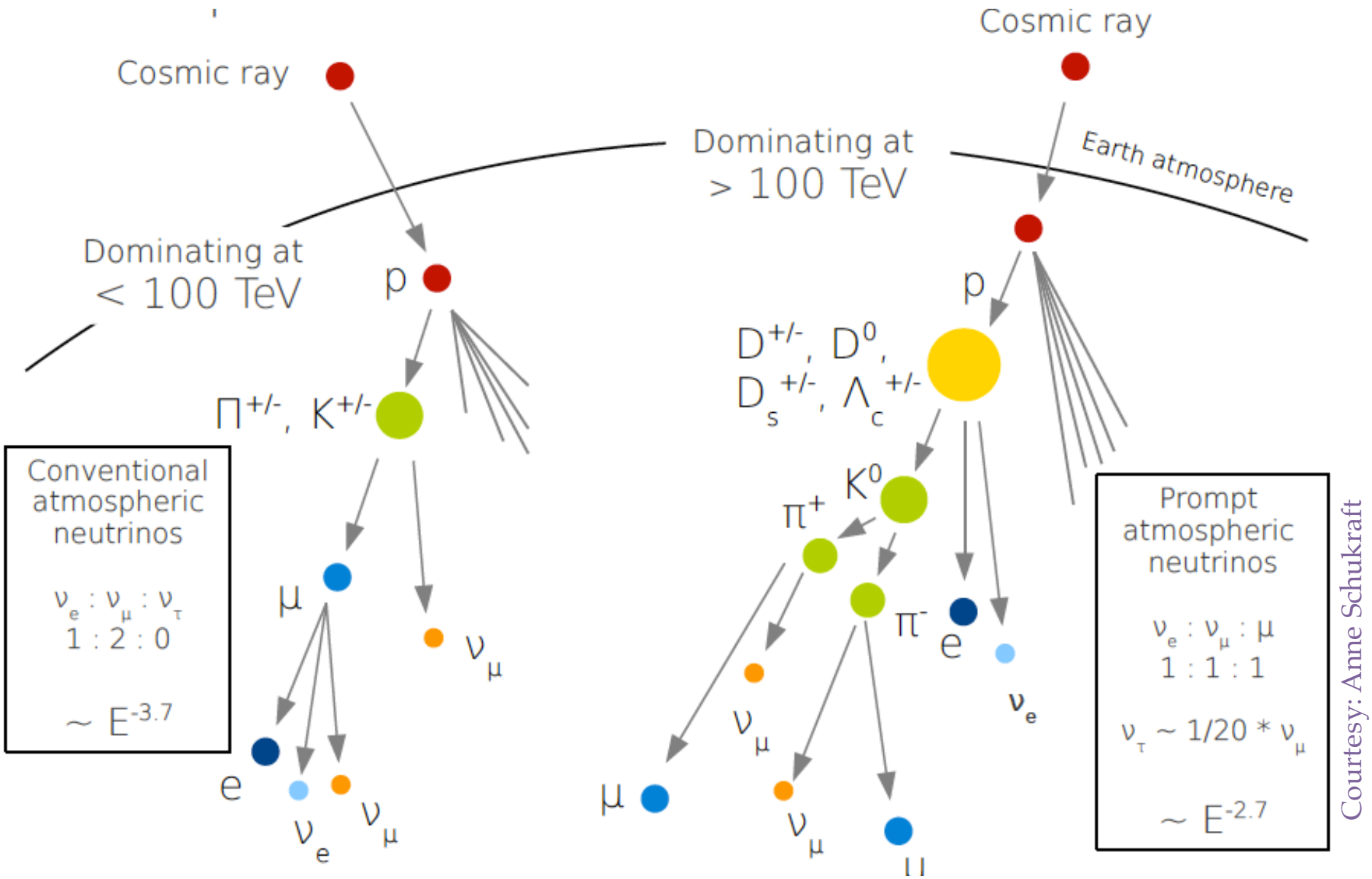
Coarse grained cumulative time bins

- 10 Epsomite paleo-detectors
- 100 g each, $\Delta t_{\rm age} \simeq 100$ Myr
- Try to detect models for evolution of star formation rate





Atmospheric ν's originating from CR interactions



Atmospheric ν's originating from CR interactions

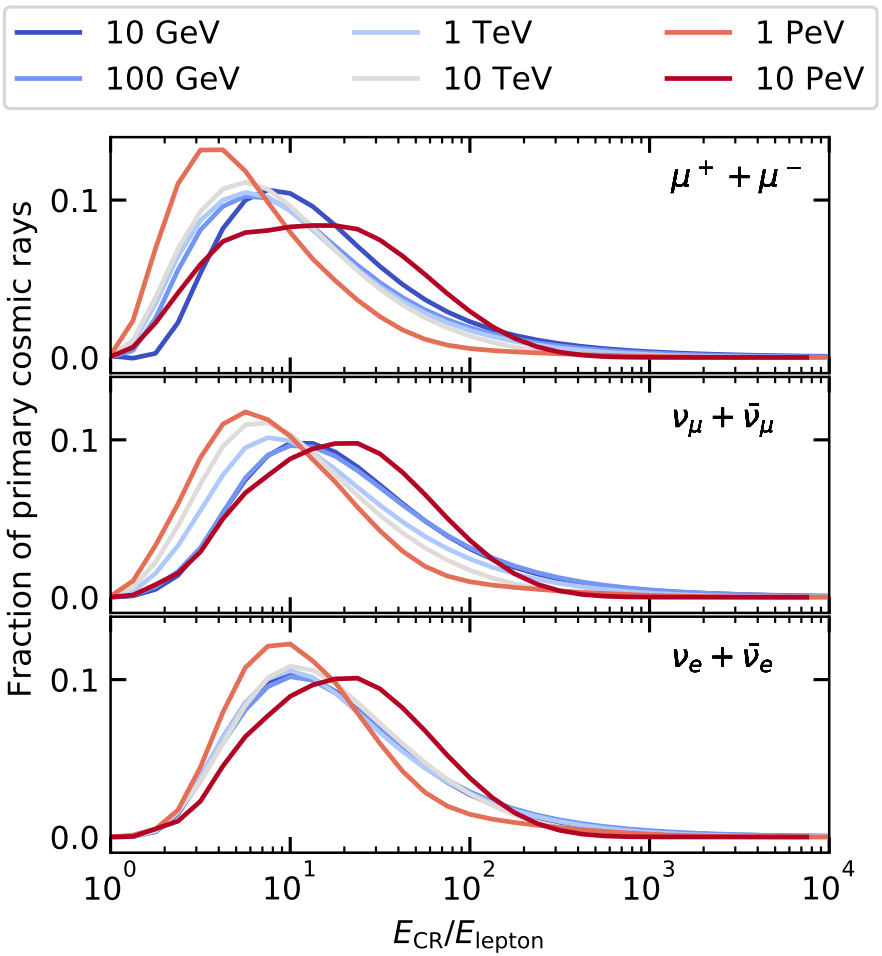


Figure: E_{CR} to leptons, 1806.04140

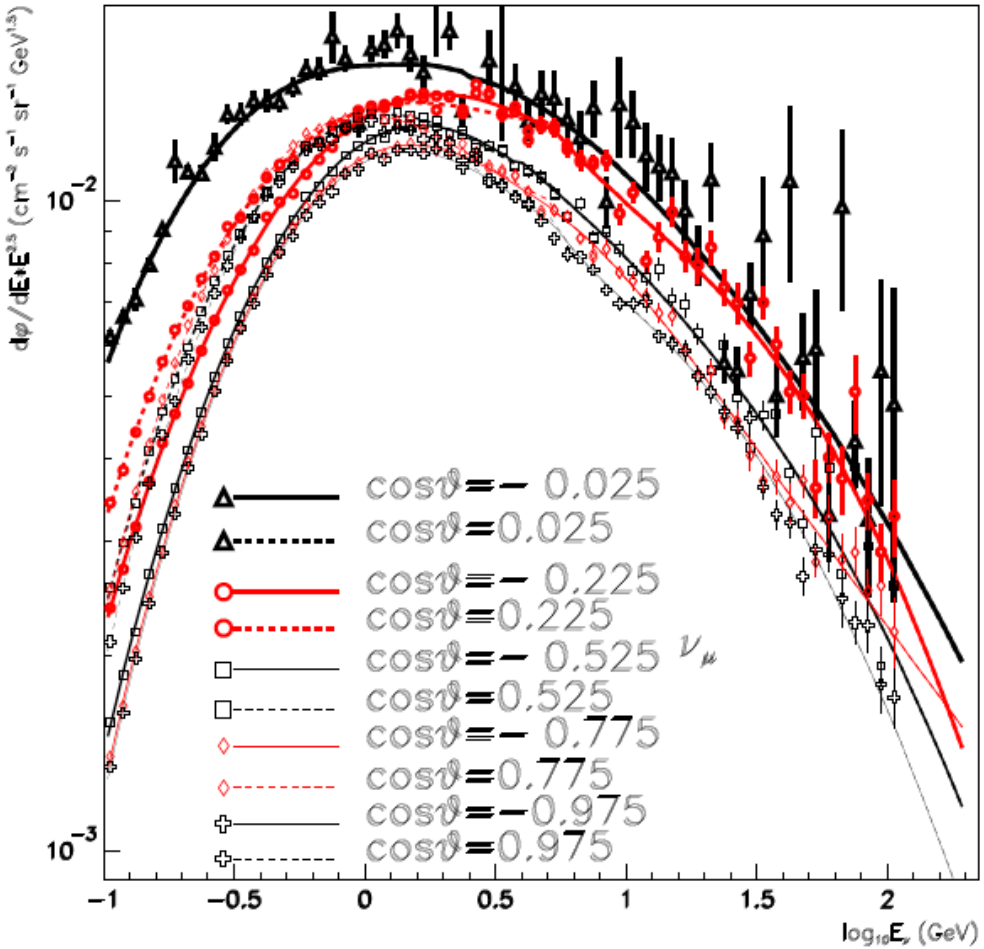


Figure: FLUKA simulation of ν_μ flux at SuperK for solar max, hep-ph/0207035

Geomagnetic field deflects lower energy CR primaries

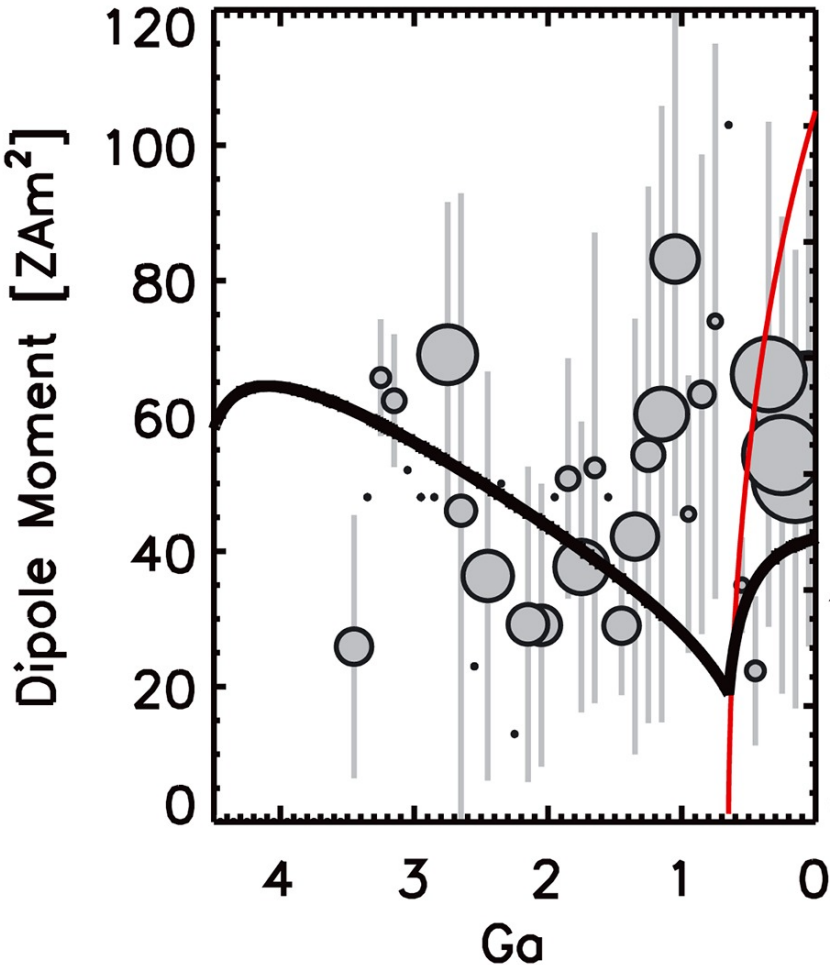
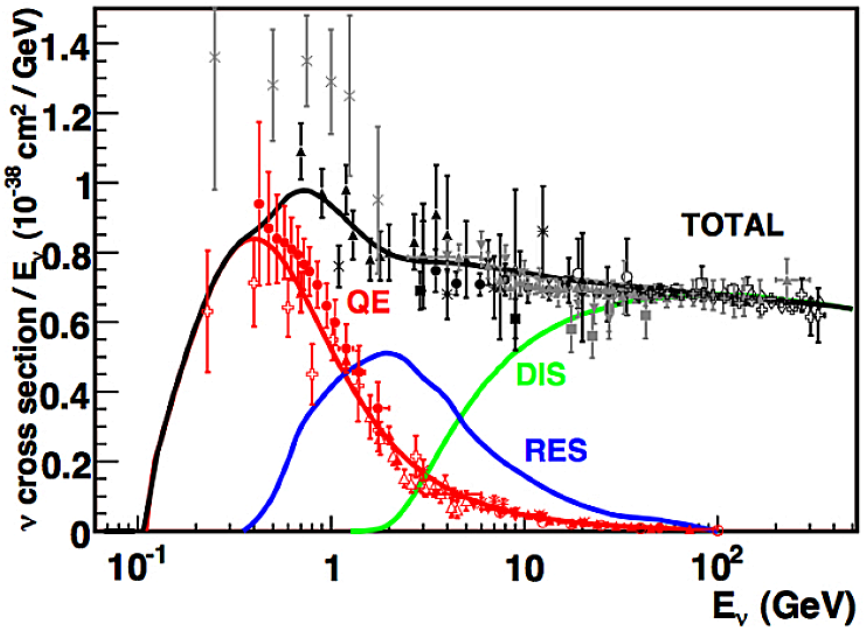


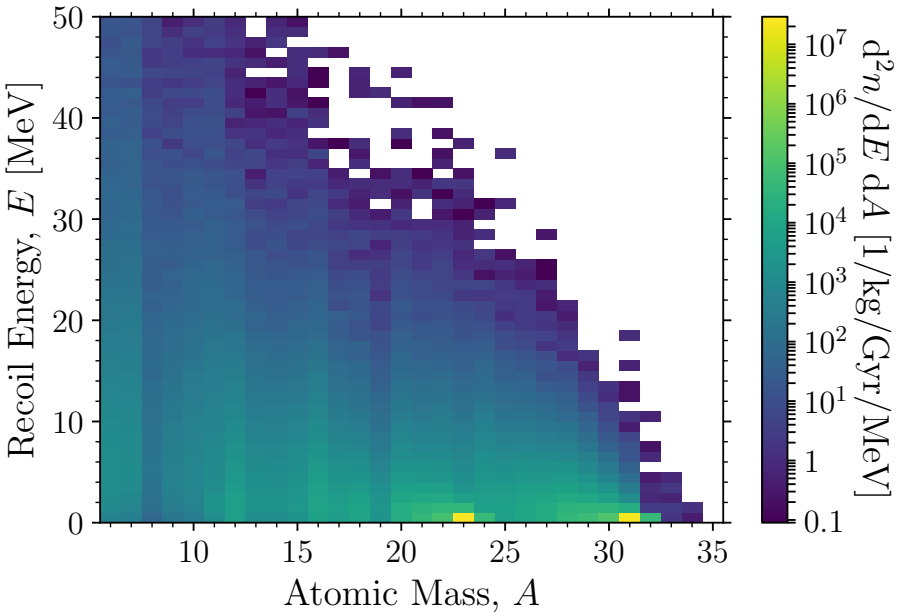
Figure: Driscoll, P. E. (2016), *Geophys. Res. Lett.*, 43, 5680-5687

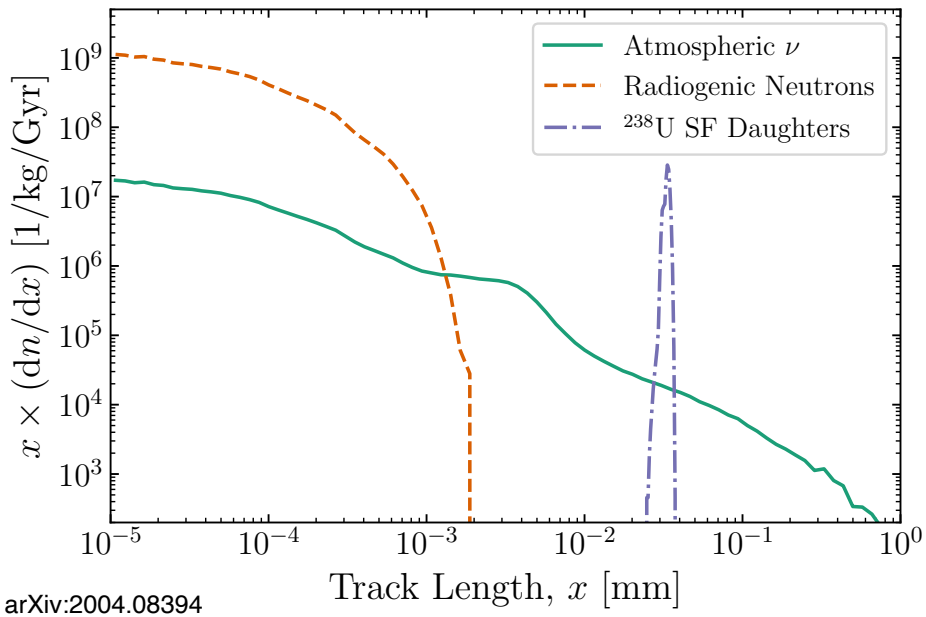
Rigidity $p_{CR}/Z_{CR} \simeq E_{CR}$ for CR protons

- Rigidity cutoff $\propto M_{dip}$ truncates atmospheric ν spectrum at low E_ν
- Maximum cutoff today $\sim 50\,\mathrm{GV}$
- Recall CR primary $E_{CR} \gtrsim 10\,E_\nu$



Recoil spectra from atmospheric ν's incident on NaCl(P)





arXiv:2004.08394

Recoils of many different nuclei

- Low energy peak from QE neutrons scattering ^{23}Na, ^{31}P
- High energy tail of lighter nuclei produced by DIS

Background free regions for $\gtrsim 1\,\mu$m

- Radiogenic n-bkg confined to low x, regardless of target
- Subdominant systematics from atmosphere, heliomagnetic field